TECHNISCHE UNIVERSITÄT MÜNCHEN
Lehrstuhl für Strahlenbiologie
Fakultät für Medizin

The role of the Peroxisome Proliferator-Activated Receptor α in radiation-induced cardiovascular disease

Vikram Subramanian

Vollständiger Abdruck der von der Fakultät für Medizin der Technischen Universität München zur Erlangung des akademischen Grades eines *Doktors der Naturwissenschaften* (Dr. rer.nat.) genehmigten Dissertation.

Vorsitzender: Prof. Dr. Dr. Stefan Engelhardt

Prüfer der Dissertation: 1. Prof. Dr. Michael J. Atkinson

2. Prof. Dr. Gabriele Multhoff

Die Dissertation wurde am 15.01.2019 bei der Technischen Universität München eingereicht und durch die Fakultät für Medizin am 17.04.2019 angenommen.

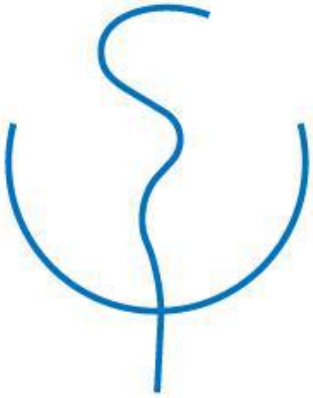

Doctoral thesis

TECHNISCHE UNIVERSITÄT MÜNCHEN

Faculty of Medicine

Chair of Radiation Biology

The role of Peroxisome Proliferator-Activated Receptor α in radiation-induced cardiovascular disease

Vikram Subramanian

Dedicated

to

My Parents and Teachers

Summary

Exposure to Ionizing radiation is an inevitable part of human existence. Although life on earth evolved in an environment with a considerable amount of ionizing radiation, excessive exposure to ionizing radiation results in a range of cancerous and non-cancerous diseases. Recent clinical and experimental models have shown that radiation-induced cardiovascular diseases belong to the spectrum of radiation-induced non-cancer effects. Epidemiological studies of atomic bomb survivors, radiotherapy patients, and nuclear workers all show an increased risk of developing a cardiovascular disease that is dependent upon the dose of ionizing radiation. Previous work using mouse models has established that an acute dose of ionizing radiation applied to the heart disturbs energy metabolism, changes cardiac structure and function and activates an inflammatory response, as well as causing myofiber impairment and local fibrosis. The molecular mechanisms behind these long-term radiation-induced damages have not yet been investigated.

The work presented in this thesis was carried out to identify the molecular targets of ionizing radiation in the heart. In particular, the roles of Peroxisome Proliferator-Activated Receptor Alpha (PPARα) and Transforming Growth Factor Beta (TGFβ), as well as their possible crosstalk in the radiation response of the heart, have been examined using a mouse and human heart samples. Quantitative proteomics and global transcriptomics techniques were used to identify radiation-induced changes in the heart. Bioinformatics tools were then used to analyze the omics data, and the results were validated by immunoblotting, bioassays (protein carbonylation, ELISA), microRNA analysis, immunohistochemistry, and electron microscopy.

In the first publication, wild-type (C57BL/6J) male mice were irradiated with a single dose of 16 Gy X-rays, applied locally to heart with shielding. A sham-irradiated (0 Gy) group served as control. This study found changes in the heart proteome and transcriptome that persisted even 40 weeks after the radiation exposure. These implied an inhibition of PPARα activity and the activation of both TGFβ mediated SMAD-dependent and SMAD-independent signaling pathways in the irradiated heart. These results suggest the involvement of an intracellular Mitogen-Activated Protein Kinase (MAPK) cascade in the regulation of crosstalk between PPARα and TGFβ mediated pathways in the irradiated heart.

In the second publication, human heart samples from three categories of nuclear workers chronically exposed to gamma-irradiation (< 100 mGy, 100–500 mGy and > 500 mGy) were studied. A global quantitative proteomic analysis revealed the dose-dependent downregulation of mitochondrial and structural proteins in the radiation-exposed hearts. This was accompanied by a dose-dependent increase in the phosphorylation (inhibitory) of the PPARα protein. The resulting reduced transcriptional activity of PPARα was consistent with the observed metabolic imbalance and suggests the increased risk of ischemic heart disease in the higher exposure groups, through modulation of structural, mitochondrial and antioxidant proteins in the irradiated heart.

In the third publication, the effect of irradiation on genetically modified male C57BL/6J mice deficient for PPARα was studied. Wild-type, PPARα heterozygous mutant, and PPARα -/- homozygous mutant animals received local heart X-irradiation (8 Gy and 16 Gy) at the age of 8 weeks. A sham-irradiated (0 Gy) Wild-type, PPARα +/- heterozygous mutant, and PPARα -/- homozygous mutant group served as control. Based on our proteomic analysis, the PPARα heterozygous mutant mice showed a far higher level of radiation-induced changes in the heart proteome than either the PPARα -/- homozygous mutant or wild-type group at both doses. The TGFβ mediated SMAD-dependent pathway was activated independently of PPARα status. Conversely, our study showed that the presence of functional PPARα was essential for radiation to induce TGFβ mediated SMAD-independent pathway. Inhibition of PPARα activity due to increased phosphorylation were also observed in wild-type and PPARα +/- heterozygous groups.

The results of these three publications provide experimental evidence for an essential role for the PPARα and TGFβ proteins in the radiation response of cardiovascular tissues. This observation may open up new therapeutic intervention to reduce radiation-induced late side effects in patients. The targeting of PPARα or TGFβ proteins by using appropriate drugs would be especially valuable in patients undergoing radiation therapy where the heart would be unavoidably exposed.

Zusammenfassung

Die Exposition durch ionisierende Strahlung ist ein unvermeidlicher Teil der menschlichen Existenz. Obwohl sich das Leben auf der Erde in einer hoch durch ionisierende Strahlung belasteten Umwelt entwickelte, führt eine übermäßige Exposition zu Krebs und weiteren Erkrankungen. Aktuelle klinische und experimentelle Studien haben gezeigt, dass strahlungsinduzierte kardiovaskuläre Herz-Kreislauf-Erkrankungen zu den nicht-karzinogenen strahlungsinduzierten Krankheiten gehören. Epidemiologische Studien mit Atombombenüberlebenden, Strahlentherapiepatienten und Beschäftigten an kerntechnischen Anlagen zeigen alle ein erhöhtes Risiko für die Entwicklung einer kardiovaskulären Herz-Kreislauf-Erkrankung, welches von der Strahlendosis abhängig ist. Frühere Arbeiten am Mausmodell ergaben, dass eine akute Exposition des Herzens durch ionisierender Strahlung den Energiestoffwechsel stört, die Struktur und Funktion des Herzens verändert und eine Entzündungsreaktion hervorruft sowie die Muskelfibrillen schädigt und lokale Fibrosen verursacht. Die molekularen Mechanismen hinter diesen langfristigen strahlungsinduzierten Schäden wurden noch nicht erforscht.

Ziel dieser Dissertation ist die Identifikation der molekularen Targets der ionisierenden Strahlung am Herzen. Insbesondere wurde die Rolle des Peroxisom-Proliferator-aktivierten Rezeptors Alpha (PPARα) und des transformierenden Wachstumsfaktors Beta (Transforming growth factor beta–TGFβ) sowie deren mögliche gegenseitige Beeinflussung in der Strahlenantwort des Herzens unter Verwendung von Herzproben von Mäusen und Menschen untersucht. Quantitative Proteomik- und globale Transkriptomik-Techniken wurden verwendet, um strahlungsinduzierte Veränderungen im Herzen zu identifizieren. Die „Omics“-Daten wurden dann mit Hilfe verschiedener Bioinformatik-Tools analysiert und die Ergebnisse wurden durch Immunblotting, Bioassays (Proteincarbonylierung, ELISA), microRNA-Analyse, Immunhistochemie und Elektronenmikroskopie validiert.

In der ersten Veröffentlichung wurden männliche Mäuse vom Wildtyp C57BL/6J mit einer einzigen Dosis Röntgenstrahlen in Höhe von 16 Gy lokal am Herzen bestrahlt. Eine schein-bestrahlte Gruppe (0 Gy) diente als Kontrolle. In dieser Studie fanden sich selbst 40 Wochen nach der Strahlenexposition Veränderungen am Herzproteom und transkriptom. Dies deutete auf eine Hemmung der PPARα-Aktivität und die Aktivierung von sowohl SMAD-abhängigen

als auch SMAD-unabhängigen TGFβ -Signalwegen im bestrahlten Herzen hin. Diese Ergebnisse lassen auf die Beteiligung einer intrazellulären MAP-Kinase (MAPK)-Signalkaskade in der Regulierung der Interaktion zwischen PPARα und TGFβ -vermittelten Signalwegen schließen.

In der zweiten Veröffentlichung wurden humane Herzproben von Beschäftigten an kerntechnischen Anlagen untersucht, die in drei Kategorien untereilt wurden, je nach Höhe ihrer chronischen Gammastrahlungsbelastung (< 100 mGy, 100 - 500 mGy und > 500 mGy). Eine globale quantitative Proteomanalyse zeigte ein dosisabhängiges Herunterregulieren der mitochondrialen und Strukturproteine im strahlenexponierten Herzen. Dies wurde von einer dosisabhängigen Erhöhung der (inhibitorischen) Phosphorylierung des PPARα-Proteins begleitet. Die daraus resultierende reduzierte Transkriptionsaktivität von PPARα stimmt mit dem beobachteten metabolischen Ungleichgewicht überein und deutet darauf hin, dass das erhöhte Risiko in den Gruppen, die einer höheren Strahlenexposition ausgesetzt waren, an einer ischämischen Herzerkrankung zu erkranken, durch die Modulation von strukturellen, mitochondrialen und antioxidativen Proteinen im bestrahlten Herzen entsteht.

In der dritten Veröffentlichung wurde die Wirkung von Strahlung auf genetisch modifizierte männliche Mäuse des Typs C57BL / 6J mit PPARα-Mangel untersucht. Wildtyp-Mäuse, PPARα +/- heterozygote Mutanten und PPARα -/- homozygot-mutierte Tiere wurden im Alter von 8 Wochen mit Röntgenstrahlen lokal am Herzen bestrahlt (8 Gy und 16 Gy). Eine schein-bestrahlte Wildtyp-Mäuse, PPARα +/- heterozygote Mutanten und PPARα -/- homozygot-mutierte Gruppe (0 Gy) diente als Kontrolle. Die Proteomanalyse zeigte, dass die Gruppe der heterozygoten PPARα-Mutanten bei beiden Dosen ein weitaus höheres Maß an strahlungsinduzierten Veränderungen im Herzen zeigte, als sowohl die homozygoten PPARα-Mutanten als auch die Wildtyp-Gruppe. Der TGFβ vermittelte SMAD-abhängige Signalweg wurde unabhängig vom PPARα-Status aktiviert. Unerwarteterweise zeigte unsere Studie, dass das Vorkommen von funktionellen PPARα wesentlich dafür war, dass die SMAD-unabhängigen TGFβ Signalwege durch die ionisierende Strahlung aktiviert wurden. Eine Hemmung der PPARα-Aktivität aufgrund einer erhöhten Phosphorylierungsrate wurde auch in der Wildtyp und PPARα +/- heterozygoten Gruppen beobachtet.

Die Ergebnisse aus diesen drei Veröffentlichungen weisen experimentell die wichtige Rolle der PPARα und TGFβ Proteine bei der Strahlenantwort des kardiovaskulären Gewebes nach. Diese Beobachtungen können neue therapeutische Wege aufzeigen, um strahleninduzierte Nebenwirkungen beim Patienten zu mindern. Mit geeigneten Medikamente bei den PPARα oder TGFβ Proteinen anzusetzen, wäre insbesondere für Patienten von Vorteil, die sich einer Behandlung unterziehen müssen, bei der es unvermeidlich zu einer Exposition des Herzens kommt.

Table of contents

Chapter 1: Introduction

Ionizing radiation is known to be an underlying factor for cardiovascular disease (CVD) in occupational, accidental or medical exposure situation [1-4]. The symptoms associated with radiation-induced cardiovascular disease appears late, decades after the ionizing radiation exposure and includes damages to pericardium, myocardium, increased inflammatory infiltrations and myocardial fibrosis [5-6]. Therefore, studies are needed to identify the different biological mechanism that contributes to radiation-induced cardiovascular disease and the risk of radiation to the heart. It is particularly relevant to identify the key proteins and signaling pathways that mediate the radiation response in the heart.

This publication-based thesis investigates the role of Peroxisome Proliferation Activated Receptor Alpha (PPARα) and Transforming Growth Factor Beta (TGFβ) in the development of radiation-induced cardiovascular disease after exposure to ionizing radiation. The first publication (Chapter 2.1) provides evidence for long-term alterations in the cardiac transcriptome and proteome due to acute local irradiation. This study identifies PPARα and TGFβ mediated signaling pathways in a mouse model of radiation-induced heart pathology. Publication two (Chapter 2.2) expands on the contribution of PPARα in the development of ischemic heart disease in the human heart when exposed to chronic external radiation. Publication three (Chapter 2.3) establishes the leading role of PPARα in the metabolic and inflammatory response of the heart to irradiation, particularly the activation of the TGFβ mediated SMAD-dependent and SMAD-independent signaling pathway in the heart after irradiation.

1.1 Concepts in Ionizing radiation

1.1.1 Ionizing radiation

In general, the term radiation refers to the physical process through which energy is released in the form of electromagnetic waves or particles into medium or space. Ionizing radiation occurs in the form of electromagnetic waves (photons), charged and uncharged sub-atomic particles (protons, neutrons) and accelerated atomic nuclei (e.g., Helium and Iron). These all characterized by their ability to transfer energy to adjacent atoms, thereby removing electrons from these atoms to create free radicles and ionized molecules. The biological

importance of ionizing radiation became apparent soon after the discovery of X-rays. Radiation poses a potential health hazard because of the damage caused to biologically relevant macromolecules such as DNA, lipids, and proteins from direct energy disposition and indirect radicle action.

1.1.2 Ionizing radiation-induced tissue damage

The radiation-induced biological damage per unit of absorbed dose varies with the type of radiation (radiation quality) or the type of tissue exposed [7]. Absorbed dose is defined as the energy deposited in a given mass of material and represented by the SI unit Gray (Gy) (1Gy = 1 J/kg). Equivalent dose is created by multiplying the absorbed dose by a radiation weighting factor that reflects the different levels of damage caused by various forms of ionizing radiation (e.g., photons and alpha particles) in biological systems. The equivalent dose is given as a Unit called Sievert (Sv) [8].

The harmful effects to tissue caused by ionizing radiation can be classified into two forms. Deterministic effects that occur as a result of immediate cell damage. Here the severity of the damage is directly dependent upon the absorbed radiation dose, and there is a threshold dose below which no damage occurs. In contrast, stochastic effects are delayed effects that result from damage that is not directly correlated to absorbed radiation dose. The probability of stochastic effects increases with radiation doses, but there is no dose below which the probability of effects can be excluded. Radiation-induced damage such as cataracts and skin burns are deterministic effects, while development of cancer and genetic abnormalities are stochastic effects [9]. It was believed that cardiovascular disease (CVD) induced by radiation was deterministic in nature on the basis of an apparent threshold for acute induced damage [6, 10]. This statement has been challenged by many recent epidemiological studies of atomic bomb survivors [4] and breast cancer patients who received radiation therapy [11]. Increased radiation doses to the heart were associated with an increased incidence of long-term cardiovascular side effects. The chance of developing cardiovascular disease increased with increased radiation dose to the heart, which subsequently leads to structural and functional dysfunction of coronary arteries, valves, myocardium and pericardium [2]. The mechanism responsible for the stochastic effect of radiation is held to be initial DNA damage during exposure, followed by misrepair leading to mutation, which is in turn followed by clonal

expansion of a cell bearing a relevant mutation. These processes are not observed in cardiovascular disease, so more studies are required to identify the molecular mechanisms behind the development of radiation-induced cardiovascular disease and the risk of radiation to the heart.

1.2 Epidemiology of radiation-induced cardiac damage

1.2.1 Therapeutic exposure

Radiation therapy (RT) is used to treat the most solid cancers. During radiotherapy treatment for breast cancer, patients may receive a cumulative radiation dose as high as 50-60 Gy, applied in a fractionated, usually at a daily dose of around 2Gy per fraction [12-13]. It has been estimated that under these circumstances the heart receives an average local dose of around 1.3 Gy to 1.7 Gy in right side breast cancer patients and 3.7 Gy to a maximum 20 Gy in left side breast cancer patients [6, 14-15]. Increased numbers of deaths were reported due to cardiovascular disease complications in patients receiving radiotherapy treatment for left side cancer than right side cancer treatment [16-17], suggesting the risk of cardiovascular disease associated with the direct heart exposure. Epidemiological data showed an increased risk of developing cardiovascular disease and cardiac mortality over a radiation dose to the heart over a range from below 2 Gy up to 16 Gy [1-2, 18-19]. Effects of radiation include damage to the pericardium, and myocardium, myocardial fibrosis, cardiomyopathy, coronary artery disease, valvular disease and arrhythmias [11, 20-23]. More recent studies where radiation therapy planning is adapted to minimize exposure to the heart to show that there is no longer a difference in death due to cardiovascular disease between left and right sided breast cancer patients [24-25].

1.2.2 Accidental and occupational exposure

An increase in the risk to human health after workplace exposure to ionizing radiation has been described. In an early 20th century, medical staff who used diagnostic and therapeutic radiation in their professional work were exposed to significant cumulative radiation doses. The study from Hauptmann et al. showed an increased incidence risk of developing ischemic heart disease among radiography technologists with a radiation dose greater than 0.3 Sv [26]. An epidemiological study of a uranium mine worker in Germany recorded an excess number

of deaths due to circulatory diseases in radiation-exposed workers [27]. A cohort study with miners exposed to radon and uranium has provided evidence for increased mortality from coronary heart disease in exposed workers compared to non-exposed workers [28-29]. A higher risk of death due to CVD was also found in Mayak plutonium enrichment plant workers exposed to external gamma irradiation [30]. Here the study by Azizova et al. found that a radiation dose equal to or higher than 1 Gy elevated the risk of ischemic heart disease when the radiation-exposed workers were compared to non-exposed workers [31], shows the risk of ischemic heart disease after accidental exposure to radiation. Exposure to radiation and its long-term damaging effect on the heart has also been studied in Japanese atomic bomb survivors. Mortality from myocardial infarction was significantly increased in exposed people 40 years after they received a single acute dose of 1-2 Gy [32].

1.3 Experimental evidence

1.3.1 *In-vivo* experiments

The clinical effects of high dose radiation in patients are complicated due to a range of confounding cardiovascular risk factors arising from the underlying disease and its treatment. So, it is necessary to have animal models to study the radiation-induced damage to the heart in which both radiation dose and the confounding risk factors can be controlled. Evidence for radiation-induced damage to the heart was provided in the late 1960s by Fajardo and Stewart who performed experimental studies on radiation-induced heart disease in the rabbit. They showed the development of pericarditis after a single dose of 16-20 Gy [33]. Radiation-induced pericarditis, accompanied by oedematous swelling, fibrotic thickening, focal myocardial damage with loss of endothelial enzymes, was also observed in rats after 4 months exposed to doses of over 10 Gy [34]. Boerma et al. showed increased expression of von Willebrand factor (vWf) in a dose and time-dependent manner in capillaries and arteries of rat heart exposed to doses of 15 Gy and 20 Gy compared to control groups [35]. This study suggests that the increased expression of vWf reflects the induction of fibrosis in the rat myocardium. Another study from Boerma et al. showed increased left ventricle posterior wall thickness and decreased left ventricle diastolic area after exposure of the hearts of rats genetically modified to be deficient for mast cells to a local 18 Gy dose [36]. A functional study from Seemann et al. observed a significant decrease in systolic and diastolic function with increased ejection

fractions in male C57BL/6J mice at 16 Gy irradiation after 40 weeks of irradiation, in this same study irradiation provoked epicardial thickness after 20 weeks and 40 weeks of post-irradiation [37], these both study shows the influence of radiation in systolic and diastolic properties in the heart.

Recent developments in biological techniques have enabled to study the damaging effects of ionizing radiation in the heart at the molecular and structural level using animal models. The biological effects of local radiation doses of 8 Gy, 16 Gy on the murine heart were studied using quantitative proteomics technology and gene expression array analysis. This study indicated most of the proteins involved in cardiac lipid metabolism and mitochondrial oxidative phosphorylation were significantly altered after irradiation. In the same study, the activity of PPARα was reduced due to increased phosphorylation (inhibitory) in the 16 Gy exposed group compared to controls [38]. A gene expression study disclosed reduced expression of PPARα target genes involved in cardiac energy metabolism and mitochondrial respiratory function, shows an impaired PPARα activity in the radiation-exposed heart. Electron microscopy analysis revealed myofibrillar alteration, focal and diffused lesion in mitochondria and decreased number of mitochondria were observed in the irradiated group at 16 Gy dose compared to controls [38]. This study concludes, impairment in PPARα activity significantly contributes to heart pathology after irradiation.

In mice, radiation-induced changes in the protein expression after 5 h and 24 h exposure to 3 Gy total body radiation were studied using isotope-coded proteomic labeling and 2D-DIGE techniques. Pathway analysis with both data sets has shown differentially expressed proteins to be involved in radiation-induced biological responses including inflammation, reorganization of structural proteins, and antioxidant defense mechanism [39]. Recently radiation-induced proteomic changes were studied in human coronary artery endothelial cells irradiated with 0.5 Gy using ICPL quantitative proteomics technique. The analysis found inhibition of Rho-GDP dissociation inhibitor (RhoGDI) and nitric oxide signaling pathways in irradiated groups [40]. This data suggests that observed molecular changes are indicative of endothelial dysfunction and supports the risk of cardiovascular disease at a 0.5 Gy dose.

1.3.2 *In-vitro* experiments

Radiation-induced modifications to the cardiovasculature have been studied using *in-vitro* cell culture models. Most of these studies have been performed using endothelial cells. Human pulmonary artery endothelial cells irradiated at 10 Gy triggered intrinsic and extrinsic apoptosis pathways with increased activation of caspases 3, 8, 9 in irradiated endothelial cells [41], this observation adds more information on the role of ionizing radiation in apoptotic pathways. Bovine pulmonary artery endothelial (BPAE) cells exposed to a single dose of 10 Gy of Cs γ rays resulted in higher endothelial permeability 3h post-irradiation, accompanied by perturbation in F-actin distribution compared to non-irradiated cells [42], suggests damaging effect of ionizing radiation in the organization of actin filaments and its influence on permeability properties of endothelial cells . Studies have shown increased production of endogenous ROS in the irradiated cells. Human U937 lymphoma cells irradiated to acute γ-irradiation (7Gy) resulted in increased ROS level and decreased mitochondrial transmembrane potential 12 h after radiation exposure compared to non-irradiated cells [43], indicates an increased risk of ROS generation and mitochondrial damage due to radiation exposure.

In a study using mice cardiac microvascular endothelial cells irradiated with 8 Gy have shown high-frequency senescence-like phenotype associated with reduced expression of genes involved in cell cycle progression and DNA replication process [44]. Another study with Human umbilical endothelial cells (HUVEC) that were subjected to chronic low dose (2.4 mGy/h and 4.1 mGy/h) radiation resulted in premature endothelial senescence through inactivation of PI3K/Akt/mTOR signaling pathway and activation of p53/p21 signaling pathway compared to non irradiated cells [45-46], both study indicates harmful effect of ionizing radiation in the induction of premature senescence in endothelial cells. Only limited experimental data are available concerning the effect of ionizing radiation on cardiomyocyte cell population. A major drawback of *in vitro* cardiomyocyte studies is the low survival rate of cardiomyocytes in the extended cell culture environment [47-48]. This makes it challenging to evaluate any direct effect of ionizing radiation on the cardiomyocyte population. A study by Friess et al. determined that primary chicken cardiomyocyte cells, irradiated at 7 Gy, revealed changes in electrophysiological properties and increased reactive oxygen species, apoptosis one-week

after irradiation [49], this suggests a detrimental effect of ionizing radiation on cardiomyocyte cell population by increasing ROS and apoptosis pathways.

1.4 Peroxisome proliferator-activated receptors (PPAR)

1.4.1 Tissue distribution of PPAR subtypes

The PPAR family of peroxisome proliferator-activated receptors is made up of three different proteins PPARα, PPARγ and PPARβ, [50]. All three PPARs belong to type II nuclear receptor family due to the presence of cysteine-rich Zinc finger DNA binding domain [51-52]. Although the three PPARs are encoded by separate genes, they share a high degree of homology in their protein structure [53-54]. They also exhibit some overlap in their tissue distribution and biological function (Table 1) [55-57]. The expression of all PPAR subtypes is higher in tissues actively involved in lipid metabolism. Thus, PPARα is a hallmark inducer of fatty acid oxidation, and its expression is higher in organs with mitochondrial and peroxisomal beta-oxidation, such as heart, liver, kidney, skeletal muscle and brown adipose tissue, where it involved in the maintenance of fatty acid homeostasis [58-60]. PPARα is also expressed in other tissues, including the adrenal gland, macrophages, smooth muscle cells, and endothelial cells [61-62]. PPARβ is expressed predominantly in kidney, adipose tissue, liver, heart, and skeletal muscle [63-64]. The principal function of PPARβ is to increase lipid catabolism in heart, adipose tissue, and skeletal muscle [65-67]. PPARβ activation can induce proliferation and differentiation [68]. The expression of PPARγ is found to be highest in adipocytes and macrophages, but it is also expressed at low levels in the vascular wall (smooth muscle cells) and skeletal muscle [69-70]. PPARγ functions as a regulator of lipid storage and plays a role in adipose tissue formation, glucose uptake, triglyceride synthesis, and storage [71-72].

PPARs	Tissue distribution	Functions
PPARα	Liver, brown adipose tissue, skeletal muscle, heart and kidney	Peroxisome proliferation (only rodents), control of lipid metabolism and inflammation, skin wound healing
PPARγ	Adipose tissue, macrophages, colon, spleen, retina, heart, skeletal muscle and vascular wall	Lipid anabolism (storage), adipocyte differentiation, inflammation control and macrophage maturation
PPARβ/δ	Kidney, adipose tissue, liver, heart, skeletal muscle and intestines	Reverse cholesterol transport, cell proliferation, apoptosis, adipocyte differentiation and skin wound healing

Table 1: Tissue distribution and functions of PPARs [73].

1.4.2 Structure and function of PPARα receptor

The peroxisome-proliferator activator receptor alpha (PPARα) is made up of multiple domains. These are the A/B domain (N-terminal region, C domain (DNA binding domain), D domain (hinge region), and the E/F domain (C-terminal region). The receptor function requires the interaction of these domains with additional proteins [74]. The A/B domain is responsible for the constitutive transcriptional activity of PPARα responsive genes during the absence of ligands [75]. The A/B domain includes the AF-1 region that performs a ligand-dependent and independent functions. These functions are modified by proteins belonging to the MAPK family [76]. The C domain contains a DNA binding domain that is made up of two zinc finger motifs that recognize PPAR response element present in the promoter region of each target gene [77]. This domain is also involved in heterodimerization of PPARα with another receptor such as retinoid X receptors (RXRs), which is essential for transcriptional activity, and co-activator binding activity [78]. The DNA binding C-domain of PPARα contains multiple phosphorylation sites that regulate its transcriptional activity [79-80]. The D domain comprises a hinge region connected the DNA binding C-domain to the ligand binding E/F domain of the receptor and is shown to act as a binding site for multiple coactivators [81-82]. Studies have shown that the hinge region contains the nuclear localization signal [83]. The E/F domain holds the ligand-binding domain (LBD) [84]. The LBD of PPARα contains an AF2 (Activating function-2) helix involved in physical interaction with coregulatory proteins to initiate transcription of genes. Ligand binding domain of PPARα contains a binding pocket for ligands that is crucial to

make dimerization with RXR [84-85]. The ligand binding domain contains a Y-shaped hydrophobic pocket into which the appropriate ligands can bind to activate or repress transactivation of the receptor [86]. The ligand binding at AF-2 region induces conformational changes which lead to accumulation of various coactivator proteins, e.g., CBP/p300 and SRC-1 on the surface of the LBD [87]. Ligand-bound PPARα associate with RXR to form heterodimer complex and binds to PPAR response elements made up of variably spaced hexameric half-sites (AGGTCA) either as direct, indirect or inverted repeats. Once bound to the PPAR response element the activated receptor complex leads to the recruitment of coactivator proteins, RNA polymerase II recruiting complexes and removal of corepressor proteins to start transcription of target genes [88]. The transcriptional activity of PPARα is increased by ligands that include saturated, monounsaturated, and polyunsaturated fatty acids, as well as their metabolites [89-90]. The activation of PPARα may be evoked by synthetic PPAR agonists and hypolipidemic drugs [89, 91].

1.4.3 Biology of PPARα protein in the heart

The healthy adult heart consumes more energy than any other organ of the body. This is achieved in part by metabolizing fatty acids to produce ATP as an energy source [92]. However, to adapt to physiological and pathological changes, the heart can switch substrate consumption between lipid and glucose catabolism [93]. These metabolic shifts are controlled and regulated by PPAR-mediated transcriptional regulation of enzymes involved in lipid and glucose metabolic pathways [94]. The role of PPARα in the heart is to modulate the energy supply to the myocardium through transcriptional regulation of genes encoding enzymes of mitochondrial fatty acid beta-oxidation pathway, uptake, and transport (Figure 1) [95]. A study with cultured neonatal cardiomyocytes showed the direct influence of fatty acids and PPARα agonist in the induction of PPARα dependent target genes involved in fatty acid uptake and fatty acid oxidation in the heart (Fig 1) [96-97].

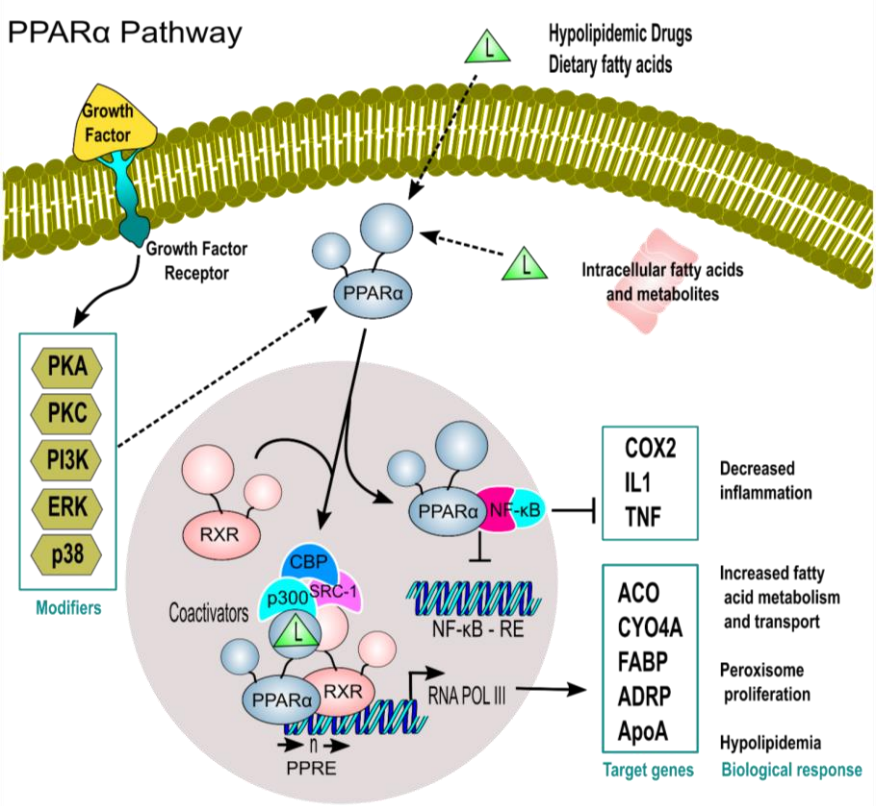

Figure 1: The role of PPARα in the cardiac system. PPARα is activated by binding of ligands including fatty acids and hypolipidemic drugs. PPARα activates transcription of target genes involved in fatty acid metabolism and transport and peroxisome proliferation. PPARα also involved in the regulation of inflammatory mechanism through the interaction of NF-kβ. PPAR alpha pathway drawing courtesy of Jack Vanden Hevel, Ph.D., nrresource.org.

Studies of cultured cardiomyocytes with adenoviral-mediated PPARα expression or treatment with PPARα activators increased the expression of PPARα target genes involved in fatty acid catabolic pathways [98-100]. In a human study, PPARα agonist fenofibrate increased the level of plasma HDL-cholesterol, while decreasing plasma level of Triglycerides, free fatty acids, and apolipoprotein C III. [101-103]. The expression of a PPARα target protein, myocardial uncoupling protein 3, was increased in rats treated with a high-fat diet and was decreased when animals were fed a low-fat diet [104]. Another PPARα receptor agonist, GW7647, resulted in improved fatty acid oxidation and reduced triglycerides in cultured human myotubes. [105-106]. Studies also have shown that PPARα plays an essential role in the regulation of heart inflammation, extracellular matrix remodeling, and oxidative stress [107].

An increased level of circulating cytokines and increased local production of profibrotic factors such as transforming growth factor beta (TGFβ) was observed due to inhibition of PPARα in Sprague Dawley rats [108], shows the importance of PPARα in the regulation of inflammation. PPARα achieves its anti-inflammatory effects through the inhibition of c-JUN and activator protein 1 (AP-1), downstream targets of TGFβ mediated SMAD-independent signaling pathway, in a mechanism called transrepression [107, 109-110]. The activation of PPARα resulted in diminished production of proteins such as endothelin-1, vascular cell adhesion molecule (VCAM)-1, and interleukin (IL)-6 [111-113], this provides support for the action of PPARα in the regulation of inflammation response in vascular cells. PPARα also exerts its inflammatory control actions indirectly through inhibition of NF-κβ activity [114-115].

1.4.4 The control of PPARα activity by phosphorylation

The first evidence on the regulatory role of PPARα phosphorylation came from the study of Shalev et al. Primary rat adipocytes were treated with insulin resulting in the increased phosphorylation of the PPARα protein at Ser 12 and 21 [116]. Studies have shown the ERK, and p38 protein kinases are responsible for PPARα phosphorylation thereby reducing its functions in the heart [83]. In rat cardiomyocytes activated ERK1/2 resulted in increased phosphorylation of PPARα at Ser 12 and 21, that leads to decreased expression of genes involved in fatty acid oxidation and transport due to impairment in the activity of PPARα protein [117], indicates the involvement of MAPK signaling pathway in the regulation of PPARα activity.

1.5. The significance of PPARα in cardiac health and disease

1.5.1 Biology of PPARα -/- null mice

PPARα -/- knockout mice were used to study the biological functions of PPARα in the myocardium [118-121]. A study with PPARα -/- null mice revealed that the constitutive expression levels of two membrane fatty acid transporters and seven mitochondrial fatty acid metabolizing proteins depend on the presence of PPARα [119], shows the importance of PPARα in the regulation of cardiac lipid metabolism. PPARα -/- null mice have an average lifespan, but they developed accelerated symptoms of cardiac toxicity, including cardiac fibrosis, abnormal mitochondrial structure, and myofibrillar fragmentation as they aged [119], suggests the role of PPARα in the prevention of such cardiac damage in aged mice. When PPARα -/-

null mice fasted for a long time, they developed hypoglycemia, hypothermia, hypoketonemia, and increased plasma free fatty acid levels compared to PPARα wild-type mice [122]. Histological analysis of hearts from PPARα -/- null mice revealed changes indicative of cardiomyocyte hypertrophy under chronic pressure overload [123]. Moreover PPARα -/- null mice showed impairment in contractile function accompanied by changes in the expression of contractile proteins, as well as increased lipid peroxidation that may contribute to the observed cardiac dysfunction [124], this may be due to a reduced rate of fatty acid oxidation that consequently leads to decreased energy production. There is an evidence that shows the presence of PPARα is necessary to stop oxidative damage that happens during normal physiological cellular metabolism or under the conditions of oxidative stress and inflammation, mainly through repressing the activity of NF-κβ, thereby reducing the production of inflammatory proteins [125], suggests that impairment of PPARα signaling pathway disturbs normal equilibrium between antioxidant defenses and oxidant production, which leads to cardiac damage.

1.5.2 Biology of PPARα +/+ overexpressing mice

The biology of PPARα +/+ overexpression in cardiac tissue was studied using transgenic mice that constitutively express PPARα in the left ventricle of heart under the control of cardiac alpha-myosin heavy chain gene promoter (MHC-PPAR). In this study mouse overexpressing PPARα resulted in increased fatty acid oxidation and uptake as well as reduced glucose uptake and oxidation, this may be due to changes in cellular lipid metabolism activated by PPARα in the heart. This study also showed the development of cardiac hypertrophy and ventricular dysfunction together with induction of hypertrophic gene markers in PPARα overexpressing mice [126], suggests that PPARα overexpression may contribute in the development of cardiac dysfunction. In another study, Finck et al. showed an increased cardiac fatty acid transport, and oxidation and reduced expression of genes involved in glucose metabolism detected in PPARα overexpressing heart [127]. Mice overexpressing PPARα exhibited increased myocardial lipid accumulation that resulted in the death of myocytes and contractile dysfunction [128], suggest the importance of PPARα regulation to have a normal biological response in the heart.

1.6 Transforming growth factor β (TGFβ)

1.6.1 Synthesis, structure and tissue distribution of TGFβ

TGFβ is a member of a superfamily of growth factors, and in mammals, TGFβ present in three different isoforms, namely TGFβ1, TGFβ2 and TGFβ3 with overlapping functions [129-130]. The isoforms are encoded by separate genes [131]. They act on target cells by binding to transmembrane cell surface receptors that induce a signal cascade that ultimately promote the expression of target genes [132]. TGFβ is secreted by several cell types, including endothelial cells, myofibroblasts, vascular smooth muscle cells (VSMCs), and macrophages [132-135]. The higher expression levels of TGFβ in the heart of mouse observed during embryonic development and adult life [136]. The three isoforms of TGFβ are synthesized as precursor proteins of 390-412 amino acids that undergo multiple processing events. Initially, the endopeptidase furin cleaves the TGFβ precursor protein between amino acids 278 and 279 [137] to generate two proteins; the N-terminal derived latency-associated peptide (LAP) and the C-terminal mature TGFβ. LAP binds non-covalently to the mature TGFβ [138]. The proteolytic cleavage of LAP by matrix metalloproteins (MMP) 2 and 9 induces destabilization of LAP-TGFβ interactions, that leads to release of active TGFβ form from its latent complex, from the extracellular matrix [139-140].

1.7 TGFβ mediated signaling pathways

1.7.1 SMAD-dependent pathway

SMAD (Single Mothers Against Decapentaplegic) proteins identified as a facilitator of intracellular signaling of TGFβ superfamily [141]. It mediates two main intracellular signaling pathways: TGFβ and bone morphogenetic protein (BMP) signaling pathways [141]. TGFβ initiates intracellular signaling by binding to transmembrane serine and threonine kinase TGFβ receptors, the type 1 (TβR-I) or type 2 (TβR-II) receptors on the cell membrane [142]. In the absence of TGFβ ligand, TβR-I and TβR-II receptors are present as inactive homodimers [143]. Upon binding of TGFβ to receptors leads to the formation of the receptor heterocomplex, in which TβR-II receptor phosphorylates serine and threonine residues reside in the TTSGSGSG motif of the TβR-I receptor, thus leads to activation of the TβR-I receptor. The activated TβR-I subsequently able to induce intracellular signaling through interaction with proteins belong

to both SMAD-dependent and SMAD-independent pathways [144]. Signaling to the nucleus from the activated TβR-I receptor is mediated by three classes of SMAD proteins, the receptor-mediated SMADs (SMAD 2 and 3), the co-SMAD (SMAD 4), and the inhibitory SMAD (SMAD 6 and 7) [145]. The activated TβR-I receptor induces phosphorylation on two serine residues in N-terminal region of receptor-mediated SMAD 2 and 3, which then form a complex with SMAD 4 in the cytoplasm. This transcriptionally active SMAD complex is translocated to the nucleus where it induces expression of TGFβ target genes (Figure 2) [144, 146]. Inhibitory SMADs, SMAD 6 and 7 are involved in counter-regulation of TGFβ signaling. The success of TGFβ signaling depends on the fine-tuned balance between R-SMAD and inhibitory SMAD 6/7 [147-148]. Studies have shown that TGFβ/SMAD signaling pathway may engage in regulation of many target genes includes Jun B [149], COL1A2 [150], SMAD 7 [151], C-Jun [149], plasminogen activated inhibitor 1 (PAI-1) [152], platelet-derived growth factor [153], integrin β5 [154] and connective tissue growth factor [155]. Furthermore, TGFβ/SMAD signaling regulates several genes belong to extracellular matrix (ECM), includes COL6A1, COL6A3, COL5A2, COL1A2, COL3A1, TIMP1 and other 60 ECM-related genes [156], these data shows the key role of SMAD signaling pathway in regulation and simultaneous activation of several fibrillar collagen genes and other ECM-related genes.

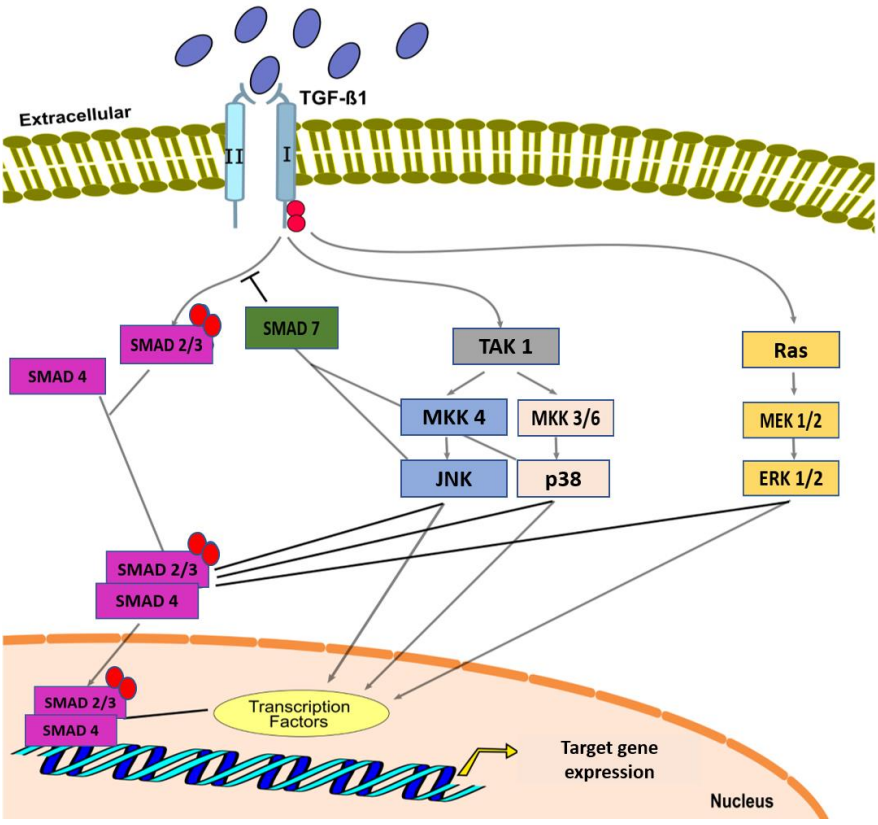

Figure 2: Activation of TGFβ mediated SMAD-dependent and SMAD-independent signaling pathways. In SMAD-dependent signaling process, activated TβR-I receptors phosphorylates SMAD 2 and 3. Then receptor-activated SMAD 2 and 3 form complexes with SMAD 4. Next, the activated SMAD complexes translocate into the nucleus and control transcription of target genes. In SMAD-independent signaling event, the activated TβR-I receptors phosphorylate and activate other signaling cascades through proteins such as TAK-1, p38, ERK, and JNK. Activation of both pathways is implicated in the pathology of cardiac system [157].

1.7.2 SMAD-independent pathway

TGFβ regulates its cellular functions not only through TGFβ/SMAD pathway but also through the SMAD-independent pathway. SMAD-independent pathways comprise of mitogen-activated protein kinases (MAPK), PI3 kinase/AKT and NF-κβ pathways, through which TGFβ mediate intracellular signaling to regulate cellular functions [158-159]. Studies have shown in various cell types that TGFβ activates extracellular regulated kinase (ERK), p38 MAPK and Jun N-terminal kinases (JNK) though SMAD-dependent and SMAD-independent transcriptional mechanisms [160-163]. The activation of ERK by TGFβ was observed in epithelial cells [164] and fibroblasts [165]. Initially, TβR-I is activated by TβR-II upon TGFβ binding and forms tetrameric receptor complex with TβR-II. The activated TβR-I promote the formation of ShcA/Grb2/Sos complex by directly phosphorylating ShcA on tyrosine and serine residues [166]. Then ShcA/Grb2/Sos complex activate Ras at the plasma membrane that leads to sequential activation of c-Raf, MEK and ERK [166], activated ERK is one of non-SMAD pathway necessary to regulate target genes involved in epithelial to mesenchymal transition (EMT) process. The SMAD-independent TGFβ/JNK/p38 pathway activated by binding of activated TβR-I to TNF receptor-associated factor 6 (TRAF 6) [167-168], leading to activation of TGFβ activated kinase 1 protein (TAK 1) [169] followed by the activation of c-Raf and MEK through the formation of a ShcA/Grb2/Sos complex at the plasma membrane. This is accompanied by phosphorylation of mitogen-activated protein kinase (MAPK) pathway members, including p38 and JNK [170-171], leading to activation of downstream JNK and p38 pathways. Studies have shown the TGFβ/TAK 1/JNK/p38 pathway is essential for activation of fibroblast [172], collagen synthesis [173] , cardiomyocyte apoptosis [174-175] and EMT process in fibroblasts [167].

1.7.3 Consequences of TGFβ signaling

The activation of SMAD signaling pathway was observed under a pathological condition with simultaneous increase of TGFβ in the heart [176-177]. Increased expression of genes related to extracellular matrix components was observed due to the activation of TGFβ/SMAD pathway [178], which potentially leads to fibrosis development in the heart. The activation of TGFβ/SMAD pathway have been reported in various type of heart diseases, including myocardial hypertrophy [179-180], myocardial infarction and transaortic construction (TAC) induced cardiac fibrosis [181], transformation of fibroblasts to myofibroblast to promote ECM deposition [130], these data indicate the role of TGFβ/SMAD signaling in the development of various pathological condition in the heart. Some studies indicate that TGFβ mediated SMAD-independent pathway plays a role in cellular homeostasis in the cardiac system. Involvement of MAPK kinase pathways in cardiac fibrosis has been well documented. A study using a mouse model of myocardial infraction exhibited increased phosphorylation of ERK1/2 and JNK that correlated with a degree of fibrosis [182], and other study using mouse model informed only increase in the phosphorylation of p38 and ERK1/2 proteins [183]. A study from Zhang et al. showed myocyte-specific overexpression of TAK1 leads to interstitial fibrosis and myocyte disorganization [184]. Overexpression of TGFβ leads to cardiac fibrosis through excessive myofibroblast differentiation [185-186], resulting in the production of extracellular matrix proteins, thus increasing ECM turnover. A recent study has also indicated the involvement of TGFβ/TAK 1/p38 MAPK pathway in the induction of hypertrophy in cardiomyocytes [187], indicating the role SMAD-independent signaling pathway in the progression of cardiomyocyte hypertrophy in the heart. Overexpression of TGFβ itself resulted in cardiac hypertrophy, interstitial fibrosis [188], dilated cardiomyopathy [189], myocardial hypertrophy, cardiomyopathy, and aortic stenosis [190-191]. Interestingly studies also have shown that the increased activation of TGFβ is also associated with radiation-induced tissue toxicity [192-193], shows the involvement of TGFβ in the initiation of radiation-induced tissue toxicity.

1.8 The role of PPARα and TGFβ in the tissue radiation response

A study by Azimzadeh et al. has provided key insight into the role of PPAR alpha-mediated mechanisms of radiation-induced damage to the heart using a mouse model. They describe radiation-induced impairment in control of both inflammation and cardiac lipid metabolism

due to a sustained increase in the inhibitory phosphorylation of PPARα that persisted even after 16 weeks of irradiation [38]. As noted above, such an inhibition of PPARα activity may itself lead to the development of cardiovascular disease [194]. A recent study from Seemann et al. found increased levels of active TGFβ1 in the heart remained at least for 40 weeks after 16 Gy exposure. They observed a progressive increase in endothelial dysfunction during this time. Despite these observations, the involvement of TGFβ and PPARα, and possible interactions between them, in radiation-induced cardiac disease remains unclear.

1.9 Working hypotheses

High dose irradiation induces acute deterministic damage to the heart (e.g., valvular damage, conductivity defects, fibrosis, and pericarditis). These arise primarily as a consequence of radiation-induced cell killing. At lower doses, where cell killing is minimal, there is epidemiological evidence to suggest that chronic CVD (e.g., perfusion defects, atherosclerosis, angina, and infarction) may develop months or years after exposure. Unlike the acute deterministic damage, there is no understanding of the mechanistic basis for the development of chronic heart diseases. Current models of chronic radiation effects (especially cancer) focus on gene mutation and clonal expansion. Clearly such a mechanism would not be involved in the genesis of cardiovascular disease. Therefore, the work included in this doctoral thesis was carried out to identify possible molecular targets of ionizing radiation and to discover the mechanisms behind radiation-induced cardiac damage.

This thesis is designed to challenge two hypotheses

1) That PPARα and TGFβ are both implicated in the development of long-term radiation-induced cardiac damage, and that their persistent inhibition and activation respectively underlie radiation-induced cardiac damage. This is addressed in publication 1 and 2.

2) That intervention in PPARα-mediated pathways (manipulation of the basal level of PPARα in the heart) will prevent the development of the CVD phenotype following exposure to radiation. This is addressed in publication 3.

The detailed information on the materials and methods used to address these hypotheses are included in the publications that form the basis for this thesis.

2.0 Strategy and methodology

2.0.1 Proteomics

The analysis of cardiac proteome can support the understanding of the biological process behind cardiovascular disease following radiation exposure. In turn, this understanding will permit more realistic extrapolation of epidemiological data, that will ultimately increase the accuracy of the assessment of risk. Unlike other techniques (transcriptomics and genomics), proteomics methods do not require amplification of the starting material and provide a direct read-out of phenotypic changes.

To study the effect of ionizing radiation on the heart, we have used label-free quantitative proteomics method for the studies included in this thesis. The workflow involved starts with sample preparation, followed by liquid chromatography coupled with tandem mass spectrometry (LC-MS/MS), and concludes with bioinformatic analysis. The work-flow for the analytical phase has been previously described in detail (Figure 3) [195-196].

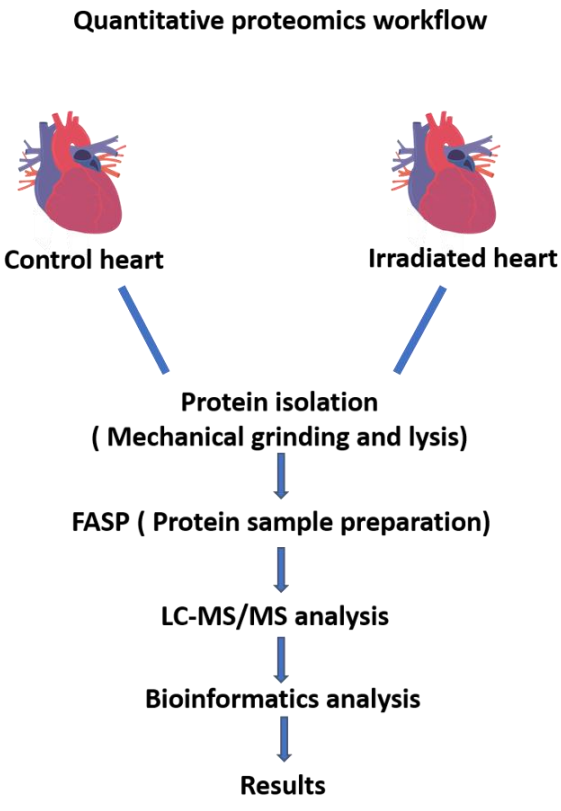

Figure 3: General workflow of comparative quantitative proteomics method. The crucial steps are heart tissue lysis, protein measurement, LC-MS/MS analysis and bioinformatics analysis of data.

Initially, heart samples from control and irradiated groups were lysed using tissue lysis buffer according to manufacturers instruction, and protein concentration was determined by using the Bradford assay. Later, protein lysates from each group were digested using modified filtered-aided sample preparation (FASP) protocol [197]. Before LC-MS/MS (Liquid chromatography-Mass spectrometry) analysis, the samples from control and irradiated groups were centrifuged, analyzed separately on mass spectrometry coupled to nano-HPLC as described previously [198-199]. The mass spectrometry is a sensitive and powerful technique used to detect, identify and quantitate molecules based on mass-to-charge (*m/z*) ratio. In the first step, protein samples are loaded into the mass spectrometer and allowed to vaporized and ionized by the ion source. In the second step, ionized molecules encounter in electric or magnetic fields from the mass analyzer; this deflects the routes of ionized molecules based on their *m/z*. In the end, successfully deflected ions from mass analyzer reach the detector and amplified for detection. The mass spectrometer is coupled together with computer-based software to measure ion frequencies, obtain mass spectra using image current detection method. In tandem mass spectrometry (MS/MS), during the first round of MS, distinct ions of interest in quadrupole filter based on their *m/z* and later fragmented by a number of dissociation methods. These fragmented ions are separated based on their individual *m/z* ratio in the second round of MS to generate mass spectra.

After mass analysis, the MS/MS spectra raw files of the individual measurements were loaded to the Progenesis QI software and analyzed as described previously [200-201]. The protein identification made by using the Mascot search engine (Matrix Science, version 2.5.0 or 2.5.1) in the Ensembl human or mouse protein database. Briefly, the summed normalized abundances of the unique peptides obtained for each protein were used for the calculation of abundance ratios and statistical analysis. The false discovery rate FDR (*q* value) calculation was used to adjust the *p*-values [202-203]. Proteins identified by more than one unique peptide and having a ratio of abundance between control and test samples greater than 1.30-fold or less than 0.77-fold ($q \leq 0.05$) were defined as being significantly differentially expressed [204-205].

2.0.2 Transcriptomics

Gene expression analysis was used to study steady-state mRNA content of irradiated tissues. The workflow involved in gene expression analysis includes RNA isolation, determination of RNA quality, amplification of RNA, hybridization of RNA to Illumina expression bead chips mouse whole genome, scanning and data analysis, was performed according to Seemann et al. [206]. For gene expression analysis, the Log2 ratio for expression of genes between control and the irradiated sample calculated according to previously published data [206]. The genes with expression ratio greater than 1.5-fold or less than 0.64-fold considered as significantly deregulated compared to control group.

2.0.3 Bioinformatics tools

Understanding of the molecular interactions is essential to elucidate the relevant biological function of any differentially expressed proteins or RNA species. Pathway analysis and predicted protein-protein interactions could both provide information on the biological relevance of any detected changes in abundance. These were studied at the protein and RNA levels using the bioinformatics software tools Ingenuity pathway analysis (IPA) (http://www.ingenuity.com/) and Search tool for the retrieval of interacting genes and proteins (STRING) (https://string-db.org/) [207]. IPA is a web-centered software application that allows analysis and understanding of complex data from microarray, proteomics, metabolomics experiments to identify the significance of data, thus enables to predict new targets (proteins or genes) or biomarkers within the setting of the biological system. STRING is a web-based biological database of predicted, and known protein-protein interactions help to identify structural, functional, evolutionary properties of expressed proteins or genes in biological analysis.

2.0.4 Supporting experiments

In this thesis, proteins and mRNA were isolated from irradiated and non-irradiated groups to study their effect on signaling pathway initiation as well as various endpoints. The expression levels of proteins belonging to the PPARα pathway, and TGFβ mediated SMAD-dependent (SMAD 4), and SMAD-independent pathways were analyzed in irradiated and non-irradiated heart samples using western blotting. The total and phosphorylation level of proteins related

to TGFβ mediated SMAD-dependent pathway such as SMAD 2, SMAD 3 were analyzed with enzyme-linked immunosorbent assay (ELISA) according to manufacturers instruction. Quantitative PCR was performed to analyze the expression of various microRNAs in irradiated and non-irradiated heart samples. Immunohistochemistry technique was used to study the severity of inflammation in irradiated and control heart samples. Briefly, all heart samples from irradiated and control groups were fixed in 4 % paraformaldehyde, embedded and processed according to previous publication [38]. Heart sections were quantified using IAS image processing software. In Transmission Electron Microscopy (TEM) study heart samples were fixed and processed according to previously published data [38]. Briefly, all the heart samples were post-fixed with 2 % osmium tetroxide, embedded and studied with the TEM. Electron micrographs with the same magnification from all groups were used to study the size and number of mitochondria in the heart. Protein carbonyl content assay were performed according to manufacturers instruction to measure biomarkers of oxidative stress to know the level of oxidative stress induced by irradiation in control and irradiated groups. The complete information on materials and methods, results, and discussion are found in the publications included in this thesis.

Chapter 2: Results and Discussion

2.1 Role of TGF-beta and PPAR alpha signaling pathways in radiation response of locally exposed heart: Integrated global transcriptomics and proteomics analysis.

2.1.1 Publication

The scientific data included in the following original research paper published in the Journal of Proteome Research.

Role of TGF Beta and PPAR Alpha Signaling Pathways in Radiation Response of Locally Exposed Heart: Integrated Global Transcriptomics and Proteomics Analysis

Vikram Subramanian, Ingar Seemann, Juliane Merl-Pham, Stefanie M. Hauck, Fiona A. Stewart, Michael J. Atkinson, Soile Tapio, and Omid Azimzadeh

J. Proteome Res, 2017, 16 (1), pp 307–318

DOI: 10.1021/acs.jproteome.6b00795

2.1.2 Aim of this study

Epidemiological studies have shown that the development of cardiovascular disease (CVD) is a late effect in radiation-exposed individuals. For radiotherapy patients the extent of the disease correlated with the dose received. However, the level of risk at lower doses is unclear, and may not be described simply by a linear no-threshold dose response. To better understand risk it is necessary to generate biologically plausible models linking radiation action to outcome. This publication examined the molecular changes found in long-term radiation-induced cardiac damage following single radiation exposure. The role of PPARα and TGFβ in this process were a special focus.

Male C57BL/6J mice were each irradiated locally to the heart with a single X-ray dose of 16 Gy. Sham-irradiated (0 Gy) mice served as control. The cardiac tissues were studied after 40 weeks of post-irradiation using global transcriptomic and quantitative proteomic techniques.

Both data sets were analyzed with Ingenuity Pathway Analysis software (IPA), and results were validated using techniques such as western blotting, ELISA and microRNA validation.

2.1.3 Summary of results

Bioinformatics analysis of the transcriptomic and proteomic data obtained from mouse hearts 40 weeks after a single dose of 16 Gy radiation was performed using Ingenuity pathway analysis (IPA) software. This predicted the activation of TGFβ and the inhibition of PPARα in both the proteomics and transcriptomics datasets. Parts of this data was further validated using western blotting, ELISA, and microRNA analysis. The proteomic profiles in irradiated heart indicated a progressive impairment in cardiac function even after 40 weeks, with significantly deregulated proteins predicted to be involved in multiple cardiac endpoints, including cardiac hypertrophy, inflammation, and fibrosis. Many proteins deregulated in the irradiated heart tissue were involved in impaired lipid metabolism and inflammatory response. Other significantly deregulated proteins contributed to the biological pathways of free radical scavenging, mitochondrial dysfunction, and nuclear factor erythroid 2-related factor 2 (Nrf-2) mediated oxidative stress response.

Gene expression analysis also showed differentially expressed genes that were involved in functional (tissue inflammation, metabolic disease) and toxic pathways (cardiac fibrosis, hypertrophy, necrosis).

The combination of both transcriptomic and proteomic data showed deregulated genes and proteins involved in progressive late effects in cardiac tissue and showed the expected low degree of correlation between mRNA levels and those of mature proteins. This is consistent with our previous observations documenting an essential role of non-coding RNAs in mediating the radiation response. Thus, the translation of proteins from mRNA is highly regulated by non-coding RNAs and produces discordant results. Indeed, increased expression of mir-21 was found in the irradiated group compared to the control group. Our data also showed the involvement of MAPK cascade in the regulation of PPARα and TGFβ signaling pathways in the irradiated heart.

This study provides evidence for persistent molecular changes accompanying cardiac damage after radiation exposure. Our data show significant changes in the cardiac transcriptome and

proteome remain, even 40 weeks after exposure. The results suggest that PPARα and TGFβ both play a role in long-term radiation-induced cardiac damage. This is presumably through activation of TGFβ and inhibition of PPARα signaling pathways.

2.1.4 Contributions

For this project, the mouse irradiation and heart sample preparation were carried out by Dr. Ingar Seemann (Netherlands Cancer Institute). I prepared protein lysate for quantitative proteomics and validation studies. For the proteomics study, I digested protein lysate into peptides from control and irradiated samples using a modified filter-aided sample preparation (FASP) method. I submitted these samples to the proteomics core facility of the HMGU for mass spectrometry. The LC-MS/MS runs and the delivery of the label-free quantification of the individual peptides were performed by Dr. Juliane Merl-Pham (Helmholtz Proteomics core facility). The gene expression profiling study on irradiated and control heart samples was performed by Dr. Ingar Seemann and Dr. Fiona A. Stewart (Netherlands Cancer Institute). I performed the bioinformatic analysis of the proteomics and transcriptomics data using bioinformatics tools under the guidance of Dr. Omid Azimzadeh. The interpretation of the result was performed by myself under the supervision of Dr. Omid Azimzadeh and was supervised by PD Dr. Soile Tapio. Additionally, I conducted the validation experiments related to the TGFβ pathways, the involvement of structural proteins and for microRNA-21 expression using western blotting, q-PCR, and ELISA techniques respectively. I was involved in the analysis and interpretation of the experimental results together with Dr. Omid Azimzadeh, PD Dr. Soile Tapio, and Prof Dr. Michael J Atkinson. I actively contributed as the first author to the preparation and writing of the manuscript under the supervision of the Dr. Omid Azimzadeh and PD Dr. Soile Tapio. Prof Dr. Michael J Atkinson edited the manuscript. All the co-authors in this manuscript contributed to the scientific discussion, corrections, and publication process.

2.1.5 Discussion

In this study, the radiation-induced changes in the transcriptome and proteome were examined 40 weeks after the radiation exposure of the mouse heart. A study from Seemann et al. showed the damaging effect of local high dose of ionizing radiation to the mouse heart

with increased inflammation, late fibrosis, wall thickening, microvascular and structural damage after 16 Gy irradiation [37].

This study aims to understand the molecular mechanism behind such long-term radiation-induced structural and functional impairments observed in experimental work from Seemann et al. using similar experimental strategy. Our global transcriptomics and proteomics data analysis revealed significant alterations in the expression of genes and proteins in irradiated samples compared to controls. Integrated analysis with transcriptomics and proteomics data uncovered that significantly deregulated genes and proteins were involved in common cardiac pathologies such as cardiac fibrosis, metabolic dysfunction, tissue inflammation, and cardiac hypertrophy. Bioinformatics analysis predicted the inhibition of PPARα and activation of TGFβ in transcriptomics and proteomics datasets. A previous study suggested that PPARα and TGFβ signaling pathways involved in the maintenance of cardiac homeostasis [208].

We have found increased activation of proteins involved in SMAD-dependent pathways such as SMAD 2/3 (increased phosphorylation) and SMAD 4 (increased total protein) in irradiated samples to controls, suggesting initiation of the SMAD-dependent pathway. The study has shown that the SMAD-independent pathway initiated through activation of TAK1, which subsequently phosphorylates proteins belonging to MAPK members such as ERK, p38, and JNK [209]. Consistent with SMAD-independent TGFβ signaling pathway, bioinformatics analysis with transcriptomics data has shown predicted activation of proteins involved in MAPK signaling pathways. This was validated by western blotting analysis, results showed increased phosphorylation of TAK1, ERK, p38, and JNK2, implying activation of SMAD-independent pathways in irradiated samples compared to controls. Crosstalk involving PPARα and TGFβ was suggested based on the involvement of TGFβ in the activation of ERK and JNK2, members of the MAPK pathway that results in phosphorylation of SMAD proteins. This data shows regulation of SMAD proteins by MAPK proteins thus changing their action in the heart [159]. Previous studies have demonstrated that radiation-induced cardiac fibrosis is mediated through activation of TGFβ and characterized by enhanced fibroblast proliferation and accumulation of collagen fibers [37, 210]. In agreement with this, our study indicated a pronounced change in the expression of decorin, biglycan, collagen 6 and 10 in irradiated heart compared to controls. Increased deposition of collagen fibers and biglycan shown to induce cardiac fibrosis and dysfunction [211-212] and also reported to be implicated in radiation-

induced heart diseases [213]. In line with this, a similar study from Seemann et al. showed diffuse amyloidosis in the irradiated myocardium due to the accumulation of abnormal fibrils, and it was suggested that the death of mice after long time exposure to irradiation due to cardiac amyloidosis [37].

In the heart, lipid metabolism is regulated by the increased activity of PPARα and reduced PPARα activity is associated with increased risk of cardiovascular disease [214]. Our proteomics data in this study showed a persistent change in cardiac metabolism due to decreased activity of PPARα, because of increased phosphorylation by ERK protein. This observation is in good agreement with previously published data [38, 198]. The function of PPARα is not limited to cardiac metabolism alone, it is reported to play a role in the regulation of inflammatory and acute phase response in the heart [215]. The protein and gene expression analysis of this study indicated many acute phase proteins and chemokines significantly altered in irradiated hearts. This observation is supported by other studies which show an increased level of inflammatory markers in irradiated cardiac endothelial cells and whole heart [37, 216].

Studies have shown the translation of both PPARα and TGFβ can be negatively regulated by miR-21 [217-218]. Our data which showed a significant increase in the expression of miR-21 in irradiated heart compared to controls. Increased expression of miR-21 has shown to be involved in heart failure [219]. Our proteomics data showed notable changes in the expression of myocardial structural proteins such as myosin heavy chain 6 and 7 in irradiated heart compared to controls. This result correlates with a study from Seemann et al. showing persistent structural damage in the irradiated heart [37]. The radiation-induced myosin heavy chain isoform switching between MYH 6 and MYH 7 seen in our study were also observed in cardiac hypertrophy in humans [220] and in rats exposed to total body irradiation [221].

In conclusion, this study provides primary evidence for long-term impairments in cardiac transcriptome and proteome after high dose local irradiation that has not been observed previously. Importantly the role of PPARα and TGFβ signaling pathways in the development of radiation-induced heart pathology is documented by this study.

Journal of proteome research

Article

pubs.acs.org/jpr

Role of TGF Beta and PPAR Alpha Signaling Pathways in Radiation Response of Locally Exposed Heart: Integrated Global Transcriptomics and Proteomics Analysis

Vikram Subramanian,[†] Ingar Seemann,[‡] Juliane Merl-Pham,[§] Stefanie M. Hauck,[§] Fiona A. Stewart,[‡] Michael J. Atkinson,[†,∥] Soile Tapio,[†] and Omid Azimzadeh*[,†]

[†]Helmholtz Zentrum München - German Research Center for Environmental Health GmbH, Institute of Radiation Biology, 85764 Neuherberg, Germany

[‡]Division of Biological Stress Response, Netherlands Cancer Institute, 1006 BE Amsterdam, The Netherlands

[§]Helmholtz Zentrum Muenchen - German Research Centre for Environmental Health GmbH, Research Unit Protein Science, 80939 Munich, Germany

[∥]Chair of Radiation Biology, Technical University of Munich, 81675 Munich, Germany

Supporting Information

ABSTRACT: Epidemiological data from patients undergoing radiotherapy for thoracic tumors clearly show the damaging effect of ionizing radiation on cardiovascular system. The long-term impairment of heart function and structure after local high-dose irradiation is associated with systemic inflammatory response, contraction impairment, microvascular damage, and cardiac fibrosis. The goal of the present study was to investigate molecular mechanisms involved in this process. C57BL/6J mice received a single X-ray dose of 16 Gy given locally to the heart at the age of 8 weeks. Radiation-induced changes in the heart transcriptome and proteome were investigated 40 weeks after the exposure. The omics data were analyzed by bioinformatics tools and validated by immunoblotting. Integrated network analysis of transcriptomics and proteomics data elucidated the signaling pathways that were similarly affected at gene and protein level. Analysis showed induction of transforming growth factor (TGF) beta signaling but inactivation of peroxisome proliferator-activated receptor (PPAR) alpha signaling in irradiated heart. The putative mediator role of mitogen-activated protein kinase cascade linking PPAR alpha and TGF beta signaling was supported by data from immunoblotting and ELISA. This study indicates that both signaling pathways are involved in radiation-induced heart fibrosis, metabolic disordering, and impaired contractility, a pathophysiological condition that is often observed in patients that received high radiation doses in thorax.

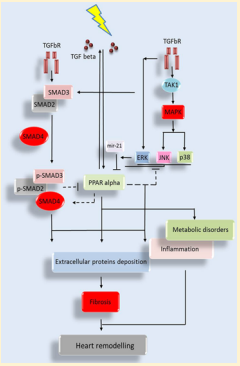

KEYWORDS: *heart, ionizing radiation, proteomics, transcriptomics, label-free quantification, PPAR alpha, TGF beta, cardiovascular disease*

INTRODUCTION

Epidemiological studies show an increased risk of cardiovascular disease (CVD) associated with high local doses of ionizing radiation to the heart. This is observed in patients after thoracic radiotherapy treatment for breast cancer, Hodgkin's disease, or childhood cancers.[1−4] A significant increase in the mortality from CVD has been reported for patients treated by radiotherapy for left-sided breast cancer compared with those with right-sided cancer.[1,5−7] The recent development of radiation therapy practice and equipment has decreased the heart dose from left-tangential radiotherapy considerably over the past 40 years; however, certain parts of the heart still receive >20 Gy in approximately half of left-sided breast cancer patients.[8] High-dose radiation leads to late adverse cardiac side effects including damage to pericardium, myocardium, valves, and coronary vessels as well as cardiomyopathy and myocardial fibrosis.[9,10] Because breast cancer is by far the most common cancer in women worldwide and most patients are treated by radiotherapy, an estimated increased risk for CVD induced by radiation (2.5%/Gy) concerns a large number of people[11] and thus remains one of the important health concerns.[12] Therefore, a deep investigation of the molecular mechanisms of CVD following irradiation of the heart is urgently needed.

We have previously shown using a mouse model (C57Bl/6J) that local cardiac high-dose radiation caused cardiac metabolic impairment that was coupled to mitochondrial dysfunction and reduction in the activity of peroxisome proliferator-activated receptor (PPAR) alpha complex.[13] It also induced a systemic inflammatory response and increased the level of free fatty acids in blood.[13,14] A similar study showed morphological disorders of the heart such as increased left ventricle (LV) wall thickening and increased interstitial collagen accumulation in LV myocardium

Special Issue: The Immune System and the Proteome 2016

Received: August 31, 2016
Published: November 2, 2016

DOI: 10.1021/acs.jproteome.6b00795
J. Proteome Res. 2017, 16, 307−318

after 40 weeks.[15] Moreover, increased structural and microvascular damage, inflammation, diffuse amyloidosis, late fibrosis, and even sudden death of some mice were observed between 30 and 40 weeks after irradiation at 16 Gy.[15]

PPAR alpha, a key regulator of the lipid metabolism in the heart, is involved in the development of CVD.[16,17] Impairment of lipid metabolism has been described as a consequence of altered transcriptional activity of PPAR alpha.[18]Inhibition of PPAR alpha is accompanied by increased levels of circulating cytokines and enhanced local production of profibrotic factors such as TGF beta.[16,19]

TGF beta family represents cytokines that are involved in the regulation of inflammation and cellular growth.[20] The increased expression of TGF beta has been found to correlate with induced myocardial hypertrophy and fibrosis in mice and humans.[21,22] Radiation-induced tissue toxicity has also been associated with TGF beta activation.[23−25] Binding of TGF beta ligands to corresponding receptors activates this canonical SMAD-dependent signaling pathway that leads to translocation of cytoplasmic SMAD proteins into the nucleus to regulate the transcription of the target genes.[26] Activated TGF beta receptors also induce non-SMAD signaling that includes participation of different members of the mitogen-activated protein kinase (MAPK) pathway.[27]

It has been shown that activated PPAR alpha complex interferes with TGF beta signaling[28,29] but the molecular mechanism is not well understood. MAPK cascade plays a regulatory role in both PPAR alpha and TGF beta signaling.[20,30] The importance of MAPK components in the control of radiation-induced cellular stress is well known.[13,14,31]

The goal of the present study was to investigate the mechanism involved in long-term radiation-induced cardiac damage, especially the role of PPAR alpha and TGF beta signaling pathways in this process. C57BL/6J mice were irradiated with single X-ray doses of 16 Gy, and the cardiac tissue was studied 40 weeks postirradiation by transcriptomics and proteomics analyses. Both omics data sets predicted the activation of TGF beta and inactivation of PPAR alpha signaling pathways. This study strongly suggests a crosstalk between the two pathways via MAPK signaling. The combined analysis on proteome and transcriptome was performed to provide a comprehensive and in depth analysis of alterations associated with radiation-induced cardiac damage including fibrosis and amyloidosis observed in the same animals by Seemann et al.[15]

EXPERIMENTAL SECTION

Animals

Male C57BL/6J mice aged 8 weeks were purchased from Charles River Laboratories, France. Animals were randomly allocated to different treatment groups of 10−15 animals and housed in a temperature-controlled room with 12 h light−dark cycle. Standard mouse chow and water was provided ad libitum. Irradiation was carried out as previously described by Seemann et al.[15] In brief, four to seven animals were irradiated with a single dose of 16 Gy locally to heart using 250 kV X-rays operating at 12 mA and filtered with 0.6 mm of copper. Mice were not anesthetized during irradiation procedure but were held in a prone position in restraining jigs with thorax fixed using adjustable hinges. The same number of age-matched controls (sham irradiated with 0 Gy) were always included, providing the appropriate comparison for irradiated groups at that time point. The dose rate was calculated as 0.94 Gy/min. The position and field size (10.6 × 15.0 mm) was determined by pilot studies using soft X-rays (25 kV, 85 mA) to visualize the heart. Up to 30% of lung volume was included in the field, and the rest of the body was shielded with a 3 mm thick lead plate. The animals were sacrificed 40 weeks after irradiation. Heart samples were prepared as described as before.[15] Experiments were in agreement with the Dutch law on animal experiments and welfare and in line with the international Guide for the Care and Use of Laboratory Animals (8th edition).

Materials

Beta-octylglucoside, SDS, and ammonium bicarbonate were obtained from Sigma (St. Louis, MO); acetone, acetonitrile (ACN), formic acid (FA), and trifluoroacetic acid (TFA) were obtained from Roth (Karlsuhe, Germany); dithiothreitol (DTT), iodoacetamide, tris-(hydroxymethyl) aminomethane (Tris), and sequencing-grade trypsin were obtained from Promega (Madison, WI). All solutions were prepared using HPLC-grade water from Roth (Karlsuhe, Germany).

Gene Expression Profiling

Gene expression analysis was performed as described before.[32] Total RNA was isolated from frozen sections (30 sections of 30 μm per mouse using four to seven mice per group) of the mid part of the horizontally cut heart using Trizol Reagent (Invitrogen, Carlsbad, CA), according to the manufacturer's protocol. The quantity of total RNA was determined spectrophotometrically (NanoDrop, Thermo Scientific, Wilmington, DE), followed by a quality check measured by an Agilent 2100 Bioanalyzer with the RNA Integrity Number (RIN) (Agilent Technologies, Santa Clara, CA). Samples with a RIN above 7 were used for DNase treatment and amplified (350 ng per sample) using Illumina Totalprep RNA Amplification kit (Ambion, Grand Island, NY). Before hybridization, individual RNA was pooled for each treatment group. Hybridization of aRNA to Illumina Expression Bead Chips Mouse Whole Genome (WG-6 vs 2.0) and subsequent washing, blocking, and detecting were performed according to the manufacturer's protocol (Illumina, San Diego, CA). Samples were scanned on the IlluminaR BeadArray 500GX Reader using IlluminaR BeadScan image data acquisition software (version 2.3.0.13). MouseWG-6 vs 2.0 BeadChip contains the full set of MouseRef-8 BeadChip probes with an additional 11 603 probes from RIKEN FANTOM2, NCBI REfSeq as well from the MEEBO database.

Before analysis, the database was normalized using robust spline normalization method within the microarray facility of The Netherlands Cancer Institute. Log2 ratio between expression of genes from control mice and expression of genes from irradiated mice were calculated as well as the sum of the expression of genes from both control and irradiated mice. Genes with sums below 6 were discarded. The threshold for standard deviation (SD) was set to 3 and mean ± nSD was calculated to identify genes that are above an expression value of 6 and above threshold 3 of SD. Among these genes, the genes with fold changes greater than 1.5 fold or less than 0.64 fold were defined as significantly differentially expressed.

Proteome Profiling

Protein Extraction and Quantification. Frozen heart samples obtained from five mice per group were lysed as previously described. Cardiac tissue was ground to a fine powder with a cold (−20 °C) mortar and pestle before being suspended in lysis buffer (SERVA).[13] The same animals were used for transcriptomics and proteomics. Protein concentration was

DOI: 10.1021/acs.jproteome.6b00795
J. Proteome Res. 2017, 16, 307−318

determined by the Bradford assay following the manufacturer's instructions (Thermo Fisher).

Protein Purification and Mass Spectrometry. Protein lysates (10 μg) from each animal were digested using a modified filter-aided sample preparation (FASP) protocol.[33] In brief, the samples were reduced with 10 mM DTT at 60 °C for 30 min, followed by alkylation with 15 mM iodoacetamide for 30 min at room temperature in the dark.[33] Samples were diluted using 8 M urea in 0.1 M Tris/HCl, pH 8.5, and centrifuged using a 30 kDa cutoff filter (Pall). After washing with 8 M urea in 0.1 M Tris/HCl, pH 8.5, and with 50 mM ammonium bicarbonate (ABC), the proteins were initially digested on the filter with 1 μg Lys-C (Wako Chemicals) in 50 mM ABC at room temperature, followed by the addition of 2 μg trypsin (Promega) and digestion overnight at 37 °C. Tryptic peptides were collected by centrifugation and acidified with trifluoric acid (TFA) to a pH of 2.0. Samples were stored at −20 °C.

Prior to LC−MS/MS analysis, the samples were centrifuged (16 000*g*) for 5 min at 4 °C. Each sample (~0.5 μg) was analyzed separately on an LTQ OrbitrapXL (Thermo Fisher Scientific) coupled to Ultimate 3000 nano-HPLC (Dionex), as previously described.[14]

Label-Free Quantification. The raw files of the individual measurements were loaded to the Progenesis QI software and analyzed as described previously.[34,35] Peptide features in the individual runs were aligned to reach a maximum overlay of at least 87%. After feature detection, the singly charged features and features with charges higher than +7 were excluded. Protein identification was performed using the Mascot search engine (Matrix Science, version 2.5.1) in the Ensembl mouse database (release 75, 23 354 020 residues, 51 771 sequences).

The following search parameters were used: 10 ppm peptide mass tolerance and 0.6 Da fragment mass tolerance, one missed cleavage was allowed, carbamidomethylation (C) was set as fixed modification, and oxidation (M) and deamidation (N, Q) were allowed as variable modifications. Search results were reimported into the Progenesis QI software, and the resulting summed normalized abundances of the unique peptides for every single protein were used for the calculation of abundance ratios and statistical analysis. For final quantifications, proteins with ratios greater than 1.30-fold or less than 0.77-fold (*t* test; $q \leq 0.05$) were defined as being significantly differentially expressed. The FDR (*q* value) calculation was used to adjust *p* values.[36,37]

Interaction and Signaling Network Analysis. For deregulated genes and proteins, interaction and signaling networks were analyzed by the software tool INGENUITY Pathway Analysis (IPA) (http://www.INGENUITY.com)[38] and the search tool STRING version 10 (http://string-db.org) coupled to the Reactome database (http://www.reactome.org).[39]

Sandwich ELISA Assay. The alteration in the phosphorylation status of SMAD 2/3 was assessed using PathScan phospho- SMAD 2 (Ser465/467)/SMAD 3 (Ser423/425) Sandwich ELISA Kits (no. 120001). The data were compared to the level of total SMAD 2/3 sandwich ELISA kit (Cell Signaling) (no. 12000C). The assays react with mouse material. The measurement was performed using three biological replicates.

Immunoblotting Analysis. Proteins separated by SDS-PAGE were transferred to nitrocellulose membranes (GE Healthcare) using a TE 77 semidry blotting system (GE Healthcare) at 1 mA/cm for 2 h. The membranes were blocked with either 5% nonfat dry milk powder or 3% BSA in TBST for 2 h at room temperature, washed four times in TBST for 5 min, and incubated overnight at 4 °C with primary antibodies using the dilutions recommended by the manufacturer. Immunoblotting analysis of heart lysates was performed using anti-ERK 44/42 (no. 9202), anti-phospho ERK 44/42 (Thr 202/Tyr 204) (no. 9101), anti-p38 (no. 9212), anti-phospho p38 (Thr 180/Tyr 182) (no. 9211), anti-PPAR alpha (sc-1982), anti-phospho PPAR alpha (Ser 12) (ab3484), anti-JNK1/JNK2 (ab179461), anti-phospho JNK1/JNK2 (Thr 183/Tyr 185) (ab4821), anti-TAK-1 (ab109526), anti-phospho TAK-1 (Thr 187) (ab192443), anti-SMAD 4 (sc-7966), anti-MYH6 (sc-168676), anti- MYH7 (sc-53089), and anti-ATPB (ab14730). Blots were washed four times with TBST after primary antibody incubation and incubated with secondary antibody conjugated with horseradish peroxidase (Santa Cruz Biotechnology) or alkaline phosphatase for 2 h at room temperature and developed using the ECL system (GE Healthcare) or 1-step NBT/BCIP method (ThermoFisher) following standard procedures. ATPB5 was not changed in the proteomic profile after 16 Gy and used as loading control. All antibodies react with mouse material. Digitized images of immunoblot bands from three biological replicates were quantified using ImageJ software (http://rsbweb.nih.gov/ij/).

MicroRNA Analysis

Total RNA was isolated from frozen heart of sham and irradiated animals and purified using the mirVana Isolation Kit (Thermo Fisher Germany) according to the manufacturer's protocol. For microRNA studies the OD ratio of 260 nm/280 nm from RNA lysates was estimated using a Nanodrop spectrophotometer. This ratio reflecting the RNA quality ranged between 2.0 and 2.1. Samples were stored at −20 °C until further analysis. Expression of single microRNA using TaqMan Single MicroRNA Assay (Thermo Fisher, Germany) was performed according to manufacturer's protocol on a StepOnePlus device (Applied Biosystems, Germany) using Taqman primers. For single microRNA analysis, the following Taqman primers were used: SnoRNA 202 (ID: PN4427975) and miR-21-5p (ID: no. 477975). All primers were purchased from Thermo Fisher, Germany. Expression levels of microRNA 21 were calculated based on the 2-ΔΔCt method with normalization to control SnoRNA 202.

Statistical Analysis

The Student's *t* test (unpaired) was used as a statistical test. Group difference was considered as statistically significant with *p* values of $p^* < 0.05$, $p^{**} < 0.01$, and $p^{***} < 0.001$. The error bars were calculated as standard deviation (SD). All experiments were done with at least three biological replicates.

Data Availability

The raw MS data can be accessed from the RBstore (https://www.storedb.org/store_v3/study.jsp?studyId=1040).[13,14]

RESULTS

Irradiation Alters Genes Involved in the Inflammatory Response

Increased levels of inflammation, diffuse amyloidosis, and fibrosis have been previously observed as late effects in locally irradiated murine heart.[15] We performed gene expression analysis to identify genes involved in these pathways.

The full list of 16 892 identified genes is provided in the Supporting Information (SI) Table S1. The analysis showed that 185 genes were significantly differentially expressed in irradiated

DOI: 10.1021/acs.jproteome.6b00795
J. Proteome Res. 2017, 16, 307−318

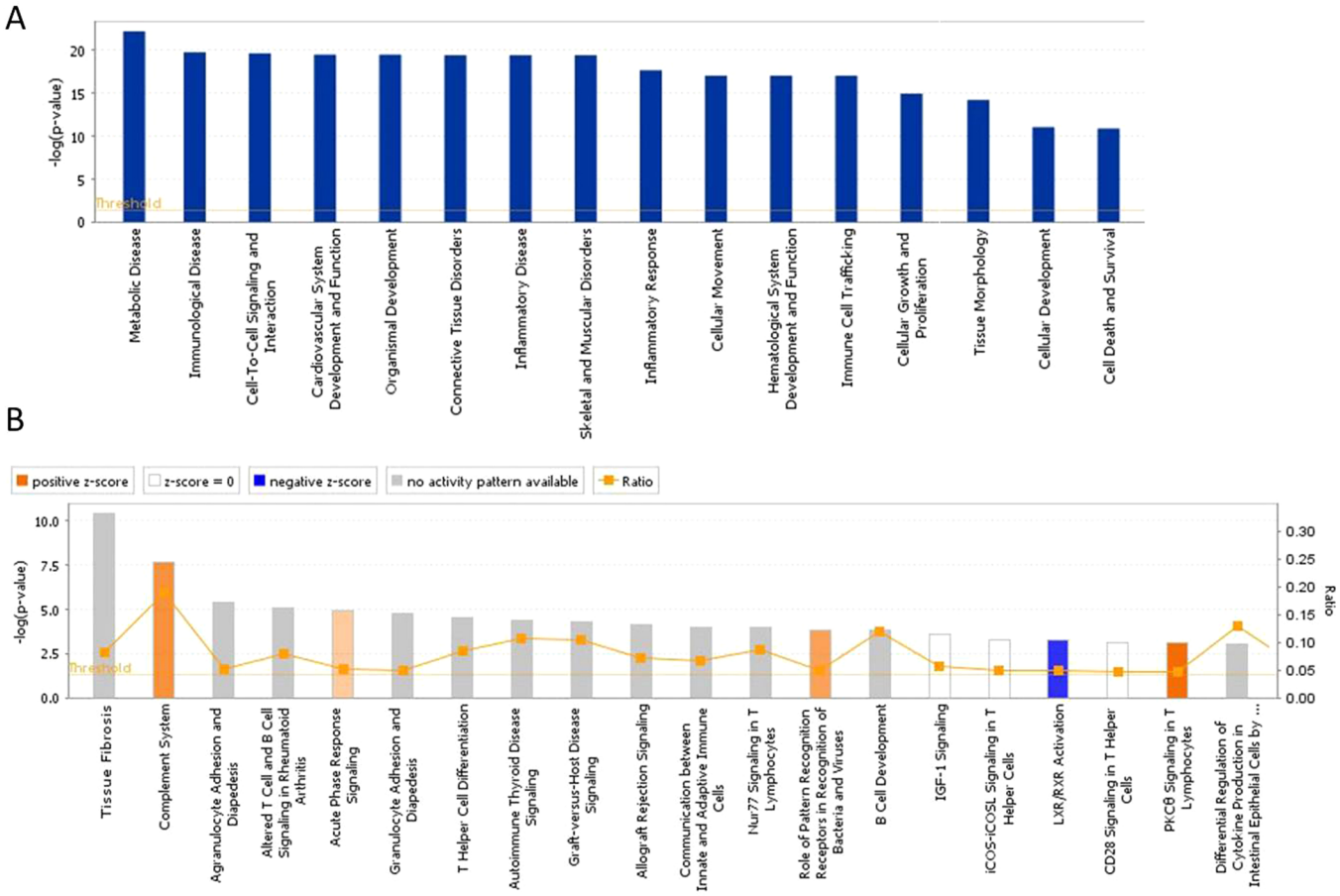

Figure 1. Pathway and network analysis of significantly differentially expressed genes in irradiated heart. Bars indicate top networks (A) and canonical pathways (B) and *y* axis displays the −(log) significance. Tall bars are more significant than short bars. A positive *z* score implies potential activation (orange) and a negative *z* score indicates potential inhibition (blue) of the pathway (http://www.INGENUITY.com).

samples compared with controls (±1.5-fold) using the statistical criteria described in the Experimental Section (Table S2 in the SI).

The analysis showed that chemokines formed the main cluster of significantly deregulated genes. Many of these genes were associated with tissue inflammation and metabolic diseases (Figure 1A and Tables S2 and S3 in the SI). The most significantly altered networks were "metabolic disease", "inflammatory disease", and "cardiovascular system development and function".

"Tissue fibrosis", "complement system", and "acute phase response signalling" were the most important deregulated functional pathways (Figure 1B and Table S3 in the SI). Differently expressed genes were associated with toxic pathways including cardiac fibrosis, hypertrophy, necrosis, and stenosis (Table S3 in the SI).

Irradiation Changes the Cardiac Proteome

To further elucidate the mechanisms of gene alterations, the cardiac proteome was analyzed after irradiation. The complete list of all identified and quantified peptides and proteins with fold changes and p and q values are shown in the Supporting Information (Tables S4, S5, S6, and S7 in the SI). Global proteomics analysis of the heart tissue identified 1038 proteins in total (Table S5 in the SI). Of 940 quantified proteins, 87 proteins were significantly changed in expression (two unique peptides; fold change ≥1.30 or ≤0.77; $q \leq 0.05$) after radiation exposure. The expression of 31 proteins was down-regulated and that of 56 proteins was up-regulated (Table S7 in SI).

A detailed analysis of functional interactions and biological pathways was performed using IPA software. Many of the altered proteins were associated with tissue skeletal disorders and metabolic and inflammatory diseases (Figure 2A and Table S8 in the SI). The analysis showed that "organismal injury and abnormalities", "free radical scavenging", and "metabolic disease" were the main networks altered in the cardiac proteome after irradiation (Table S8 in the SI).

The pathways "actin cytoskeleton signalling", "mitochondrial dysfunction", and "acute phase response signalling" as well as "nuclear factor (erythroid-derived 2)-like 2, NFE2L2-mediated oxidative stress response" were significantly affected in irradiated hearts (Figure 2B and Table S8 in the SI).

The majority of significantly altered proteins were associated with different heart diseases including heart hypertrophy, inflammation, heart failure, and heart fibrosis (Table S8 in the SI).

Common Regulatory Pathways Are Affected in Both Gene and Protein Data Sets

On the basis of IPA upstream regulator analysis, TGF beta 1 was predicted to be activated after irradiation in both data sets (Figure 3A,B and Tables S3 and S8 in the SI), whereas PPAR alpha was deactivated (Figure 3C,D and Tables S3 and S8 in the SI). Furthermore, the analysis of both data sets predicted the

DOI: 10.1021/acs.jproteome.6b00795
J. Proteome Res. 2017, 16, 307−318

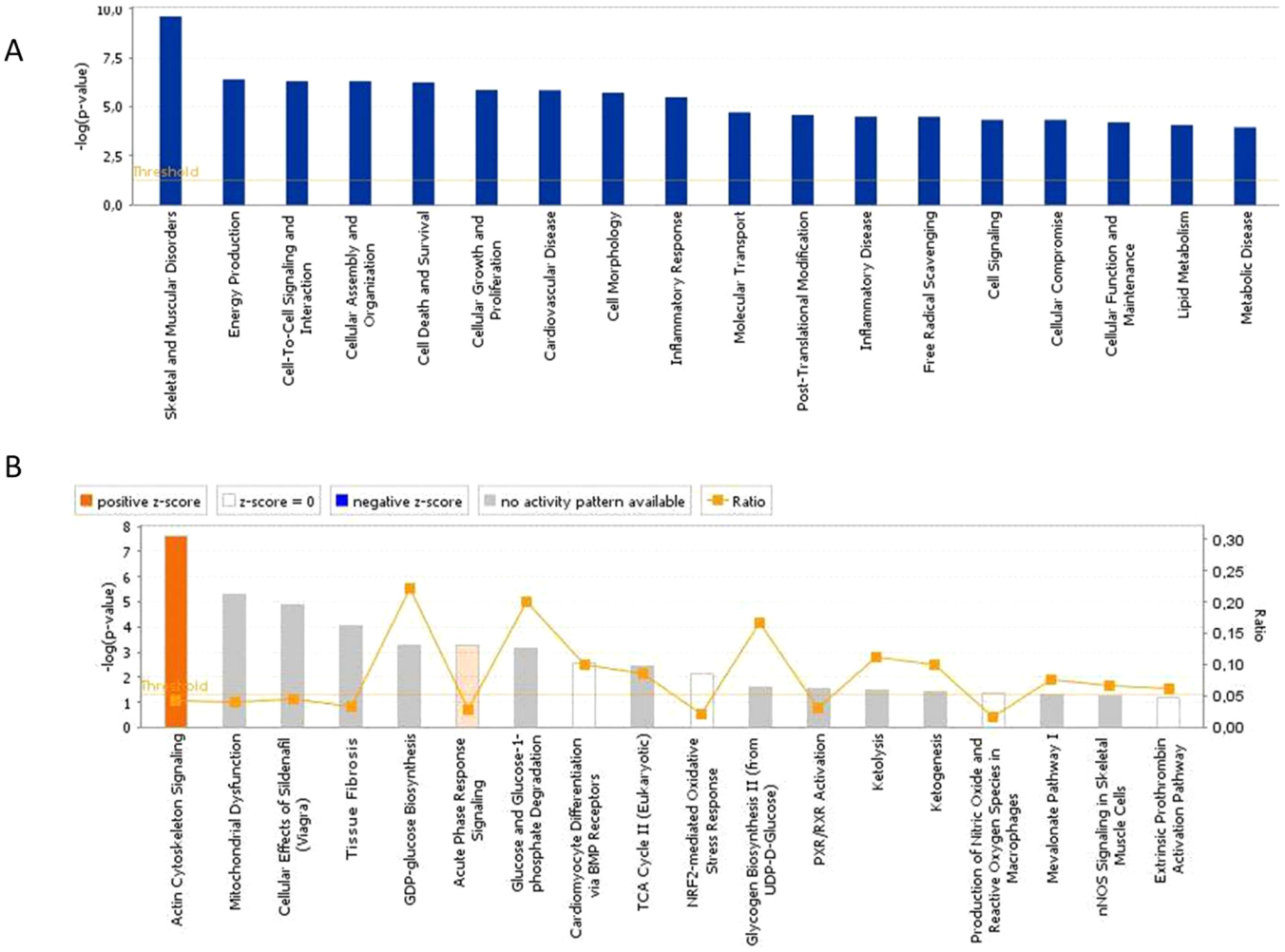

Figure 2. Pathway and network analysis of significantly differentially expressed proteins in irradiated heart. Bars indicate top networks (A) and canonical pathways (B) and *y* axis displays the −(log) significance. Tall bars are more significant than short bars. A positive *z* score implies potential activation (orange) and a negative *z* score indicates potential inhibition (blue) of the pathway (http://www.INGENUITY.com).

induction of different interleukins including IL6 and IL1A in irradiated hearts (Figure S1A,B).

p38 was also predicted to be activated after irradiation (Figure S2A,B in the SI). Other components of TGF beta signaling including SMAD 3 and ERK and JNK were predicted to be induced only at the gene expression level after radiation exposure (Figure S3A−C in the SI).

The analysis also showed that several significantly deregulated genes and proteins formed an amyloid precursor protein (APP)-related protein cluster supporting cardiac amyloidosis previously observed in these animals[15] (Figure S4 in the SI).

TGF Beta Induces SMAD-Dependent and SMAD-Independent Pathways after Irradiation

As SMAD proteins mediate the TGF beta signaling, the levels of SMAD 2 and 3 proteins were measured. The analysis showed a significant increase in the ratio of phosphorylated/total level of SMAD 2 and 3 after exposure (Figure 4A, $p < 0.05$), suggesting the activation of SMAD 2/3. Active SMAD 2 and 3 are known to interact with SMAD 4 to assemble a complex that is required for efficient TGF beta SMAD-dependent signal transduction.[26] In good agreement with this, enhanced protein level of SMAD 4 was detected in the irradiated heart (Figure 4B, $p < 0.05$).

In addition, the protein components of SMAD-independent pathway, TGF beta associated kinase 1 (TAK1), and JNK1/2 and their phosphorylated forms were analyzed (Figure 4C,D). Significant increase in the ratio of phosphorylated/total level of TAK 1 and JNK 2 was found in the irradiated heart (Figure 4C,D, $p < 0.05$). Active TGF beta is known to induce MAPK signaling.[40] Therefore, the protein expression of components of the MAPK pathway, ERK 42 and 44, and p38 and their phosphorylated forms was measured (Figure 4C,D). The ratio of phosphorylated/total ERK 42 and p38 was significantly increased (Figure 4C,D, $p < 0.05$) at irradiated hearts compared with control, whereas there was no significant effect on the ratio of phosphorylated/total level of ERK 44 (Figure 4C,D).

Transcription Factor PPAR Alpha Is Inactivated by Irradiation

The predicted inhibition of PPAR-alpha was analyzed by measuring the level of phosphorylated (inactive) and total protein. The ratio of phosphorylated/total PPAR alpha was significantly increased in irradiated hearts compared with control (Figure 4C,D, $p < 0.05$), suggesting reduced PPAR alpha transcriptional activity.

miR-21 Is Induced in Irradiated Heart

As miR-21 is known to regulate the activity of PPAR alpha[41] and TGF beta,[42] the expression level of miR-21 was compared in irradiated to control hearts. The analysis showed that the

DOI: 10.1021/acs.jproteome.6b00795
J. Proteome Res. 2017, 16, 307−318

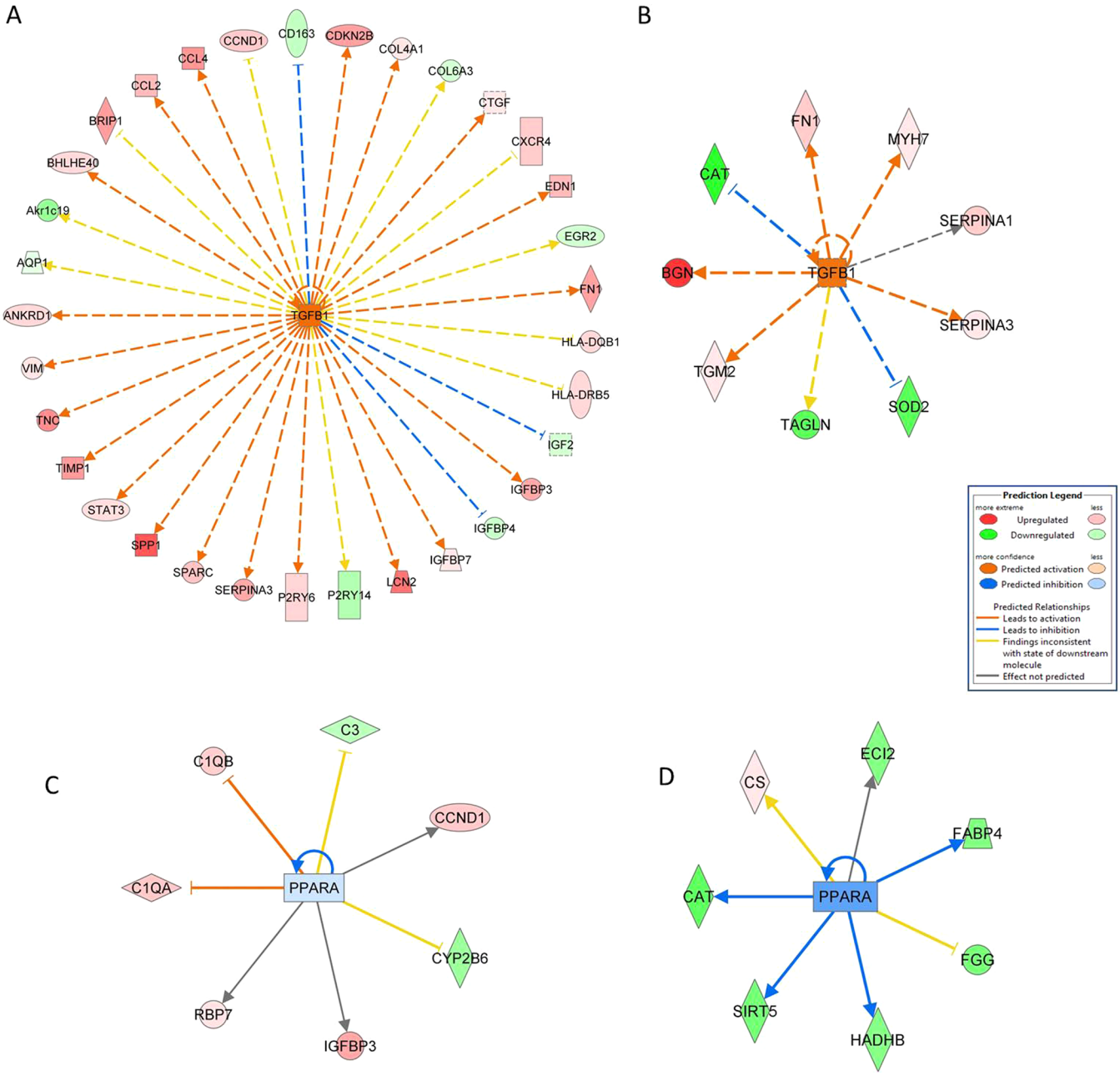

Figure 3. Analysis of transcriptomics and proteomics upstream regulators. Graphical representation of the deregulated genes (A and C) and proteins (B and D) networks with their upstream transcriptional regulators at 16 Gy is shown (http://www.INGENUITY.com). The up-regulated proteins are marked in red and the down-regulated are marked in green. The nodes in blue and orange represent transcription factors PPAR alpha and TGF beta, respectively. The genes and protein IDs are available in Tables S2, S3, S7, and S8 in the SI.

expression of miR-21 was significantly increased after irradiation compared with the control (Figure 5A, $p < 0.01$).

Protein Expression of Myosin Heavy Chain Isoforms Is Altered after Irradiation

To validate the changes in the structural proteins indicated by the proteomics analysis, the levels of cardiac myosin heavy chain isoforms 6 (MYH 6) and 7 (MYH 7) were measured using immunoblotting. The level of MYH 6 was significantly decreased and MYH 7 significantly increased in irradiated hearts compared with control (Figure 5B,C, $p < 0.05$). The shift of MYH 6 to MYH 7 is a known human heart pathology.[43]

Integration of All Omics Data Indicates PPAR Alpha and TGF Beta As Common Regulators of Radiation Response

Among the significantly deregulated genes and proteins, annexin A1, fibronectin, and serine (or cysteine) peptidase inhibitor 3 were found in both data sets to be up-regulated, suggesting a similar response to radiation exposure at gene and protein level (Tables S2 and S7 in the SI).

A reconstruction of integrative networks of all deregulated genes and proteins indicated a high degree of interconnectivity between the two data sets with PPAR alpha and TGF beta as common regulators (Figure 6).

DOI: 10.1021/acs.jproteome.6b00795
J. Proteome Res. 2017, 16, 307−318

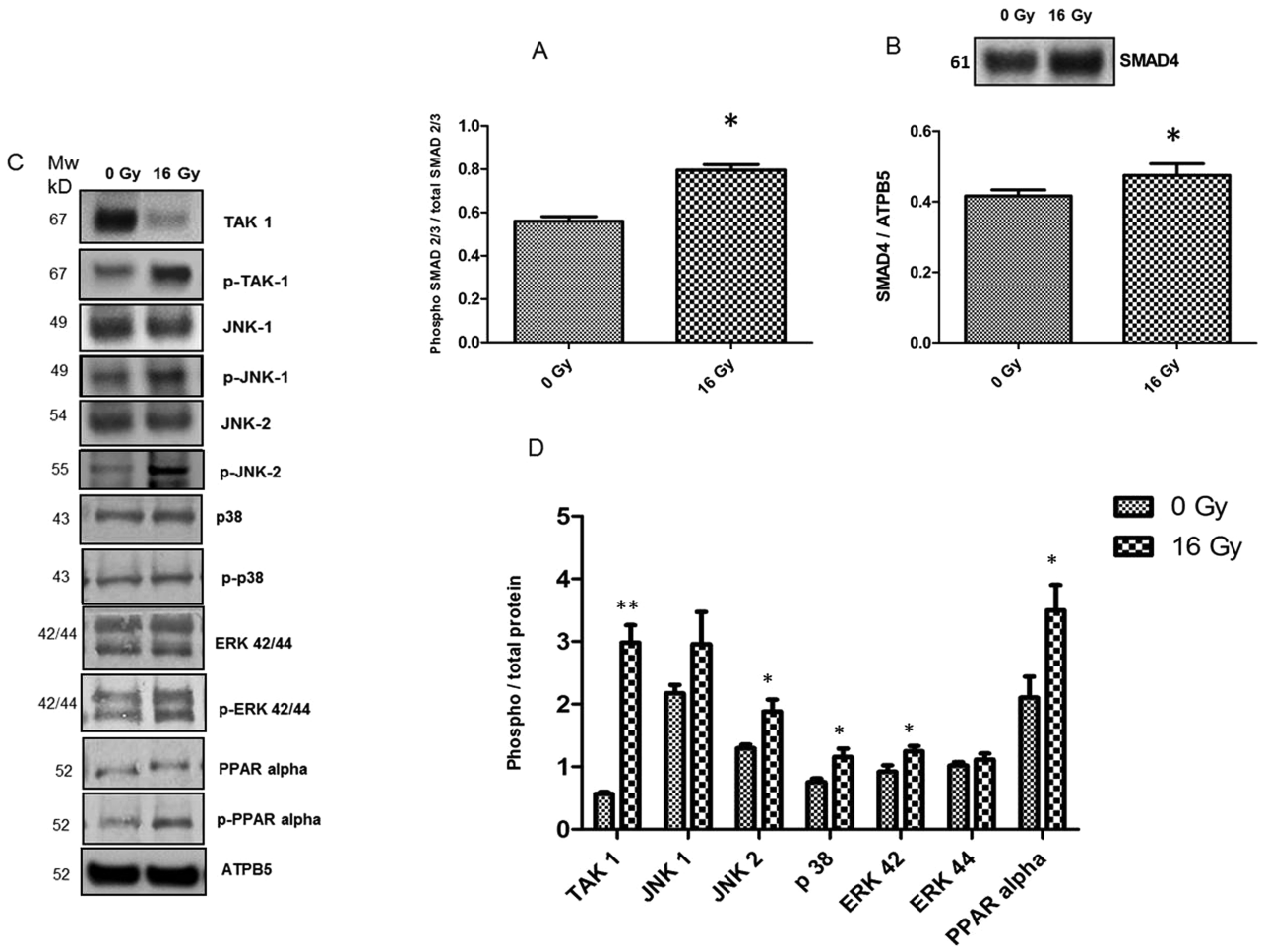

Figure 4. (A) Validation of TGF beta and PPAR alpha signaling pathways. Immunoblot analysis of the levels of TAK-1, phospho TAK-1, JNK1/JNK2, phospho JNK1/JNK2, ERK 44/42, phospho ERK 44/42, p38, phospho p38, PPAR alpha, and phospho PPAR alpha is shown. (B) Columns represent the average ratios of relative protein expression in sham- and irradiated samples after background correction and normalization to ATPB5 expression (*t* test; * $p < 0.05$, ** $p < 0.01$; $n = 3$).

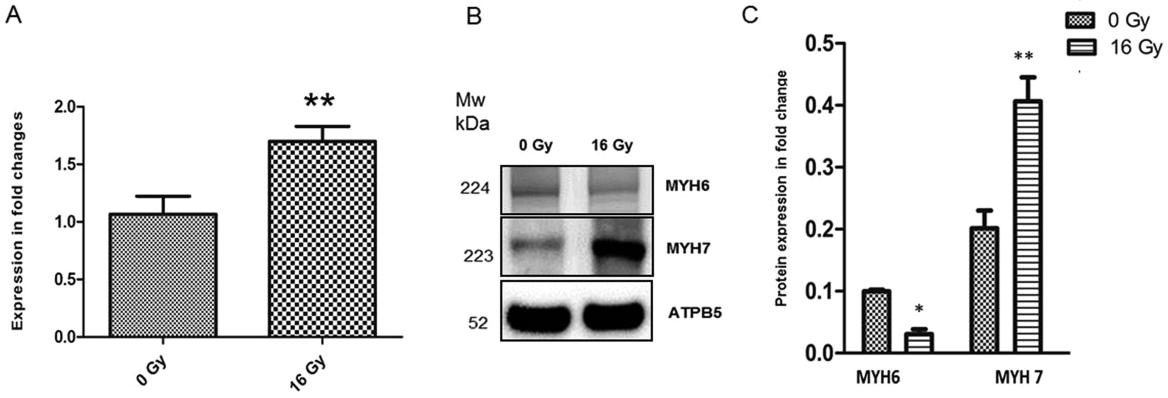

Figure 5. Analysis of radiation-induced changes in miR-21 and the myosin heavy chain isoforms. The analysis showed significant upregulation of miR-21 in the irradiated heart compared with controls (A) (*t* test; *$p < 0.05$, **$p < 0.01$; $n = 3$). (B) Immunoblot analysis of the levels of myosin heavy chain 6 (MYH 6) and myosin heavy chain 7 (MYH 7). (C) Columns represent the average ratios of relative protein expression in sham and irradiated samples after background correction and normalization to ATPB5 expression (*t* test; *$p < 0.05$, **$p < 0.01$; $n = 3$).

DISCUSSION

In this study, radiation-induced transcriptome and proteome changes were examined in mouse heart tissue 40 weeks after local radiation exposure (16 Gy). A similar study done by Seemann et al. showed functional disorders in the irradiated heart including microvascular damage, inflammation, diffuse amyloidosis, and late fibrosis.[15] The goal of the present study was to investigate molecular mechanism involved in such long-term radiation-induced cardiac damage using exactly similar experimental design (age-at-exposure, dose, and time point) as in the previous study.[15]

DOI: 10.1021/acs.jproteome.6b00795
J. Proteome Res. 2017, 16, 307−318

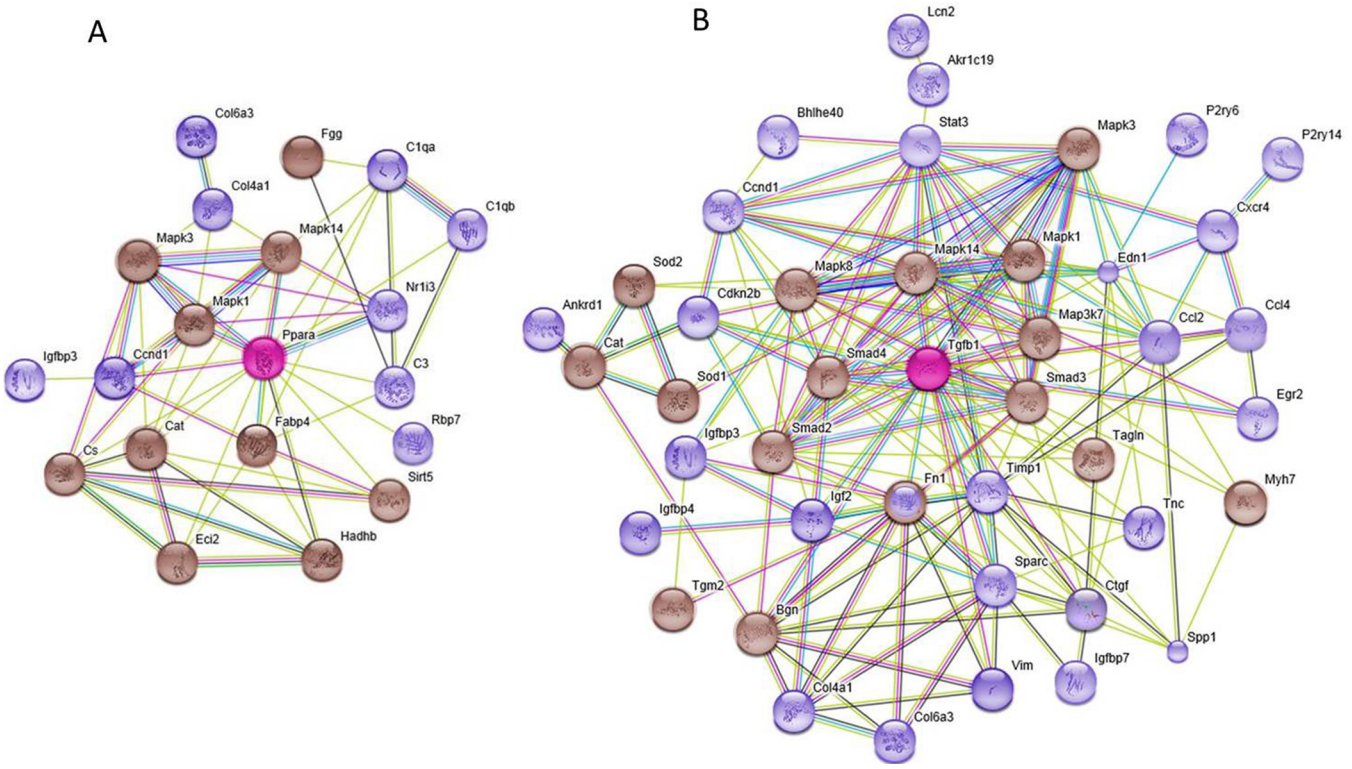

Figure 6. Combined analysis for common regulatory networks of all significantly deregulated cardiac genes and proteins. The TGF beta (A) and PPAR alpha (B) networks were generated by introducing all proteins and genes found significantly up- or downregulated in this study to the STRING software. Proteins are shown in brown and genes in purple balls. The protein and gene IDs are available in Tables S2 and S7 in the SI. Mapk3: ERK1; Mapk1: ERK2; Mapk8: JNK; map3k7: TAK1; and Mapk14: p38.

The novelty of the present study is to correlate radiation-induced proteome and transcriptome changes to the functional impairments observed before.[15] We noticed only modest direct correlation between gene and protein expression. This is in agreement with previous data showing poor or even negative correlation between gene and protein expression levels.[44,45] One reason for this is the different regulatory mechanisms for gene and protein expression,[46,47] such as gene expression regulation by noncoding RNAs or protein expression regulation by post-translational modifications.[47]

Despite expression differences between individual genes and proteins, both profiles revealed same biological processes affected by irradiation. The integrated analysis elucidated the signaling pathways that are commonly deregulated in proteome and transcriptome level. These processes were closely related to heart pathologies such as cardiac remodelling, hypertrophy, metabolic perturbation, and fibrosis.

The activation of TGF beta[22,48] was predicted in both transcriptomics and proteomics data sets. TGF beta signaling is able to initiate both canonical SMAD-dependent and non-canonical SMAD-independent transduction pathways.[40] Here we show enhanced phosphorylation of SMAD 2 and 3 and increased level of SMAD 4 after radiation exposure, suggesting an activation of the SMAD-dependent pathway.

The so-called SMAD-independent pathway initiates with activation of TAK1, followed by a series of phosphorylation events of MAPK members such as ERK, p38, and JNK.[40] The transcriptomic analysis of this study predicted radiation-induced activation of these factors that was confirmed by immunoblot analysis showing increased phosphorylation of TAK1, p38, ERK 42, and JNK 2. These data suggest an alteration in both canonical and noncanonical TGF beta signaling. Cross-talk between the two signaling pathways has been previously suggested as TGF beta induced activation of the ERK and JNK kinases, resulting in phosphorylation of SMAD proteins and thus regulation their activation.[40]

Enhanced levels of TGF beta are involved in radiation-induced cardiac fibrosis that is characterized by excess fibroblast proliferation and deposition of collagen fibers.[15,49] In line with this, our study showed a marked alteration in the expression of extracellular matrix proteins such as biglycan, decorin, and collagens 6 and 10 in the irradiated heart. Excessive accumulation of collagen fibers leading to cardiac fibrosis and dysfunction has previously been reported in different cardiac diseases[50,51] including radiation-induced heart disease.[52] In agreement with this, similarly treated as used in this study showed diffuse amyloidosis caused by extracellular deposition of insoluble, abnormal fibrils that derived from aggregation of misfolded proteins in the myocardium.[15] It was suggested that the sudden death of nearly half of the irradiated mice was caused by this cardiac amyloidosis.[15] In good agreement with this finding, transcriptomics and proteomics data of the present study show that significantly altered extracellular matrix genes and proteins form a cluster of APP-related factors.

Consistent with our previous data,[13,14,53] this study indicated a persistent alteration of cardiac metabolism due to decreased PPAR alpha activity related to its increased phosphorylation.[30] PPAR alpha regulates lipid metabolism in the heart, and reduced PPAR alpha activity is associated with the development of CVD.[16,17] The activity of PPAR alpha transcription factor is known to be regulated at the phosphorylation level by MAPK-ERK and p38 pathways.[54] The enhanced phosphorylation of

DOI: 10.1021/acs.jproteome.6b00795
J. Proteome Res. 2017, 16, 307−318

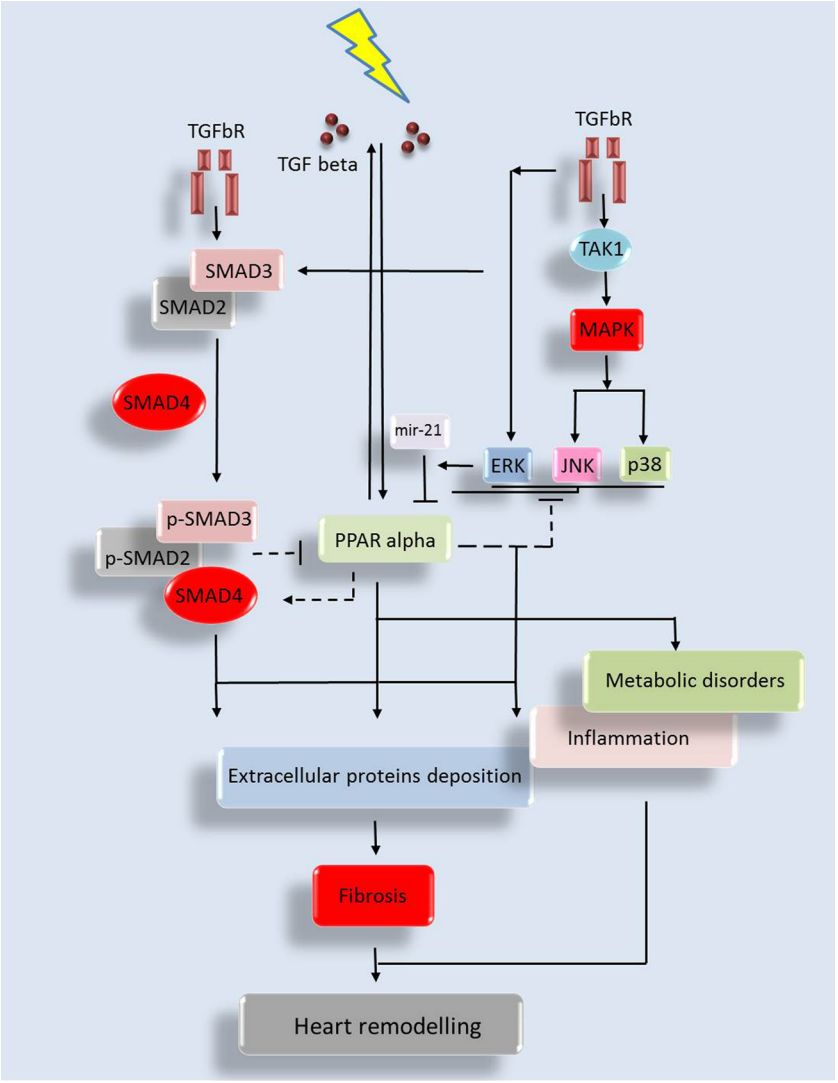

Figure 7. Proposed model for the role of TGF beta and PPAR alpha pathways in radiation-induced cardiac damage.

ERK found in this study strongly indicates that increased phosphorylation and subsequent inactivation of PPAR alpha results from the activation of MAPK pathway.[30]

Besides metabolism, the expression of genes involved in the inflammatory and acute phase response is regulated by PPAR alpha activation.[55] The gene and protein expression analysis of this study showed that the inflammation-related factors including acute phase proteins and different chemokines were markedly and permanently affected in irradiated hearts. The gene expression profiling predicted activation of different interleukins. This is supported by previous studies showing enhanced levels of inflammatory markers in serum, cardiac endothelial cells, and heart tissue in mice after local heart irradiation.[15,56] Consistent with this finding, the persistent inhibition of the PPAR alpha signaling pathway is suggested to lead to pro-inflammatory homeostasis in irradiated heart.[53]

PPAR alpha and TGF beta signaling pathways are contributing to the cardiac homeostasis. The regulatory cross-talk between PPAR alpha and TGF beta was reported previously.[57,58] TGF beta-treated cardiac myocytes showed significantly suppressed fatty acid oxidation due to impaired PPAR alpha activity.[57] In line with this, PPAR alpha agonist significantly inhibited fibrotic LV remodelling[59] that is extremely prevalent in PPAR alpha knockout mice.[28] Agonist-activated PPAR alpha has been shown to inhibit TGF beta signal transduction by suppression of c-JUN expression, a downstream target of JNK.[58,60] On the contrary, JNK activation inhibited PPAR alpha gene expression and fatty acid oxidation in mouse hearts and in a human cardiomyocyte-derived cell line.[61] Furthermore, the interaction between PPAR alpha and SMAD pathways has been previously suggested in mouse heart.[57]

PPAR alpha and TGF beta are known to be regulated by miR-21.[41,42] This study showed significant upregulation of miR-21 expression in the irradiated heart. Increased levels of mir-21 have been reported in heart failure and radiation-induced cardiac ischemia.[53,62,63]

Both cardiac fibrosis and cardiac energy metabolism impairment are known to affect the heart contractile function.[64,65] Proteomics data of this study showed significant changes in the cardiac structural proteins. This correlates well with previous data showing progressive structural damage in locally irradiated murine hearts.[15] The myosin isoform switching between MYH 6 and MYH 7 shown in the present study is a well-known human heart pathology[43,66] that was also detected in rats irradiated with a total body high-dose exposure.[67]

DOI: 10.1021/acs.jproteome.6b00795
J. Proteome Res. 2017, 16, 307−318

CONCLUSIONS

This study provides evidence of long-term alterations in the cardiac transcriptome and proteome after local irradiation. The integrated analysis of transcriptome and proteome shows a complex and complementary network of genes and proteins involved in the radiation-induced heart pathology. A putative model for the role of PPAR alpha and TGF beta signaling pathways is presented in Figure 7. It proposes that radiation-induced activation of MAPK cascade connects these pathways and modulates them, resulting in metabolic disordering, fibrosis, and inflammation.

ASSOCIATED CONTENT

Supporting Information

The Supporting Information is available free of charge on the ACS Publications website at DOI: 10.1021/acs.jproteome.6b00795.

Figure S-1. IPA of transcriptomics and proteomics upstream regulators. Figure S-2. IPA of transcriptomics and proteomics upstream regulators. Figure S-3. IPA of transcriptomics upstream regulators. Figure S-4. IPA of transcriptomics and proteomics upstream regulators. (PDF)

Table S-1. The list of all identified and quantified genes in irradiated heart. (XLS)

Table S-2. Significantly deregulated genes in irradiated heart. (XLS)

Table S-3. IPA Analysis summary of significantly deregulated genes in irradiated heart. (XLS)

Table S-4. All peptides identified and quantified by label-free quantification approach. (XLS)

Table S-5. All proteins identified by label-free quantification approach. (XLS)

Table S-6. All proteins quantified by label-free quantification approach. (XLS)

Table S-7. List of significantly deregulated proteins in irradiated heart. (XLS)

Table S-8. IPA Analysis summary of significantly deregulated proteins in irradiated heart. (XLS)

AUTHOR INFORMATION

Corresponding Author

*E-mail: omid.azimzadeh@helmholtz-muenchen.de. Phone: +49-89-3187-3887. Fax: +49-89-3187-3378.

Notes

The authors declare no competing financial interest.

ACKNOWLEDGMENTS

V.S. is recipient of a scholarship from the German Academic Exchange Service (DAAD). The sample collection was funded by a grant from the European Community's Seventh Framework Programme (EURATOM) contract no. 211403 (CARDIORISK). We thank Stefanie Winkler and Fabian Gruhn for excellent technical assistance.

ABBREVIATIONS

PPAR alpha, peroxisome proliferator activated receptor alpha; TGF beta 1, transforming growth factor beta 1; IPA, Ingenuity Pathway Analysis; LC−ESI−MS/MS, liquid chromatography−electron spray ionization−tandem mass spectrometry; Gy, gray

REFERENCES

(1) Darby, S. C.; Ewertz, M.; McGale, P.; Bennet, A. M.; Blom-Goldman, U.; Bronnum, D.; Correa, C.; Cutter, D.; Gagliardi, G.; Gigante, B.; Jensen, M. B.; Nisbet, A.; Peto, R.; Rahimi, K.; Taylor, C.; Hall, P. Risk of ischemic heart disease in women after radiotherapy for breast cancer. *N. Engl. J. Med.* **2013**, *368* (11), 987−98.

(2) Swerdlow, A. J.; Higgins, C. D.; Smith, P.; Cunningham, D.; Hancock, B. W.; Horwich, A.; Hoskin, P. J.; Lister, A.; Radford, J. A.; Rohatiner, A. Z.; Linch, D. C. Myocardial infarction mortality risk after treatment for Hodgkin disease: a collaborative British cohort study. *J. Natl. Cancer Inst* **2007**, *99* (3), 206−14.

(3) Carr, Z. A.; Land, C. E.; Kleinerman, R. A.; Weinstock, R. W.; Stovall, M.; Griem, M. L.; Mabuchi, K. Coronary heart disease after radiotherapy for peptic ulcer disease. *Int. J. Radiat. Oncol., Biol., Phys.* **2005**, *61* (3), 842−50.

(4) Tukenova, M.; Guibout, C.; Oberlin, O.; Doyon, F.; Mousannif, A.; Haddy, N.; Guerin, S.; Pacquement, H.; Aouba, A.; Hawkins, M.; Winter, D.; Bourhis, J.; Lefkopoulos, D.; Diallo, I.; de Vathaire, F. Role of cancer treatment in long-term overall and cardiovascular mortality after childhood cancer. *J. Clin. Oncol.* **2010**, *28* (8), 1308−15.

(5) Darby, S.; McGale, P.; Peto, R.; Granath, F.; Hall, P.; Ekbom, A. Mortality from cardiovascular disease more than 10 years after radiotherapy for breast cancer: nationwide cohort study of 90 000 Swedish women. *Bmj* **2003**, *326* (7383), 256−7.

(6) Darby, S. C.; McGale, P.; Taylor, C. W.; Peto, R. Long-term mortality from heart disease and lung cancer after radiotherapy for early breast cancer: prospective cohort study of about 300,000 women in US SEER cancer registries. *Lancet Oncol.* **2005**, *6* (8), 557−65.

(7) Guven, M.; Guven, G. S.; Oz, E.; Ozaydin, A.; Batar, B.; Ulutin, T.; Hacihanefioglu, S.; Domanic, N. DNA repair gene XRCC1 and XPD polymorphisms and their association with coronary artery disease risks and micronucleus frequency. *Heart Vessels* **2007**, *22* (6), 355−60.

(8) Taylor, C. W.; Povall, J. M.; McGale, P.; Nisbet, A.; Dodwell, D.; Smith, J. T.; Darby, S. C. Cardiac dose from tangential breast cancer radiotherapy in the year 2006. *Int. J. Radiat. Oncol., Biol., Phys.* **2008**, *72* (2), 501−7.

(9) Cuzick, J.; Stewart, H.; Rutqvist, L.; Houghton, J.; Edwards, R.; Redmond, C.; Peto, R.; Baum, M.; Fisher, B.; Host, H. Cause-specific mortality in long-term survivors of breast cancer who participated in trials of radiotherapy. *J. Clin. Oncol.* **1994**, *12* (3), 447−453.

(10) Shimizu, Y.; Pierce, D. A.; Preston, D. L.; Mabuchi, K. Studies of the mortality of atomic bomb survivors. Report 12, part II. Noncancer mortality: 1950−1990. *Radiat. Res.* **1999**, *152* (4), 374−389.

(11) Little, M. P.; Azizova, T. V.; Bazyka, D.; Bouffler, S. D.; Cardis, E.; Chekin, S.; Chumak, V. V.; Cucinotta, F. A.; de Vathaire, F.; Hall, P.; Harrison, J. D.; Hildebrandt, G.; Ivanov, V.; Kashcheev, V. V.; Klymenko, S. V.; Kreuzer, M.; Laurent, O.; Ozasa, K.; Schneider, T.; Tapio, S.; Taylor, A. M.; Tzoulaki, I.; Vandoolaeghe, W. L.; Wakeford, R.; Zablotska, L. B.; Zhang, W.; Lipshultz, S. E. Systematic review and meta-analysis of circulatory disease from exposure to low-level ionizing radiation and estimates of potential population mortality risks. *Environ. Health Perspect* **2012**, *120* (11), 1503−11.

(12) Baker, J. E.; Moulder, J. E.; Hopewell, J. W. Radiation as a risk factor for cardiovascular disease. *Antioxid. Redox Signaling* **2011**, *15* (7), 1945−56.

(13) Azimzadeh, O.; Sievert, W.; Sarioglu, H.; Yentrapalli, R.; Barjaktarovic, Z.; Sriharshan, A.; Ueffing, M.; Janik, D.; Aichler, M.; Atkinson, M. J.; Multhoff, G.; Tapio, S. PPAR Alpha: A Novel Radiation Target in Locally Exposed Mus musculus Heart Revealed by Quantitative Proteomics. *J. Proteome Res.* **2013**, *12* (6), 2700−2714.

(14) Azimzadeh, O.; Sievert, W.; Sarioglu, H.; Merl-Pham, J.; Yentrapalli, R.; Bakshi, M. V.; Janik, D.; Ueffing, M.; Atkinson, M. J.; Multhoff, G.; Tapio, S. Integrative proteomics and targeted transcriptomics analyses in cardiac endothelial cells unravel mechanisms of long-term radiation-induced vascular dysfunction. *J. Proteome Res.* **2015**, *14* (2), 1203−19.

(15) Seemann, I.; Gabriels, K.; Visser, N. L.; Hoving, S.; te Poele, J. A.; Pol, J. F.; Gijbels, M. J.; Janssen, B. J.; van Leeuwen, F. W.; Daemen, M. J.; Heeneman, S.; Stewart, F. A. Irradiation induced modest changes in

DOI: 10.1021/acs.jproteome.6b00795
J. Proteome Res. 2017, 16, 307−318

murine cardiac function despite progressive structural damage to the myocardium and microvasculature. *Radiother. Oncol.* **2012**, *103* (2), 143−50.
(16) Smeets, P. J.; Planavila, A.; van der Vusse, G. J.; van Bilsen, M. Peroxisome proliferator-activated receptors and inflammation: take it to heart. *Acta Physiol.* **2007**, *191* (3), 171−88.
(17) Fruchart, J. C. Peroxisome proliferator-activated receptor-alpha (PPARalpha): at the crossroads of obesity, diabetes and cardiovascular disease. *Atherosclerosis* **2009**, *205* (1), 1−8.
(18) Finck, B. N. The PPAR regulatory system in cardiac physiology and disease. *Cardiovasc. Res.* **2007**, *73* (2), 269−77.
(19) Diep, Q. N.; Benkirane, K.; Amiri, F.; Cohn, J. S.; Endemann, D.; Schiffrin, E. L. PPAR alpha activator fenofibrate inhibits myocardial inflammation and fibrosis in angiotensin II-infused rats. *J. Mol. Cell. Cardiol.* **2004**, *36* (2), 295−304.
(20) Derynck, R.; Zhang, Y. E. Smad-dependent and Smad-independent pathways in TGF-beta family signalling. *Nature* **2003**, *425* (6958), 577−584.
(21) Hein, S.; Arnon, E.; Kostin, S.; Schönburg, M.; Elsässer, A.; Polyakova, V.; Bauer, E. P.; Klövekorn, W.-P.; Schaper, J. Progression from compensated hypertrophy to failure in the pressure-overloaded human heart: structural deterioration and compensatory mechanisms. *Circulation* **2003**, *107* (7), 984−991.
(22) Rosenkranz, S.; Flesch, M.; Amann, K.; Haeuseler, C.; Kilter, H.; Seeland, U.; Schlüter, K.-D.; Böhm, M. Alterations of beta-adrenergic signaling and cardiac hypertrophy in transgenic mice overexpressing TGF-beta(1). *American journal of physiology. Heart and circulatory physiology* **2002**, *283* (3), H1253−62.
(23) Anscher, M. S. Targeting the TGF-beta1 pathway to prevent normal tissue injury after cancer therapy. *Oncologist* **2010**, *15* (4), 350−9.
(24) Barcellos-Hoff, M. H.; Derynck, R.; Tsang, M. L.; Weatherbee, J. A. Transforming growth factor-beta activation in irradiated murine mammary gland. *J. Clin. Invest.* **1994**, *93* (2), 892−9.
(25) Scharpfenecker, M.; Kruse, J. J.; Sprong, D.; Russell, N. S.; Ten Dijke, P.; Stewart, F. A. Ionizing radiation shifts the PAI-1/ID-1 balance and activates notch signaling in endothelial cells. *Int. J. Radiat. Oncol., Biol., Phys.* **2009**, *73* (2), 506−13.
(26) Shi, Y.; Massague, J. Mechanisms of TGF-beta signaling from cell membrane to the nucleus. *Cell* **2003**, *113* (6), 685−700.
(27) Zhang, Y. E. Non-Smad pathways in TGF-beta signaling. *Cell Res.* **2009**, *19* (1), 128−39.
(28) Lakatos, H. F.; Thatcher, T. H.; Kottmann, R. M.; Garcia, T. M.; Phipps, R. P.; Sime, P. J. The Role of PPARs in Lung Fibrosis. *PPAR Res.* **2007**, *2007*, 71323.
(29) Lee, C. H.; Kim, H. D.; Shin, S. M.; Kim, S. G. A Novel Mechanism of PPARgamma Regulation of TGFbeta1: Implication in Cancer Biology. *PPAR Res.* **2008**, *2008*, 762398.
(30) Barger, P. M.; Brandt, J. M.; Leone, T. C.; Weinheimer, C. J.; Kelly, D. P. Deactivation of peroxisome proliferator-activated receptor-alpha during cardiac hypertrophic growth. *J. Clin. Invest.* **2000**, *105* (12), 1723−30.
(31) Munshi, A.; Ramesh, R. Mitogen-activated protein kinases and their role in radiation response. *Genes Cancer* **2013**, *4* (9−10), 401−8.
(32) Seemann, I.; Te Poele, J. A.; Luikinga, S. J.; Hoving, S.; Stewart, F. A. Endoglin haplo-insufficiency modifies the inflammatory response in irradiated mouse hearts without affecting structural and mircovascular changes. *PLoS One* **2013**, *8* (7), e68922.
(33) Wisniewski, J. R.; Zougman, A.; Nagaraj, N.; Mann, M. Universal sample preparation method for proteome analysis. *Nat. Methods* **2009**, *6* (5), 359−62.
(34) Hauck, S. M.; Dietter, J.; Kramer, R. L.; Hofmaier, F.; Zipplies, J. K.; Amann, B.; Feuchtinger, A.; Deeg, C. A.; Ueffing, M. Deciphering membrane-associated molecular processes in target tissue of autoimmune uveitis by label-free quantitative mass spectrometry. *Mol. Cell. Proteomics* **2010**, *9* (10), 2292−305.
(35) Merl, J.; Ueffing, M.; Hauck, S. M.; von Toerne, C. Direct comparison of MS-based label-free and SILAC quantitative proteome profiling strategies in primary retinal Muller cells. *Proteomics* **2012**, *12* (12), 1902−11.
(36) Chen, J. J.; Wang, S. J.; Tsai, C. A.; Lin, C. J. Selection of differentially expressed genes in microarray data analysis. *Pharmacogenomics J.* **2007**, *7* (3), 212−20.
(37) Storey, J. D.; Tibshirani, R. Statistical significance for genomewide studies. *Proc. Natl. Acad. Sci. U. S. A.* **2003**, *100* (16), 9440−5.
(38) Wu, J.; Liu, W.; Bemis, A.; Wang, E.; Qiu, Y.; Morris, E. A.; Flannery, C. R.; Yang, Z. Comparative proteomic characterization of articular cartilage tissue from normal donors and patients with osteoarthritis. *Arthritis Rheum.* **2007**, *56* (11), 3675−84.
(39) D'Eustachio, P. Reactome knowledgebase of human biological pathways and processes. *Methods Mol. Biol.* **2011**, *694*, 49−61.
(40) Derynck, R.; Zhang, Y. E. Smad-dependent and Smad-independent pathways in TGF-beta family signalling. *Nature* **2003**, *425* (6958), 577−84.
(41) Zhou, J.; Wang, K. C.; Wu, W.; Subramaniam, S.; Shyy, J. Y.; Chiu, J. J.; Li, J. Y.; Chien, S. MicroRNA-21 targets peroxisome proliferators-activated receptor-alpha in an autoregulatory loop to modulate flow-induced endothelial inflammation. *Proc. Natl. Acad. Sci. U. S. A.* **2011**, *108* (25), 10355−60.
(42) Wang, T.; Zhang, L.; Shi, C.; Sun, H.; Wang, J.; Li, R.; Zou, Z.; Ran, X.; Su, Y. TGF-beta-induced miR-21 negatively regulates the antiproliferative activity but has no effect on EMT of TGF-beta in HaCaT cells. *Int. J. Biochem. Cell Biol.* **2012**, *44* (2), 366−76.
(43) Miyata, S.; Minobe, W.; Bristow, M. R.; Leinwand, L. A. Myosin heavy chain isoform expression in the failing and nonfailing human heart. *Circ. Res.* **2000**, *86* (4), 386−390.
(44) Koussounadis, A.; Langdon, S. P.; Um, I. H.; Harrison, D. J.; Smith, V. A. Relationship between differentially expressed mRNA and mRNA-protein correlations in a xenograft model system. *Sci. Rep.* **2015**, *5*, 10775.
(45) Vogel, C.; Marcotte, E. M. Insights into the regulation of protein abundance from proteomic and transcriptomic analyses. *Nat. Rev. Genet.* **2012**, *13* (4), 227−32.
(46) Olivares-Hernandez, R.; Bordel, S.; Nielsen, J. Codon usage variability determines the correlation between proteome and transcriptome fold changes. *BMC Syst. Biol.* **2011**, *5*, 33.
(47) Wu, G.; Nie, L.; Zhang, W. Integrative analyses of posttranscriptional regulation in the yeast Saccharomyces cerevisiae using transcriptomic and proteomic data. *Curr. Microbiol.* **2008**, *57* (1), 18−22.
(48) Dobaczewski, M.; Chen, W.; Frangogiannis, N. G. Transforming growth factor (TGF)-beta signaling in cardiac remodeling. *J. Mol. Cell. Cardiol.* **2011**, *51* (4), 600−6.
(49) Sun, W.; Ni, X.; Sun, S.; Cai, L.; Yu, J.; Wang, J.; Nie, B.; Sun, Z.; Ni, X.; Cao, X. Adipose-Derived Stem Cells Alleviate Radiation-Induced Muscular Fibrosis by Suppressing the Expression of TGF-beta1. *Stem Cells Int.* **2016**, *2016*, 5638204.
(50) Diez, J. Altered degradation of extracellular matrix in myocardial remodelling: the growing role of cathepsins and cystatins. *Cardiovasc. Res.* **2010**, *87* (4), 591−2.
(51) Westermann, D.; Mersmann, J.; Melchior, A.; Freudenberger, T.; Petrik, C.; Schaefer, L.; Lullmann-Rauch, R.; Lettau, O.; Jacoby, C.; Schrader, J.; Brand-Herrmann, S. M.; Young, M. F.; Schultheiss, H. P.; Levkau, B.; Baba, H. A.; Unger, T.; Zacharowski, K.; Tschope, C.; Fischer, J. W. Biglycan is required for adaptive remodeling after myocardial infarction. *Circulation* **2008**, *117* (10), 1269−76.
(52) Taunk, N. K.; Haffty, B. G.; Kostis, J. B.; Goyal, S. Radiation-induced heart disease: pathologic abnormalities and putative mechanisms. *Front. Oncol.* **2015**, *5*, 39.
(53) Azimzadeh, O.; Azizova, T.; Merl-Pham, J.; Subramanian, V.; Bakshi, M. V.; Moseeva, M.; Zubkova, O.; Hauck, S. M.; Anastasov, N.; Atkinson, M. J.; Tapio, S. A dose-dependent perturbation in cardiac energy metabolism is linked to radiation-induced ischemic heart disease in Mayak nuclear workers. *Oncotarget* **2016**, DOI: 10.18632/oncotarget.10424.
(54) Gervois, P.; Torra, I. P.; Chinetti, G.; Grotzinger, T.; Dubois, G.; Fruchart, J. C.; Fruchart-Najib, J.; Leitersdorf, E.; Staels, B. A truncated human peroxisome proliferator-activated receptor alpha splice variant

DOI: 10.1021/acs.jproteome.6b00795
J. Proteome Res. 2017, 16, 307−318

with dominant negative activity. *Mol. Endocrinol.* **1999**, *13* (9), 1535−49.
(55) Marx, N.; Kehrle, B.; Kohlhammer, K.; Grub, M.; Koenig, W.; Hombach, V.; Libby, P.; Plutzky, J. PPAR activators as antiinflammatory mediators in human T lymphocytes: implications for atherosclerosis and transplantation-associated arteriosclerosis. *Circ. Res.* **2002**, *90* (6), 703−10.
(56) Sievert, W.; Trott, K. R.; Azimzadeh, O.; Tapio, S.; Zitzelsberger, H.; Multhoff, G. Late proliferating and inflammatory effects on murine microvascular heart and lung endothelial cells after irradiation. *Radiother. Oncol.* **2015**, *117* (2), 376−81.
(57) Sekiguchi, K.; Tian, Q.; Ishiyama, M.; Burchfield, J.; Gao, F.; Mann, D. L.; Barger, P. M. Inhibition of PPAR-alpha activity in mice with cardiac-restricted expression of tumor necrosis factor: potential role of TGF-beta/Smad3. *Am. J. Physiol Heart Circ Physiol* **2006**, *292* (3), H1443−H1451.
(58) Kintscher, U.; Lyon, C.; Wakino, S.; Bruemmer, D.; Feng, X.; Goetze, S.; Graf, K.; Moustakas, A.; Staels, B.; Fleck, E.; Hsueh, W. A.; Law, R. E. PPARalpha inhibits TGF-beta-induced beta5 integrin transcription in vascular smooth muscle cells by interacting with Smad4. *Circ. Res.* **2002**, *91* (11), e35−44.
(59) Iglarz, M.; Touyz, R. M.; Viel, E. C.; Paradis, P.; Amiri, F.; Diep, Q. N.; Schiffrin, E. L. Peroxisome proliferator-activated receptor-alpha and receptor-gamma activators prevent cardiac fibrosis in mineralocorticoid-dependent hypertension. *Hypertension* **2003**, *42* (4), 737−43.
(60) Ogata, T.; Miyauchi, T.; Irukayama-Tomobe, Y.; Takanashi, M.; Goto, K.; Yamaguchi, I. The peroxisome proliferator-activated receptor alpha activator fenofibrate inhibits endothelin-1-induced cardiac fibroblast proliferation. *J. Cardiovasc. Pharmacol.* **2004**, *44* (Suppl1), S279−82.
(61) Drosatos, K.; Drosatos-Tampakaki, Z.; Khan, R.; Homma, S.; Schulze, P. C.; Zannis, V. I.; Goldberg, I. J. Inhibition of c-Jun-N-terminal kinase increases cardiac peroxisome proliferator-activated receptor alpha expression and fatty acid oxidation and prevents lipopolysaccharide-induced heart dysfunction. *J. Biol. Chem.* **2011**, *286* (42), 36331−9.
(62) Cheng, Y.; Zhang, C. MicroRNA-21 in cardiovascular disease. *J. Cardiovasc Transl Res.* **2010**, *3* (3), 251−5.
(63) Thum, T.; Gross, C.; Fiedler, J.; Fischer, T.; Kissler, S.; Bussen, M.; Galuppo, P.; Just, S.; Rottbauer, W.; Frantz, S.; Castoldi, M.; Soutschek, J.; Koteliansky, V.; Rosenwald, A.; Basson, M. A.; Licht, J. D.; Pena, J. T.; Rouhanifard, S. H.; Muckenthaler, M. U.; Tuschl, T.; Martin, G. R.; Bauersachs, J.; Engelhardt, S. MicroRNA-21 contributes to myocardial disease by stimulating MAP kinase signalling in fibroblasts. *Nature* **2008**, *456* (7224), 980−4.
(64) Doenst, T.; Nguyen, T. D.; Abel, E. D. Cardiac metabolism in heart failure: implications beyond ATP production. *Circ. Res.* **2013**, *113* (6), 709−24 (1524−4571 (Electronic))..
(65) Khan, R.; Sheppard, R. Fibrosis in heart disease: understanding the role of transforming growth factor-beta in cardiomyopathy, valvular disease and arrhythmia. *Immunology* **2006**, *118* (1), 10−24.
(66) Lowes, B. D.; Minobe, W.; Abraham, W. T.; Rizeq, M. N.; Bohlmeyer, T. J.; Quaife, R. A.; Roden, R. L.; Dutcher, D. L.; Robertson, A. D.; Voelkel, N. F.; Badesch, D. B.; Groves, B. M.; Gilbert, E. M.; Bristow, M. R. Changes in gene expression in the intact human heart. Downregulation of alpha-myosin heavy chain in hypertrophied, failing ventricular myocardium. *J. Clin. Invest.* **1997**, *100* (9), 2315−2324.
(67) Litten, R. Z.; Fein, H. G.; Gainey, G. T.; Walden, T. L.; Smallridge, R. C. Alterations in rat cardiac myosin isozymes induced by whole-body irradiation are prevented by 3,5,3′-L-triiodothyronine. *Metab., Clin. Exp.* **1990**, *39* (1), 64−68.

DOI: 10.1021/acs.jproteome.6b00795
J. Proteome Res. 2017, 16, 307−318

2.2 A dose-dependent perturbation in cardiac energy metabolism is linked to radiation-induced ischemic heart disease in Mayak nuclear workers

2.2.1 Publication

The scientific data included in the following original research paper published in Oncotarget.

A dose-dependent perturbation in cardiac energy metabolism is linked to radiation-induced ischemic heart disease in Mayak nuclear workers

Omid Azimzadeh, Tamara Azizova, Juliane Merl-Pham, Vikram Subramanian, Mayur V. Bakshi, Maria Moseeva, Olga Zubkova, Stefanie M. Hauck, Nataša Anastasov, Michael J. Atkinson, Soile Tapio.

Oncotarget. 2017; 8:9067-9078

DOI: 10.18632/oncotarget.10424.

2.2.2 Aim of this study

An epidemiological study of the Mayak nuclear worker cohort has identified an increase in the incidence of ischemic heart disease (IHD) among workers exposed to external gamma-ray doses above 500mGy. Based on our previous work it was possible to use heart material from these workers to determine if the changes we have observed in the mouse are also occurring in humans. The study of heart tissue obtained from Mayak workers aims to examine changes in PPARα activity in irradiated hearts and investigate a possible involvement in radiation-induced ischemic heart disease. To answer this question, a quantitative proteomics study was performed on cardiac left ventricle samples from control (non-irradiated) and radiation-exposed male workers. The radiation exposed samples were grouped into three dose categories based on the registered cumulative dose (< 100 mGy, 100–500 mGy and > 500 mGy).

2.2.3 Summary of results

Global quantitative proteomics revealed a dose-dependent increase in the number of deregulated proteins relative to the non-exposed group. Thus 101 proteins were deregulated in the group exposed to a cumulative dose below 100 mGy, 225 proteins in workers exposed to a dose of 100–500 mGy and 431 proteins in the group exposed to the highest dose category of > 500 mGy. In total, 72 proteins were common to all three irradiated groups. Interestingly, a large portion of the deregulated proteins belonged to the cytoskeletal and mitochondrial proteomes.

To understand the biological function of the deregulated proteins, proteomics list from all three dose categories were analyzed by ingenuity pathway analysis software. This analysis determined that in all irradiated groups most of the deregulated proteins were involved in mitochondrial dysfunction and metabolic impairment, with a decrease in the expression of proteins belongs to mitochondrial respiratory complexes I, III and V seen at all doses, whilst complexes II and IV were only affected in the highest dose group. A set of proteins contributing to the energy production pathways associated with fatty acid oxidation (lipid metabolism, kerbs cycle) and glycolysis were also downregulated in a dose-dependent way compared to control groups. These data indicate that there is a reduction in energy production and supply pathways in the heart after irradiation. Most of the significantly deregulated proteins were found to be involved in cardiac disease including cardiac hypertrophy and left ventricle dysfunction in the heart. Also, deregulated proteins belonging to the actin cytoskeleton or calcium signaling pathways were over-represented in a dose-dependent manner in the irradiated groups.

Our bioinformatics analysis of deregulated proteins predicted the inhibition of PPARα in all irradiated groups. In accord with predicted inactivation, immunoblotting analysis showed a significant increase in the level of phosphorylated form of PPARα in pooled samples of irradiated groups compared to the control group. To confirm this finding at the individual level, the expression of total PPARα protein and the phosphorylated form of PPARα from all individual samples were also studied. Our results showed significant increase in the phosphorylated form of PPARα in irradiated samples of the two highest groups with no change in total PPARα protein expression in irradiated and control groups. This study also

showed an increased expression of miR-21 and miR-146-a (a potential biomarker for heart disease) in the highest dose group compared to the control groups.

Immunoblotting analysis indicated the downregulation of antioxidant defense proteins such as superoxide dismutase 2 (SOD2), peroxiredoxin 5 (PRDX5) and structural proteins such as troponin T (TNNT2), tropomyosin 2 (TPM2), and myosin light chain 2 (MYL2) in radiation-exposed groups. The expression of Nrf2 protein, a central regulator of the antioxidative response was significantly downregulated in the highest dose group.

This proteomic study of ventricle heart samples from irradiated individuals highlights a potential role for PPARα in the development of radiation-induced heart disease in man and is consistent with previous observations in the mouse. Based on our quantitative proteomics data this study showed reduced expression of proteins involved in energy metabolism such as fatty acid beta-oxidation and glycolytic pathways. It also suggests that the risk of developing ischemic heart disease after chronic exposure to an external radiation dose increases due to malfunction of PPARα signaling pathways.

2.2.4 Contribution

This study aimed to elucidate the role of PPARα in radiation-induced ischemic heart disease (IHD) in man. Dr. Tamara Azizova, Mari Moseeva, and Olga Zubkova (Southern Urals Biophysics Institute) contributed by collecting human heart sample from Mayak workers and controls included in this study. They also provided dosimetry estimates for each individual. I pulverized the human heart tissues, measured protein concentrations, and prepared protein lysate for the quantitative proteomics study.

I prepared the protein lysate from control and irradiated groups using modified filter-aided sample preparation (FASP) method for label-free mass spectrometry analysis. The LC-MS/MS run was performed by Dr. Juliane Merl-Pham (PROT/HMGU). I performed the western blotting experiments to validate the expression of PPAR alpha protein (total and phosphorylated level), as well as the structural and antioxidant proteins. Dr. Natasa Anastasov and Dr. Mayur Bakshi contributed the microRNA expression analysis. PD Dr. Soile Tapio and Dr. Omid Azimzadeh supervised the experiments and wrote the manuscript. All the

co-authors in this manuscript contributed to scientific discussion, corrections, and publication process.

2.2.5 Discussion

In this study, dose-dependent alterations in the cardiac proteome were observed in three groups of nuclear workers exposed to < 100 mGy, 100–500 mGy or > 500 mGy chronic radiation. The radiation-induced changes were seen in proteins involved in cardiac structure and function in a dose-dependent manner. This supports epidemiological data that found a dose-dependent increase in the ischemic heart disease (IHD) incidence in the Mayak radiation exposed worker cohort [222-223]. The quantitative proteomics analysis in this study showed downregulation of mitochondrial proteins that are in good agreement with data from our previous mouse model studies [38, 224-225]. A dose-dependent deregulation of these mitochondrial proteins suggests impaired mitochondrial function consistent with changes observed in other aetiologies of IHD [226]. Specifically, we found a dose-dependent reduction in the expression of proteins that belong to the mitochondrial respiratory complexs I, III and V in the irradiated heart. It has been shown that local heart irradiation in mice resulted in similar changes accompanied by mitochondrial dysfunction combined with the declined activity of respiratory complex I and III after 40 weeks of radiation [224]. Such a decreased mitochondrial respiration rate has been previously shown to increase reactive oxygen species(ROS) production in rats heart [227].

In previous study, we have shown in mice after local heart irradiation rises mitochondrial ROS levels [224, 228]. This current study showed a dose-dependent decrease in the expression of the Nrf2 protein, an antioxidant response regulator. Proteomics data have demonstrated reduced expression of Nrf2 target proteins and oxidative response proteins in the highest radiation dose group. The proteins are targets of Nrf2, peroxiredoxins (PRDX1, PRDX2, PRDX3, PRDX5, and PRDX6), superoxide dismutase (SOD1 and SOD2), catalase and glutathione-S-transferases (kappa1, mu2, mu3, omega1, and pi1). The downregulation of these proteins was associated with a reduced antioxidant competence expressed as increased protein carbonylation. This suggests a radiation-induced increased production of ROS. Study have shown expression of miRNA-146a is increased by oxidative stress [229]. Our result indicated increased expression of

miRNA-146a in the highest dose group. Interestingly our data revealed downregulation of SOD2, a target protein of miRNA-146a [229] in this group.

Increased ROS synthesis leads to contractile impairment by damaging actin-myosin interactions through blocking actin-myosin polymerization process [230]. It has been shown that change in the redox system sensitizes cytoskeletal proteins to oxidative stress [231]. Our study revealed significant downregulation of many structural proteins (actin isoforms, tubulin, troponin, desmin, tropomyosin and heavy and light isoforms of myosin) in the highest radiation dose groups. The study has shown that both antioxidant response and myofibrillar structure have been influenced by PPARα in the heart [232]. Thus, an active link between PPARα deficiency and contractile dysfunction due to increased oxidative damage to myosin was observed in PPARα -/- mice [124]. So, the observed inhibition of PPARα activity after radiation exposure may intensify structural impairments and oxidative stress phenotypes seen in irradiated hearts

In this study (Chapter 2.2), we were able to predict a decrease in the transcriptional activity of PPARα from the observed dose-dependent reduction in the expression of PPAR target proteins. Data showed increased phosphorylation of PPARα in the irradiated workers. This is in good agreement with results from mouse studies presented in Chapter 2.1. Moreover, it is consistent with previously published data showing diminished cardiac fatty acid oxidation due to impaired activity of PPARα after high dose irradiation in mice [38]. This suggests that reduced activity of PPARα results in a metabolic impairment, and it is accompanied by a reduced expression of target proteins in heart.

In many cells and tissues, the level PPARα and expression of mitochondrial proteins were regulated by miR-21 [218, 233-234]. Our results showed upregulated expression of miR-21 in the left ventricle samples of the highest dose group. This relates to the observed downregulation of mitochondrial proteins in highest dose group. Interestingly increased expression of miR-21 is also observed in various heart diseases such as heart failure and ischemia [219, 235-236].

This study highlights the essential function of PPARα in radiation-induced ischemic heart disease.

www.impactjournals.com/oncotarget/ Oncotarget, 2017, Vol. 8, (No. 6), pp: 9067-9078

Research Paper

A dose-dependent perturbation in cardiac energy metabolism is linked to radiation-induced ischemic heart disease in Mayak nuclear workers

Omid Azimzadeh[1], Tamara Azizova[2], Juliane Merl-Pham[3], Vikram Subramanian[1], Mayur V. Bakshi[1], Maria Moseeva[2], Olga Zubkova[2], Stefanie M. Hauck[3], Nataša Anastasov[1], Michael J. Atkinson[1,4], Soile Tapio[1]

[1]Helmholtz Zentrum München-German Research Center for Environmental Health (GmbH), Institute of Radiation Biology, Neuherberg, Germany

[2]Southern Urals Biophysics Institute, Russian Federation, Ozyorsk, Russia

[3]Helmholtz Zentrum München-German Research Center for Environmental Health (GmbH), Research Unit Protein Science, Munich, Germany

[4]Chair of Radiation Biology, Technical University of Munich, Munich, Germany

Correspondence to: Soile Tapio, **email:** soile.tapio@helmholtz-muenchen.de

Keywords: *ionising radiation, proteomics, heart disease, PPAR alpha, mitochondrial dysfunction*

Received: *April 08, 2016* ***Accepted:*** *June 17, 2016* ***Published:*** *July 06, 2016*

ABSTRACT

Epidemiological studies show a significant increase in ischemic heart disease (IHD) incidence associated with total external gamma-ray dose among Mayak plutonium enrichment plant workers. Our previous studies using mouse models suggest that persistent alteration of heart metabolism due to the inhibition of peroxisome proliferator-activated receptor (PPAR) alpha accompanies cardiac damage after high doses of ionising radiation. The aim of the present study was to elucidate the mechanism of radiation-induced IHD in humans. The cardiac proteome response to irradiation was analysed in Mayak workers who were exposed only to external doses of gamma rays. All participants were diagnosed during their lifetime with IHD that also was the cause of death. Label-free quantitative proteomics analysis was performed on tissue samples from the cardiac left ventricles of individuals stratified into four radiation dose groups (0 Gy, < 100 mGy, 100–500 mGy, and > 500 mGy). The groups could be separated using principal component analysis based on all proteomics features. Proteome profiling showed a dose-dependent increase in the number of downregulated mitochondrial and structural proteins. Both proteomics and immunoblotting showed decreased expression of several oxidative stress responsive proteins in the irradiated hearts. The phosphorylation of transcription factor PPAR alpha was increased in a dose-dependent manner, which is indicative of a reduction in transcriptional activity with increased radiation dose. These data suggest that chronic external radiation enhances the risk for IHD by inhibiting PPAR alpha and altering the expression of mitochondrial, structural, and antioxidant components of the heart.

INTRODUCTION

Mayak Production Association (PA), located 150 km south-east of Ekaterinburg, is one of the biggest nuclear facilities in the Russian Federation. Individual dosimetric monitoring of external exposure performed at Mayak PA showed that the total external gamma-ray doses ranged widely from below 100 mGy to more than 5 Gy, with 32.6% of the workers having a total dose greater than 1 Gy [1]. Epidemiological studies in this cohort showed a significant increase in ischemic heart disease (IHD) incidence associated with total external gamma-ray dose after correction for multiple competing factors such as smoking and alcohol consumption [1–3]. The risk estimates for IHD in relation to chronic external radiation dose are generally compatible with those reported in other large occupational studies and the Japanese A-bomb survivors [4].

Mitochondrial dysfunction plays a key role in the pathogenesis of IHD [5]. A high rate of mitochondrial catabolism of carbohydrates and fatty acids is crucial for furnishing the energy supply necessary for heart function [6]. Under normal conditions the adult heart relies mostly on fatty acids for this energy production via the oxidative phosphorylation (OXPHOS) process, with only 10% to 30% of total ATP being derived from glucose [7]. However, a normal heart can easily switch between fatty acids and glucose for ATP production, depending on energy demand and substrate availability [8]. In pathological conditions such as IHD this flexibility is lost and either superseded by a preference for glucose over fat [9] or an overall reduction of mitochondrial oxidative metabolism independent of the energy source [10]. Both scenarios are associated with the reduction in the level of active peroxisome proliferator-activated receptor (PPAR) alpha in cardiac ventricles [11]. PPAR alpha functions as a key regulator of cardiac metabolism and is essential for fatty acid oxidation [6].

We have previously shown that local heart irradiation in mice persistently decreases the respiratory capacity of cardiac mitochondria [12, 13], reduces their number, and results in damage to the cristae structure [14]. Importantly, the activity of the transcription factor PPAR alpha is reduced by a dose-dependent increase in phosphorylation [14].

Although mouse models are widely used to study cardiac disease, there are functional differences between mouse and human hearts [15]. Infarction is virtually unknown in mice, probably due to their short life span, and differences in the heart physiology and diet. Even though mouse models have led to important observations on the causes of radiation-induced IHD, the question of their clinical relevance remains.

The aim of the present study was to examine whether alteration in cardiac metabolism, and its key regulator PPAR alpha, contribute to radiation-induced IHD in man. Here, we investigated human left ventricle proteome profiles in Mayak workers who had been occupationally exposed to different cumulative doses of external gamma rays. All participants had previously been diagnosed with IHD that also was the primary cause of death [1, 16]. The proteomic analysis revealed a dose-dependent series of alteration in the levels of proteins involved in the left ventricle function and structure. These include proteins critical for mitochondrial energy metabolism and cardiac cytoskeleton. A significant inactivation of PPAR alpha by phosphorylation was observed in the highest dose group (> 500 mGy). The present study provides, for the first time, a proteomics signature of radiation-induced human heart ischemia. This is coherent with the observations made using irradiated mice upon the radiation dose.

RESULTS

Chronic irradiation alters the heart proteome in a dose-dependent manner

Global proteomics analysis identified 1,281 proteins in total (Supplementary Table S1). Of the quantified proteins, 101, 225 and 431 proteins were significantly changed in expression (2 unique peptides; fold change ≥ 1.30 or ≤ 0.77; $q < 0.05$) after exposure to doses of < 100 mGy, 100–500 mGy and > 500 mGy, respectively. This indicated a dose-dependent increase in the number of deregulated proteins (Supplementary Tables S2–S4), as seen in irradiated mouse heart models [14]. A large number (72) of deregulated proteins were shared between all three irradiated groups compared to the control (Table 1). The majority of these shared proteins belonged to mitochondria (24 proteins) or cytoskeleton (13 proteins).

To investigate differences in the proteome profiles between the different dose groups, a PCA based on all proteomics features was performed. Control and irradiated samples clustered into four groups according to the dose (Figure 1). The distance between the cluster that represents the control group and the clusters representing the irradiated groups increased with increasing dose. Even though the workers exposed to the highest dose (> 500 mGy) were generally older than the members of other groups, the PCA did not show any clustering based on age. Similarly, no clustering was observed based on smoking status or index, alcohol consumption, or body mass index (Supplementary Table S10).

Some outliers were identified in each irradiated group, namely donors 3, 25 and 46 (Figure 1). Sample number 25, belonging to the group < 100 mGy, was exposed to the very low dose of 6 mGy, and unsurprisingly showed proteomics features that were more similar to those of the control group. Sample number 3, belonging to the dose group of 100–500 mGy, was exposed to the dose of 114 mGy and showed similarity with the group of < 100 mGy. Sample number 46, a member of the dose group 100–500 mGy, was exposed to the dose of 483 mGy, and was placed in close proximity to the group exposed to the highest dose (> 500 mGy) (Figure 1 and Supplementary Table S10). These deviations strengthen the evidence for a dose-response relationship.

A detailed analysis of functional interactions and biological pathways was performed using IPA (http://www.INGENUITY.com) (Supplementary Tables S5 and S6). Mitochondrial dysfunction and metabolic impairment were indicated in all irradiated groups compared to the control group (Figure 2A). A dose-dependent reduction was found in the expression of proteins of the respiratory complexes I, III and V. The complexes II and IV were affected only

Table 1: Significantly deregulated proteins shared in all radiation dose groups

#	Symbol	Entrez Gene Name	ratio	ratio	ratio	GO - Molecular function
			< 100 mGy/ control	100–500 mGy/ controls	> 500 mGy/ controls	
1	ACAT1	acetyl-CoA acetyltransferase 1	0.77	0.68	0.42	metabolic activity (GO:0003824)
2	AHSG	alpha-2-HS-glycoprotein	0.47	0.63	0.33	metabolic activity (GO:0003824)
3	AIFM1	apoptosis-inducing factor, mitochondrion-associated, 1	0.65	0.62	0.40	antioxidant activity (GO:0016209)
4	AK2	adenylate kinase 2	0.74	0.76	0.48	metabolic activity (GO:0003824)
5	ALDOA	aldolase A, fructose-bisphosphate	0.63	0.63	0.42	metabolic activity (GO:0003824)
6	ANXA11	annexin A11	0.77	0.73	0.53	structural molecule activity (GO:0005198)
7	ATP5B	ATP synthase, H+ transporting, beta	0.62	0.62	0.38	metabolic activity (GO:0003824)
8	CCT3	chaperonin containing TCP1, subunit 3 (gamma)	0.65	0.76	0.52	ATP binding (GO:0005524)
9	CHCHD3	coiled-coil-helix-coiled-coil-helix domain containing 3	0.46	0.6	0.34	structural molecule activity (GO:0005198)
10	CKM	creatine kinase, muscle	0.66	0.65	0.38	metabolic activity (GO:0003824)
11	COQ9	coenzyme Q9	0.73	0.55	0.38	metabolic activity (GO:0003824)
12	DBI	GABA receptor modulator, acyl-CoA binding protein	0.73	0.68	0.41	metabolic activity (GO:0003824)
13	DECR1	2,4-dienoyl CoA reductase 1, mitochondrial	0.7	0.57	0.39	metabolic activity (GO:0003824)
14	DLD	dihydrolipoamide dehydrogenase	0.74	0.64	0.51	metabolic activity (GO:0003824)
15	ECI1	enoyl-CoA delta isomerase 1	0.7	0.65	0.44	metabolic activity (GO:0003824)
16	FH	fumarate hydratase	0.71	0.61	0.40	metabolic activity (GO:0003824)
17	GLRX5	glutaredoxin 5	0.52	0.5	0.37	antioxidant activity (GO:0016209)
18	HADH	hydroxyacyl-CoA dehydrogenase	0.67	0.58	0.37	metabolic activity (GO:0003824)
19	HNRNPA1L2	heterogeneous nuclear ribonucleoprotein A1-like 2	0.77	0.73	0.56	nucleotide binding (GO:0000166)
20	HNRNPA2B1	heterogeneous nuclear ribonucleoprotein A2/B1	0.77	0.77	0.44	nucleotide binding (GO:0000166)
21	HSD17B10	hydroxysteroid (17-beta) dehydrogenase 10	0.76	0.66	0.42	metabolic activity (GO:0003824)
22	LDHB	lactate dehydrogenase B	0.78	0.6	0.49	metabolic activity (GO:0003824)
23	LGALS1	lectin, galactoside-binding, soluble, 1	0.59	0.53	0.32	nucleotide binding (GO:0000166)
24	LGALS3	lectin, galactoside-binding, soluble, 3	0.48	0.49	0.29	nucleotide binding (GO:0000166)
25	MCCC1	methylcrotonoyl-CoA carboxylase 1 (alpha)	0.62	0.52	0.39	ATP binding (GO:0005524)
26	MCEE	methylmalonyl CoA epimerase	0.64	0.63	0.47	metabolic activity (GO:0003824)
27	MDH2	malate dehydrogenase 2, NAD (mitochondrial)	0.73	0.68	0.44	metabolic activity (GO:0003824)
28	ME3	malic enzyme 3, NADP(+)-dependent, mitochondrial	3.8	6.21	4.45	metabolic activity (GO:0003824)
29	MECR	mitochondrial trans-2-enoyl-CoA reductase	0.62	0.55	0.38	metabolic activity (GO:0003824)
30	MYBPC3	myosin binding protein C, cardiac	0.74	0.57	0.45	structural molecule activity (GO:0005198)
31	MYH10	myosin, heavy chain 10, non-muscle	2.16	2.91	1.92	structural molecule activity (GO:0005198)
32	MYH11	myosin, heavy chain 11, smooth muscle	0.45	0.56	0.52	structural molecule activity (GO:0005198)
33	MYL2	myosin, light chain 2, regulatory, cardiac, slow	0.63	0.65	0.40	structural molecule activity (GO:0005198)
34	MYL3	myosin, light chain 3, alkali; ventricular, skeletal, slow	0.67	0.65	0.41	structural molecule activity (GO:0005198)
35	MYL6	myosin light chain 6,smooth muscle and non-muscle	0.54	0.68	0.38	structural molecule activity (GO:0005198)
36	MYOM1	myomesin 1	0.76	0.58	0.44	structural molecule activity (GO:0005198)
37	MYOM2	myomesin 2	0.7	0.51	0.39	structural molecule activity (GO:0005198)
38	NDUFA3	NADH dehydrogenase (ubiquinone) 1 alpha	0.41	0.56	0.29	metabolic activity (GO:0003824)
39	NID1	nidogen 1	0.69	0.67	0.42	extracellular matrix binding (GO:0050840)
40	NMT1	N-myristoyltransferase 1	3.4	16.63	23.75	apoptotic activity (GO:0006915)
41	NPM1	nucleolar phosphoprotein B23, numatrin	0.72	0.77	0.44	histone binding (GO:0042393)
42	PARK7	protein deglycase DJ-1	0.73	0.72	0.46	nucleic acid binding transcription factor activity (GO:0001071)
43	PCMT1	protein-L-isoaspartate (D-aspartate) O-methyltransferase	0.71	0.68	0.53	metabolic activity (GO:0003824)
44	PDHA1	pyruvate dehydrogenase (lipoamide) alpha 1	0.77	0.63	0.47	metabolic activity (GO:0003824)
45	PDHB	pyruvate dehydrogenase (lipoamide) beta	0.76	0.56	0.46	metabolic activity (GO:0003824)
46	PGAM2	phosphoglycerate mutase 2 (muscle)	0.7	0.55	0.36	metabolic activity (GO:0003824)
47	PGK1	phosphoglycerate kinase 1	0.67	0.59	0.40	metabolic activity (GO:0003824)

48	PGM1	phosphoglucomutase 1	0.7	0.48	0.35	metabolic activity (GO:0003824)
49	PKM	pyruvate kinase, muscle	0.73	0.56	0.38	metabolic activity (GO:0003824)
50	PLEC	plectin	0.73	0.64	0.43	structural molecule activity (GO:0005198)
51	PPP1CB	protein phosphatase 1, beta isozyme	1.61	2.09	1.62	structural molecule activity (GO:0005198)
52	PRDX3	peroxiredoxin 3	0.76	0.73	0.49	antioxidant activity (GO:0016209)
53	PRDX5	peroxiredoxin 5	0.74	0.64	0.40	antioxidant activity (GO:0016209)
54	PRDX6	peroxiredoxin 6	0.74	0.72	0.47	antioxidant activity (GO:0016209)
55	PRKAR1A	protein kinase, cAMP-dependent, regulatory, type I, A	0.73	0.65	0.50	cAMP binding (GO:0030552)
56	PSMA5	proteasome (prosome, macropain) subunit, alpha type, 5	0.71	0.67	0.41	protein polyubiquitination (GO:0000209)
57	PSMA6	proteasome (prosome, macropain) subunit, alpha type, 6	0.64	0.62	0.46	protein polyubiquitination (GO:0000209)
58	PTRF	polymerase I and transcript release factor	0.65	0.65	0.46	poly(A) RNA binding (GO:0044822)
59	PYGM	phosphorylase, glycogen, muscle	0.54	0.49	0.24	metabolic activity (GO:0003824)
60	RPS27A	ribosomal protein S27a	0.74	0.62	0.44	structural molecule activity (GO:0005198)
61	SDPR	serum deprivation response	0.71	0.75	0.48	protein kinase C binding (GO:0005080)
62	SOD2	superoxide dismutase 2, mitochondrial	0.73	0.61	0.42	antioxidant activity (GO:0016209)
63	SPTA1	spectrin, alpha, erythrocytic 1	4.36	4.62	4.87	structural molecule activity (GO:0005198)
64	SUCLG1	succinate-CoA ligase, alpha subunit	0.72	0.74	0.45	metabolic activity (GO:0003824)
65	SUCLG2	succinate-CoA ligase, beta subunit	0.66	0.67	0.42	metabolic activity (GO:0003824)
66	TOM1L2	target of myb1 like 2 membrane trafficking protein	1.8	1.83	1.50	metabolic activity (GO:0003824)
67	TPM2	tropomyosin 2 (beta)	0.49	0.5	0.33	structural molecule activity (GO:0005198)
68	TUBA8	tubulin, alpha 8	0.55	0.56	0.38	structural molecule activity (GO:0005198)
69	TXN	thioredoxin	0.69	0.54	0.38	antioxidant activity (GO:0016209)
70	UQCR10	ubiquinol-cytochrome c reductase, subunit X	0.56	0.46	0.37	metabolic activity (GO:0003824)
71	UQCRC2	ubiquinol-cytochrome c reductase core protein II	0.63	0.57	0.39	metabolic activity (GO:0003824)
72	VCAN	versican	3.05	4.11	2.31	structural molecule activity (GO:0005198)

The accession number, protein ID, full name and fold change after exposure to < 100 mGy, 100–500 mGy or > 500 mGy is shown for each protein.

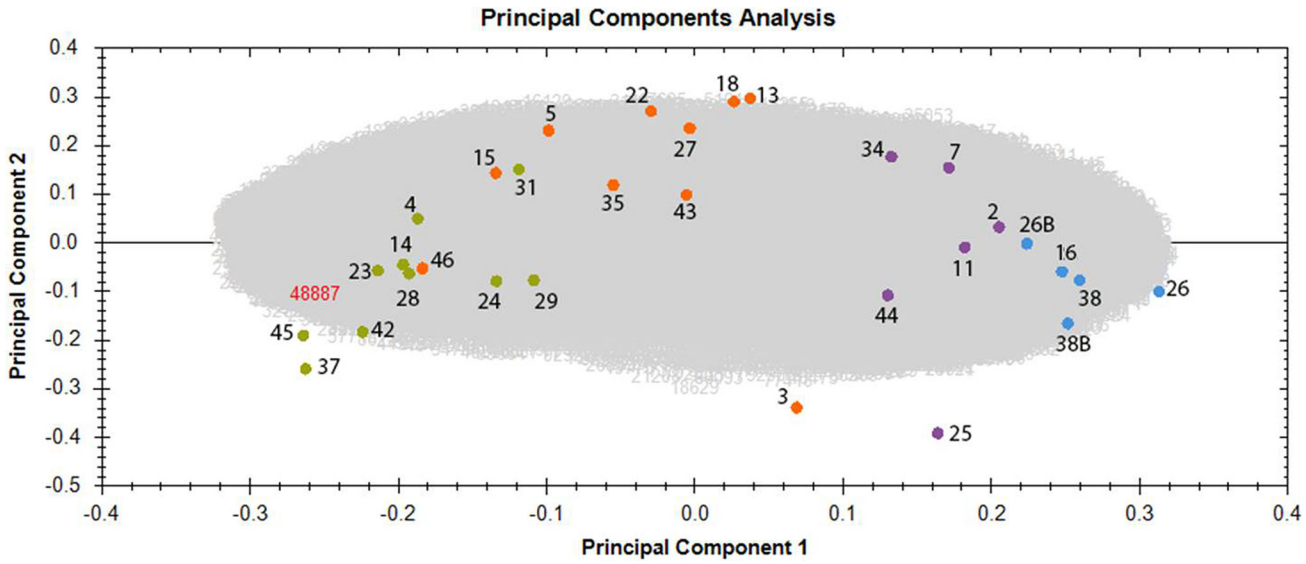

Figure 1: Principal component analysis (PCA) based on all proteomic features in the left ventricle of sample donors in different dose groups. The PCA used features with charges +2 to +7 resulting in PC1 and PC2 as follows: PC1 23.65% and PC2 8.36%. The control samples with the corresponding donor number are represented as blue spots, the samples exposed to < 100 mGy in purple, the samples exposed to 100–500 mGy in orange and the samples exposed to > 500 mGy in green. Samples number 26 and 38 were run as 2 technical replicates and are indicated as 26, 26B and 38, 38B. Detailed information of the sample donors and the exact doses are given in Supplementary Table S10. The analysis was performed using the Progenesis QI software (http://www.nonlinear.com).

in the two high-dose groups (Figure 2B). The number of deregulated mitochondrial proteins increased with the radiation dose (Figure 2C–2E and Supplementary Table S6).

Several proteins belonging to energy production pathways associated with fatty acid oxidation (lipid metabolism, Krebs cycle) were downregulated by irradiation (Figure 2A and Supplementary Table S6). Also several enzymes in the glycolysis pathway were downregulated (Supplementary Figure S1 and Supplementary Table S6), suggesting a general depletion of energy supply, rather than a glucose/lipid switch.

In addition, the number of deregulated proteins belonging to actin cytoskeleton or calcium signalling was increased in a dose-dependent manner (Supplementary Figure S2 and Supplementary Table S6). The majority of significantly altered proteins were associated with heart diseases including left ventricle dysfunction and heart hypertrophy (Supplementary Figure S3 and Supplementary Table S7).

Immunoblotting confirms radiation-induced downregulation of structural and antioxidant proteins

Consistent with the proteomics data, immunoblotting showed markedly decreased levels of the antioxidant defence proteins peroxiredoxin 5 (PRDX 5), and superoxide dismutase 2 (SOD2) after irradiation (Figure 3). The expression of transcription factor Nrf2, the central regulator of the antioxidative response, was significantly downregulated in the highest dose group (Figure 3). Significantly reduced expression of structural proteins myosin light chain 2 (MYL2), tropomyosin 2 (TPM2) and troponin T (TNNT2) was found in the highest dose group (Figure 3).

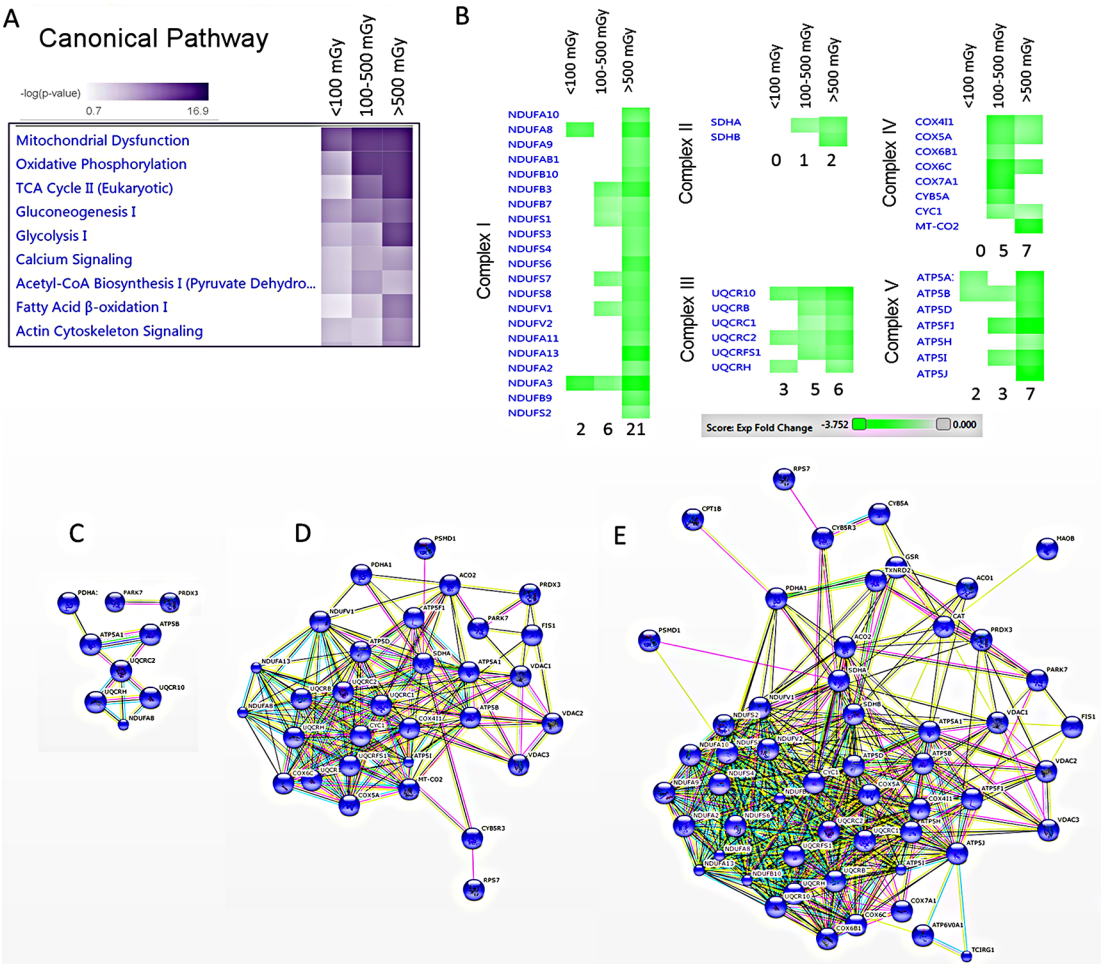

Figure 2: Pathway and network analysis of significantly differentially expressed mitochondrial proteins. A dose-dependent alteration is observed in the pathways involved in the energy production. The pathway scores are displayed using a purple colour gradient, where darker purple corresponds to higher scores (increased statistical significance). The score is the negative log of the *p*-value derived from the Fisher's Exact test. By default, the rows (pathways) with the highest total score across the set of observations are sorted to the top (**A**). Heat map for the expression values of differentially expressed OXPHOS proteins between dose groups is displayed using a green colour gradient for downregulated proteins, where dark green corresponds to large downregulation. The numbers shows how many proteins were deregulated in each subunit (**B**) (http://www.INGENUITY.com). Protein-protein interaction analysis of the significantly differentially expressed proteins showing the networks of deregulated mitochondrial proteins in the dose groups < 100 mGy (**C**), 100–500 mGy (**D**) and > 500 mGy (**E**) (http://string-db.org).

Irradiation enhances protein oxidation

As the proteomics and immunoblotting data indicated alterations in the oxidative stress response, the level of protein carbonylation (protein oxidation marker) was measured in the pooled samples from each of the different dose groups. A significant increase in protein carbonylation was found in the highest dose group compared to the control (Figure 4A).

Cardiac miRNAs are altered in irradiated hearts

MicroRNAs miR-21 and miR-146a are potential biomarkers of heart disease [17–19]. The expression of miR-21 and miR-146a was significantly upregulated in the highest dose group compared to the control and lower dose groups (Figure 4B, Supplementary Tables S8–S9).

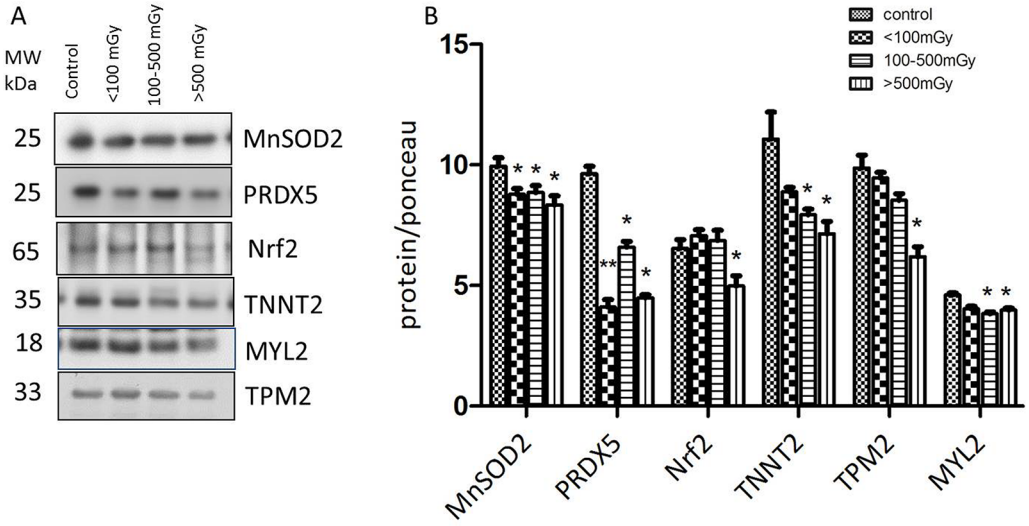

Figure 3: Immunoblot validation of the proteomics data. The heart protein lysates from each individual sample were pooled within the dose groups and tested using anti-Troponin T (TNNT2), anti-Tropomyosin 2 (TPM2), anti- Myosin light chain (MYL2), anti-Mn superoxide dismutase (SOD2), and anti-Peroxiredoxin 5 (PRDX5) (**A**).The columns represent the average ratios of relative protein expression in control and irradiated samples. The amount of the total protein was measured by Ponceau S staining for accurate comparison between the groups. The error bars represent standard error of the mean (± SEM) (**B**) (*t*-test; *$p < 0.05$, **$p < 0.01$; $n = 3$).

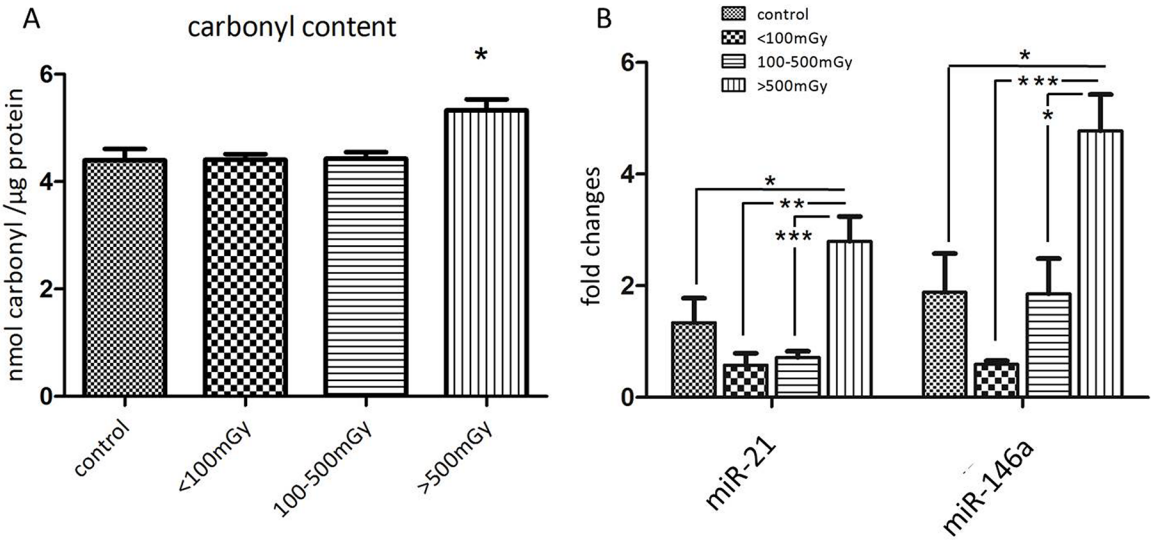

Figure 4: Analysis of the protein carbonyl levels and miR-21 and miR-146a in different dose groups. The total amount of carbonylated protein was measured in individual samples from each dose group. The samples in the control group were run in two technical replicates. Significantly increased level of carbonylated proteins was shown in the dose group > 500 mGy (**A**). Analysis of miR-21 and miR-146a from samples of all dose groups showed significant upregulation of both miRNAs in the dose group > 500 mGy (**B**) The error bars represent standard error of the mean (+ SEM) (*t*-test; * $p < 0.05$; **$p < 0.01$; *** $p < 0.001$).

Transcription factor PPAR alpha is inactivated by irradiation

Analysis of deregulated proteins predicted a significant inactivation of PPAR alpha in all exposed groups (Figure 5A–5C). The number of PPAR alpha target proteins found to have altered expression increased in a dose-dependent manner (Figure 5A–5C). Phosphorylation of PPAR alpha leads to its deactivation in the heart [20]. In agreement with the predicted inactivation, the analysis showed a significant increase in the phosphorylated form of PPAR alpha in pooled samples representing different irradiated groups (Figure 5D). To confirm this at the individual level, the expression of total PPAR alpha and its phosphorylated form were measured separately in all samples (Supplementary Figure S4). The total amount of PPAR alpha was not changed by irradiation (Figure 5E) but there was a significant increase in phospho-PPAR alpha in the irradiated samples in the highest dose groups (Figure 5F).

DISCUSSION

The aim of the present study was to elucidate potential biological mechanisms involved in the radiation-induced IHD in human. For this purpose, we analysed post-mortem samples from the cardiac left ventricle taken from Mayak workers previously exposed to different external radiation doses. This study shows that chronic radiation exposure is able to alter the heart proteome in a dose-dependent manner. The data indicate pronounced radiation-induced changes in proteins involved in the heart function and structure, thereby supporting epidemiological evidence of a significant dose-dependent increase in the IHD incidence reported in the Mayak cohort [2, 3, 21].

In agreement with our previous data obtained in mouse models [12–14, 22, 23] the proteomics analysis shows downregulation of several mitochondrial proteins. The number of deregulated mitochondrial proteins was increased in a dose-dependent manner, indicating increasing mitochondrial dysfunction, a critical pathologic

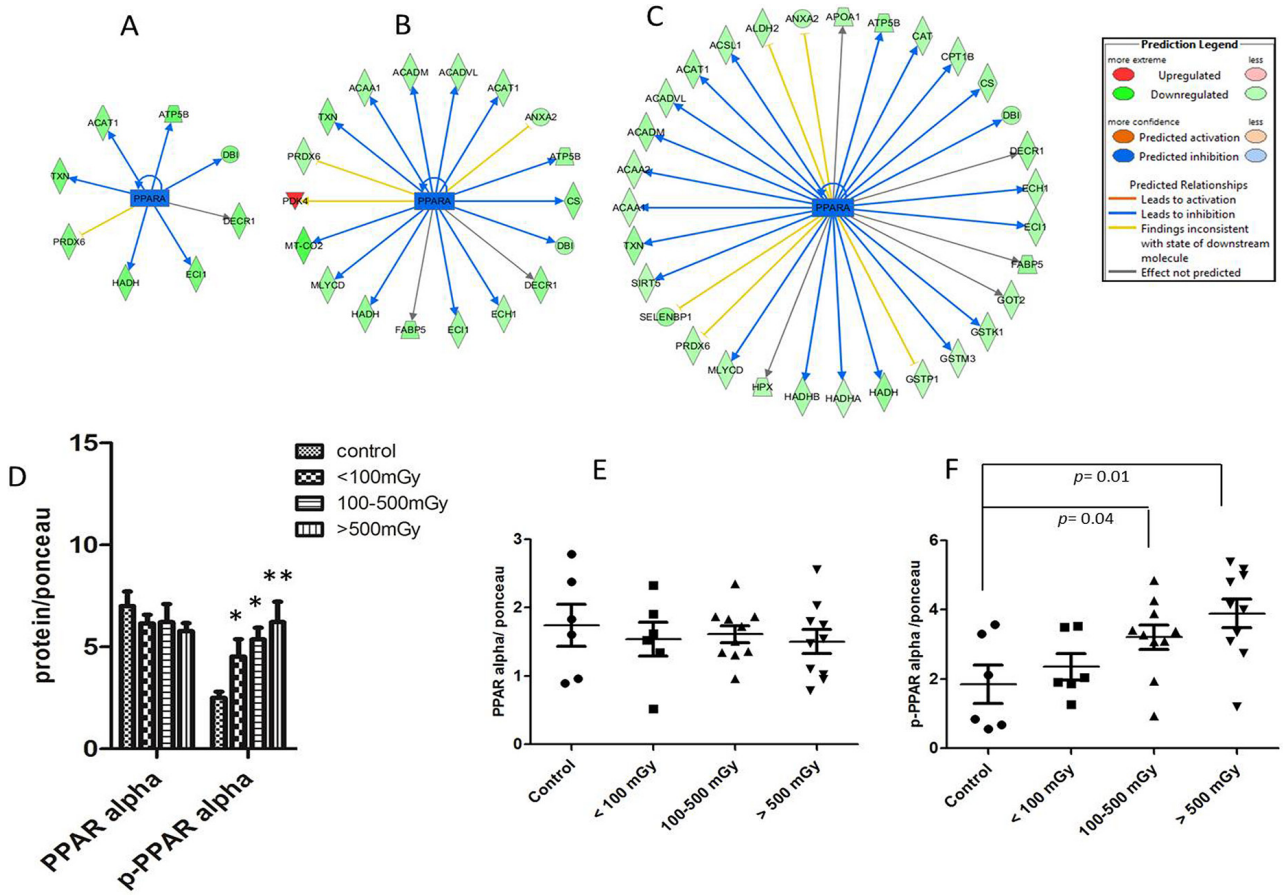

Figure 5: Analysis of the activation status of PPAR alpha. IPA prediction of inactivation of PPAR alpha based on the deregulated proteins from proteomics analysis in the dose groups < 100 mGy (**A**), 100–500 mGy (**B**) and > 500 mGy (**C**). The upregulated proteins are marked in red and the down-regulated in green. The blue colour of the node (PPAR alpha) indicates inactivation. The list of proteins is available in Supplementary Tables S2–S4. Immunoblot analysis of total and phospho-PPAR alpha (Ser12) in pooled samples is shown (**D**). The columns represent the average ratios of relative protein expression in control and irradiated samples. Immunoblot analysis of total PPAR alpha (**E**) and phospho-PPAR alpha (**F**) in individual samples from each dose group is shown. The icons represent individual samples in different dose groups. The samples in the control group were run in two technical replicates. The amount of the total protein was confirmed by Ponceau S staining for accurate comparison between the groups (*t*-test; $*p < 0.05$).

event in IHD [10]. In particular, the expression of proteins belonging to mitochondrial complexes I and III were significantly downregulated. We have previously reported that local heart irradiation in mice induces persistent functional and proteome alterations in cardiac mitochondria that are associated with reduced activity of complexes I and III [13]. Ischemic damage to the heart is also associated with defaults in the activity of complexes I and III [24, 25]. As the control group used in this study was also suffering from IHD, it can be suggested that chronic radiation worsens the respiratory complex impairment, at least on the proteome level.

A decrease in the mitochondrial respiration rate has been reported to enhance reactive oxygen species (ROS) production [26]. We have shown previously that local heart irradiation permanently increases mitochondrial ROS levels in mice [12, 13]. This study now shows a dose-dependent decrease in the level of the antioxidant response regulator protein Nrf2. The expression of many Nrf2 target proteins, as well as other proteins of oxidative response, were significantly downregulated (up to 50%) in the highest dose group. These included superoxide dismutases (SOD1 and SOD2), peroxiredoxins (1, 2, 3, 5, and 6), glutathione-S-transferases (kappa1, mu2, mu3, omega 1, pi1) and catalase. This marked downregulation of antioxidant capacity, coupled with increased carbonylation, suggests an increased radiation-induced ROS production. The expression of miR-146a is increased by oxidative stress [27]. This miRNA was markedly increased in the highest dose group. A target protein of miR-146a is SOD2 [27] which was indeed downregulated in this group.

Mitochondria are not only the main source and but also a target of oxidative damage. As oxidative stress-induced protein modifications such as carbonylation lead to increased protein degradation [28] or inactivation [29], increased oxidation of mitochondrial proteins may explain the vigorous downregulation in their expression seen in this study.

Mitochondria are physically associated with myofibrils, and increased mitochondrial ROS production may lead to impaired contractility through disruption of actin-myosin interactions [30]. Cytoskeletal proteins are considered to be sensitive to redox alterations and the association between oxidative stress and structural damage has been well documented [31]. The oxidation of actin has been shown to result in a strong inhibition of protein polymerisation and in complete disruption of actin-filament organisation [31]. This study shows a significant downregulation of actin isoforms together with many other structural proteins (tubulin, troponin, tropomyosin, desmin and different isoforms of light and heavy myosin). These proteins are major constituents of the contractile apparatus and the severe downregulation seen in the high-dose groups may negatively influence cardiac contractility. Cardiac troponin, a sensitive and specific marker for heart damage, is significantly reduced in the two highest dose groups, in comparison to the controls [32].

Prompted by the bioinformatics prediction based mainly on downregulated metabolic and oxidative response proteins, we show here that ionising radiation increases the level of phosphorylation of PPAR alpha and thereby inhibits this transcription factor in a dose-dependent manner [6, 20]. This is in agreement with our previous study showing that high-dose local heart irradiation impairs the cardiac fatty acid oxidation due to inhibition of PPAR alpha activity in mice [14]. The PPAR alpha pathway has been shown to influence antioxidant response and myofibrillar structure [33]. Increased oxidative stress and reduced contractility due to oxidation of myosin have been reported in PPAR alpha knock-out mice [34]. We suggest that inactivation of PPAR alpha following radiation exposure adds to the oxidative stress and structural impairment phenotype observed in irradiated hearts.

The level of PPAR alpha and that of several mitochondrial proteins is regulated by mir-21 in different cells and tissues [35–37]. We found significant upregulation in the expression of miR-21 in the left ventricle samples of the highest dose group. This corresponds to the observed downregulation of mitochondrial proteins. Increased levels of mir-21 in heart failure and ischemia have been reported [19, 38, 39].

MATERIALS AND METHODS

Samples

Biological samples were collected post-mortem from donors who had previously given informed consent to participate in the study and who had consented to the processing of their personal data in accordance with the Russian Federal Laws No 323-FL of 27.09.2013 and No 261-FL of 25.07.2011. The study was approved by the Southern Urals Biophysics Institute´s Institutional Review Board.

The individuals were male Mayak plutonium enrichment plant workers who were exposed only to external gamma rays. The control subjects were non-Mayak workers living in the same area. All participants were diagnosed multiple times with IHD during their lifetime and the primary cause of death was IHD. Workers exposed to internal plutonium (Pu alpha-activity in urine > 0.5 kBq), or who had been diagnosed with cancer or other major somatic diseases were excluded from the study.

All individuals were placed in a cold-room (+4°C) immediately after the death (approximately within 1 h). All autopsies were performed within first 12–24 h after the death. The cardiac left ventricle was collected at autopsy and immediately frozen. Heart tissues from 29 individuals were allocated between four dose groups as follows: 3 individuals to the control group (0 Gy), 6 to

the dose group < 100 mGy, 10 individuals to the group receiving doses between 100–500 mGy, and 10 individuals to the dose group > 500 mGy (Supplementary Table S10). The smoking status and index, alcohol consumption and body mass index of each individual is indicated in Supplementary Table S10.

To expand the number of participants, formalin-fixed paraffin-embedded (FFPE) samples from 15 donors were used for miRNA analysis as follows: 3 individuals from control group, 3 individuals from the dose group <100 mGy, 4 individuals from the group representing doses between 100–500 mGy, and 5 individuals from the dose group > 500 mGy (Supplementary Table S10). Four participants (5, 16, 26 and 27) were donors of both frozen and FFPE samples.

Protein extraction

Frozen heart samples were lysed as described previously [14]. Cardiac left ventricle was ground to a fine powder with a cold (–20°C) mortar and pestle before being suspended in lysis buffer (SERVA) [14]. Protein concentration was determined by the Bradford assay following the manufacturer's instructions (Thermo Fisher).

Protein purification and mass spectrometry

Protein lysates (10 µg) were digested using a modified filter-aided sample preparation (FASP) protocol [40]. Briefly, the samples were reduced with 10 mM DTT at 60°C for 30 min, followed by alkylation with 15 mM iodoacetamide for 30 min at room temperature [40]. Samples were diluted using 8 M urea in 0.1 M Tris/HCl, pH 8.5, and centrifuged using a 30 kDa cut-off filter (Pall Corporation). After washing with 8 M urea in 0.1 M Tris/HCl, pH 8.5, and with 50 mM ammonium bicarbonate (ABC), the proteins were initially digested on the filter with 1 µg Lys-C (Wako Chemicals GmbH) in 50 mM ABC at room temperature, followed by addition of 2 µg trypsin (Promega) and digestion overnight at 37°C. Tryptic peptides were collected by centrifugation and acidified with trifluoric acid (TFA) to a pH of 2.0. Samples were stored at –20°C.

Prior to LC-MS/MS analysis the samples were centrifuged (16,000 g) for 5 min at 4°C. Each sample (0.5 µg) representing one donor was analysed separately on a LTQ OrbitrapXL (Thermo Fisher Scientific) coupled to Ultimate 3000 nano-HPLC (Dionex) as described previously [41].

Label-free quantification

The raw files of the individual measurements were loaded to the Progenesis QI software and analysed as described previously [42, 43]. Briefly, peptide features in the individual runs were aligned in order to reach a maximum overlay of at least 85%. After feature detection, the singly charged features and features with charges higher than +7 were excluded. The samples were grouped according to the radiation dose as described above. Protein identification was performed using the Mascot search engine (Matrix Science, version 2.5.0) with the Ensembl Human database (version 68, 40047886 residues, 105288 sequences).

The following search parameters were used: 10 ppm peptide mass tolerance and 0.6 Da fragment mass tolerance, one missed cleavage was allowed, carbamidomethylation (C) was set as fixed modification, and oxidation (M) and deamidation (N, Q) were allowed as variable modifications. Search results were reimported into the Progenesis QI software and the resulting summed normalised abundances of unique peptides for every single protein were used for the calculation of abundance ratios and statistical analysis (Student's *t*-test).

A principal component analysis (PCA) was performed using Progenesis QI software (http://www.nonlinear.com), based on all features with charges +2 to +7 resulting in the PC1 of 23.65% and PC2 of 8.36%.

For final quantifications, proteins with ratios greater than 1.30-fold or less than 0.77-fold (*t*-test; $p \leq 0.05$) were defined as being significantly differentially expressed. The FDR (q value) calculation was used to adjust *p*-values [44, 45]. The calculation was performed using modified BenjaminiHochberg created by Manuel Weinkauf (https://marum.de/Software_and_Programs.html), licensed under a Creative Commons Attribution-NonCommercial-ShareAlike 3.0 Unported License (http://creativecommons.org/licenses/by-nc-sa/3.0/deed.en_GB). All *p*-values below the corrected significance level q were considered to represent significant results.

Protein-protein interaction and signalling network

For deregulated proteins, protein-protein interaction and signalling networks were analysed by the software tool INGENUITY Pathway Analysis (IPA) (http://www.INGENUITY.com) [46] and the search tool STRING version 10 (http://string-db.org), coupled to the Reactome database (http://www.reactome.org) [47].

Immunoblot analysis

Protein lysates from pooled or individual (total and phospho-PPAR alpha) samples were analysed by immunoblotting. For pooled samples, similar amount of protein from each individual belonging to the same radiation dose group (control, < 100 mGy, 100–500 mGy and > 500 mGy) was combined into a batch representing that group. Proteins separated by 4–12% SDS-PAGE were transferred to nitrocellulose membranes (GE Healthcare) using a TE 77 semidry blotting system (GE Healthcare) at 1 mA/cm for 1h. The membranes were blocked using 3 % BSA in TBS, pH 7.4, for 1 h at room temperature, washed three times in 10 mM Tris-

HCl, pH 7.4, 150 mM NaCl for 5 min and incubated overnight at 4°C with primary antibodies using dilutions recommended by the manufacturer (Abcam). Immunoblot analysis of heart protein lysate was performed using anti-PPAR alpha (# ab2779), anti-phospho-PPAR alpha (Ser12)(# ab3484), anti-troponin T(# ab156852), anti-SOD2 (# ab13533), anti-peroxiredoxin 5 (# ab119712), anti-myosin light chain 2 (# ab 92721), anti-tropomyosin 2 (# ab96073) and anti-Nrf2 (# ab31163). After washing three times, the blots were incubated with the appropriate horseradish peroxidase-conjugated or alkaline phosphatase-conjugated anti-mouse, anti-rabbit or anti-goat secondary antibody (Santa Cruz Biotechnology) for 2 h at room temperature and developed using the ECL system (GE Healthcare) or 1-step™ NBT/BCIP method (ThermoFisher) following standard procedures. Reversible Ponceau staining was used as the loading control. Quantification of digitised images of immunoblot bands was done using ImageJ (http://rsbweb.nih.gov/ij/). Three technical replicates were performed from each pooled sample. For individual analysis, the samples in the control group were run in two technical replicates, all others in one technical replicate.

Protein carbonylation analysis

To detect the level of protein oxidation, protein carbonylation was measured using the assay kit (Biovision) according to the manufacturer´s instructions.

RNA isolation from FFPE blocks and TaqMan-miRNA assays

Heart tissue was immediately fixed in 4% buffered formalin for 24 h and dehydrated with a graded series of ethanol before embedding in paraffin. FFPE blocks were stored in the dark at room temperature. For miRNA analysis, multiple 10 µm sections were cut after initial trimming to remove air exposed surfaces. Total RNA was isolated using phenol chloroform gradient as described previously [48] and quantified using NanoDrop spectrophotometer (PeqLab Germany).

Quantitative PCR (Applied Biosystems, Forster City, CA, USA) was performed to analyse the expression of miR-21 (# 4427975, assay id 000397) and miR-146a (#4427975, assay id 000468) with the StepOnePlus Detection System (Applied Biosystems, Foster City, CA) according to the manufacturer´s instructions. Relative expression values of each miRNA were calculated using the 2–ΔΔCT method, normalised to the control miRNA RNU44 (# 4427975, assay id 001094) as described earlier [49]. Relative expression values from control and exposed groups were used for further calculations. All samples were analysed at least in duplicate.

Statistical analysis

Comparative analysis of the data was carried out using the Student´s *t*-test (two-paired and unpaired). The significance levels were $*p < 0.05$ (5%); $**p < 0.01$ (1%) and $***p < 0.001$ (0.1%). The error bars represent the standard error of the mean (± SEM).

Data availability

The raw MS data can be accessed from the RBstore database http://www.storedb.org/store_v3/study.jsp?studyId=1038.

CONCLUSIONS

This data emphasizes the critical role of PPAR alpha and defect fatty acid oxidation in the radiation-induced IHD. Furthermore, the reduced energy flow from beta oxidation may not be compensated with increased uptake of glucose as the majority of the enzymes in the glycolysis pathway were also downregulated in a dose-dependent manner. This may lead to severe ATP depletion in the irradiated heart. Improving the function of PPAR alpha may serve as a useful preventive tool in radiation-induced IHD.

ACKNOWLEDGMENTS AND FUNDING

This work was supported by grants from Federal Office for Radiation Protection (BfS) (# 3611S30022), from the European Community's Seventh Framework Program (EURATOM) (# 295823 PROCARDIO), and Federal Medical Biological Agency (FMBA Russia). We thank Fabian Gruhn, Katrin Linder, Olga Teplyakova and Stefanie Winkler for technical assistance.

CONFLICTS OF INTEREST

The authors declare no conflicts of interest.

REFERENCES

1. Azizova TV, Muirhead CR, Druzhinina MB, Grigoryeva ES, Vlasenko EV, Sumina MV, O'Hagan JA, Zhang W, Haylock RG, Hunter N. Cardiovascular diseases in the cohort of workers first employed at Mayak PA in 1948–1958. Radiat Res. 2010; 174:155–168.
2. Azizova TV, Grigoryeva ES, Haylock RG, Pikulina MV, Moseeva MB. Ischaemic heart disease incidence and mortality in an extended cohort of Mayak workers first employed in 1948–1982. Br J Radiol. 2015; 88:20150169.
3. Simonetto C, Azizova TV, Grigoryeva ES, Kaiser JC, Schollnberger H, Eidemuller M. Ischemic heart disease

in workers at Mayak PA: latency of incidence risk after radiation exposure. PLoS One. 2014; 9:e96309.

4. Yamada M, Wong FL, Fujiwara S, Akahoshi M, Suzuki G. Noncancer disease incidence in atomic bomb survivors, 1958–1998. Radiat Res. 2004; 161:622–632.
5. Stanley WC, Hoppel CL. Mitochondrial dysfunction in heart failure: potential for therapeutic interventions? Cardiovasc Res. 2000; 45:805–806.
6. Finck BN. The PPAR regulatory system in cardiac physiology and disease. Cardiovasc Res. 2007; 73:269–277.
7. Lopaschuk GD, Opie LH. Introduction to JMCC symposium on myocardial energy metabolism in health and disease. J Mol Cell Cardiol. 2002; 34:1075–1076.
8. Walters AM, Porter GA, Jr., Brookes PS. Mitochondria as a drug target in ischemic heart disease and cardiomyopathy. Circ Res. 2012; 111:1222–1236.
9. Lehman JJ, Kelly DP. Gene regulatory mechanisms governing energy metabolism during cardiac hypertrophic growth. Heart Fail Rev. 2002; 7:175–185.
10. Fillmore N, Mori J, Lopaschuk GD. Mitochondrial fatty acid oxidation alterations in heart failure, ischaemic heart disease and diabetic cardiomyopathy. Br J Pharmacol. 2014; 171:2080–2090.
11. Barger PM, Kelly DP. PPAR signaling in the control of cardiac energy metabolism. Trends Cardiovasc Med. 2000; 10:238–245.
12. Barjaktarovic Z, Schmaltz D, Shyla A, Azimzadeh O, Schulz S, Haagen J, Dorr W, Sarioglu H, Schafer A, Atkinson MJ, Zischka H, Tapio S. Radiation-induced signaling results in mitochondrial impairment in mouse heart at 4 weeks after exposure to X-rays. PLoS One. 2011; 6:e27811.
13. Barjaktarovic Z, Shyla A, Azimzadeh O, Schulz S, Haagen J, Dorr W, Sarioglu H, Atkinson MJ, Zischka H, Tapio S. Ionising radiation induces persistent alterations in the cardiac mitochondrial function of C57BL/6 mice 40 weeks after local heart exposure. Radiother Oncol. 2013; 106:404–410.
14. Azimzadeh O, Sievert W, Sarioglu H, Yentrapalli R, Barjaktarovic Z, Sriharshan A, Ueffing M, Janik D, Aichler M, Atkinson MJ, Multhoff G, Tapio S. PPAR Alpha: A Novel Radiation Target in Locally Exposed Mus musculus Heart Revealed by Quantitative Proteomics. J Proteome Res. 2013; 12:2700–2714.
15. Breckenridge R. Heart failure and mouse models. Dis Model Mech. 2010; 3:138–143.
16. Azizova TV, Day RD, Wald N, Muirhead CR, O'Hagan JA, Sumina MV, Belyaeva ZD, Druzhinina MB, Teplyakov, II, Semenikhina NG, Stetsenko LA, Grigoryeva ES, et al. The "clinic" medical-dosimetric database of Mayak production association workers: structure, characteristics and prospects of utilization. Health Phys. 2008; 94:449–458.
17. Schulte C, Zeller T. microRNA-based diagnostics and therapy in cardiovascular disease-Summing up the facts. Cardiovasc Diagn Ther. 2015; 5:17–36.
18. Bronze-da-Rocha E. MicroRNAs expression profiles in cardiovascular diseases. Biomed Res Int. 2014; 2014:985408.
19. Thum T, Gross C, Fiedler J, Fischer T, Kissler S, Bussen M, Galuppo P, Just S, Rottbauer W, Frantz S, Castoldi M, Soutschek J, Koteliansky V, et al. MicroRNA-21 contributes to myocardial disease by stimulating MAP kinase signalling in fibroblasts. Nature. 2008; 456:980–984.
20. Barger PM, Brandt JM, Leone TC, Weinheimer CJ, Kelly DP. Deactivation of peroxisome proliferator-activated receptor-alpha during cardiac hypertrophic growth. J Clin Invest. 2000; 105:1723–1730.
21. Azizova TV, Muirhead CR, Moseeva MB, Grigoryeva ES, Vlasenko EV, Hunter N, Haylock RG, O'Hagan JA. Ischemic heart disease in nuclear workers first employed at the Mayak PA in 1948–1972. Health Phys. 2012; 103:3–14.
22. Azimzadeh O, Scherthan H, Sarioglu H, Barjaktarovic Z, Conrad M, Vogt A, Calzada-Wack J, Neff F, Aubele M, Buske C, Atkinson MJ, Tapio S. Rapid proteomic remodeling of cardiac tissue caused by total body ionizing radiation. Proteomics. 2011; 11:3299–3311.
23. Azimzadeh O, Scherthan H, Yentrapalli R, Barjaktarovic Z, Ueffing M, Conrad M, Neff F, Calzada-Wack J, Aubele M, Buske C, Atkinson MJ, Hauck SM, Tapio S. Label-free protein profiling of formalin-fixed paraffin-embedded (FFPE) heart tissue reveals immediate mitochondrial impairment after ionising radiation. J Proteomics. 2012; 75:2384–2395.
24. Lesnefsky EJ, Chen Q, Slabe TJ, Stoll MS, Minkler PE, Hassan MO, Tandler B, Hoppel CL. Ischemia, rather than reperfusion, inhibits respiration through cytochrome oxidase in the isolated, perfused rabbit heart: role of cardiolipin. Am J Physiol Heart Circ Physiol. 2004; 287:H258–267.
25. Tompkins AJ, Burwell LS, Digerness SB, Zaragoza C, Holman WL, Brookes PS. Mitochondrial dysfunction in cardiac ischemia-reperfusion injury: ROS from complex I, without inhibition. Biochim Biophys Acta. 2006; 1762:223–231.
26. Heather LC, Carr CA, Stuckey DJ, Pope S, Morten KJ, Carter EE, Edwards LM, Clarke K. Critical role of complex III in the early metabolic changes following myocardial infarction. Cardiovasc Res. 2010; 85:127–136.
27. Ji G, Lv K, Chen H, Wang T, Wang Y, Zhao D, Qu L, Li Y. MiR-146a regulates SOD2 expression in H2O2 stimulated PC12 cells. PLoS One. 2013; 8:e69351.
28. Dukan S, Farewell A, Ballesteros M, Taddei F, Radman M, Nystrom T. Protein oxidation in response to increased transcriptional or translational errors. Proc Natl Acad Sci U S A. 2000; 97:5746–5749.
29. Tai Y, Inoue H, Sakurai T, Yamada H, Morito M, Ide F, Mishima K, Saito I. Protective effect of lecithinized SOD on reactive oxygen species-induced xerostomia. Radiat Res. 2009; 172:331–338.
30. Bayeva M, Ardehali H. Mitochondrial dysfunction and oxidative damage to sarcomeric proteins. Curr Hypertens Rep. 2010; 12:426–432.

31. Dalle-Donne I, Rossi R, Giustarini D, Gagliano N, Lusini L, Milzani A, Di Simplicio P, Colombo R. Actin carbonylation: from a simple marker of protein oxidation to relevant signs of severe functional impairment. Free Radic Biol Med. 2001; 31:1075–1083.

32. Skeik N, Patel DC. A review of troponins in ischemic heart disease and other conditions. Int J Angiol. 2007; 16:53–58.

33. Lee WS, Kim J. Peroxisome Proliferator-Activated Receptors and the Heart: Lessons from the Past and Future Directions. PPAR Res. 2015; 2015:271983.

34. Guellich A, Damy T, Lecarpentier Y, Conti M, Claes V, Samuel JL, Quillard J, Hebert JL, Pineau T, Coirault C. Role of oxidative stress in cardiac dysfunction of PPARalpha$^{-/-}$ mice. Am J Physiol Heart Circ Physiol. 2007; 293:H93–H102.

35. Zhou J, Wang KC, Wu W, Subramaniam S, Shyy JY, Chiu JJ, Li JY, Chien S. MicroRNA-21 targets peroxisome proliferators-activated receptor-alpha in an autoregulatory loop to modulate flow-induced endothelial inflammation. Proc Natl Acad Sci U S A. 2011; 108:10355–10360.

36. Kida K, Nakajima M, Mohri T, Oda Y, Takagi S, Fukami T, Yokoi T. PPARalpha is regulated by miR-21 and miR-27b in human liver. Pharm Res. 2011; 28:2467–2476.

37. Gomez IG, MacKenna DA, Johnson BG, Kaimal V, Roach AM, Ren S, Nakagawa N, Xin C, Newitt R, Pandya S, Xia TH, Liu X, Borza DB, et al. Anti-microRNA-21 oligonucleotides prevent Alport nephropathy progression by stimulating metabolic pathways. J Clin Invest. 2015; 125:141–156.

38. Cheng Y, Zhang C. MicroRNA-21 in cardiovascular disease. J Cardiovasc Transl Res. 2010; 3:251–255.

39. Schroen B, Heymans S. Small but smart--microRNAs in the centre of inflammatory processes during cardiovascular diseases, the metabolic syndrome, and ageing. Cardiovasc Res. 2012; 93:605–613.

40. Wisniewski JR, Zougman A, Nagaraj N, Mann M. Universal sample preparation method for proteome analysis. Nat Methods. 2009; 6:359–362.

41. Azimzadeh O, Sievert W, Sarioglu H, Merl-Pham J, Yentrapalli R, Bakshi MV, Janik D, Ueffing M, Atkinson MJ, Multhoff G, Tapio S. Integrative proteomics and targeted transcriptomics analyses in cardiac endothelial cells unravel mechanisms of long-term radiation-induced vascular dysfunction. J Proteome Res. 2015; 14:1203–1219.

42. Hauck SM, Dietter J, Kramer RL, Hofmaier F, Zipplies JK, Amann B, Feuchtinger A, Deeg CA, Ueffing M. Deciphering membrane-associated molecular processes in target tissue of autoimmune uveitis by label-free quantitative mass spectrometry. Mol Cell Proteomics. 2010; 9:2292–2305.

43. Merl J, Ueffing M, Hauck SM, von Toerne C. Direct comparison of MS-based label-free and SILAC quantitative proteome profiling strategies in primary retinal Muller cells. Proteomics. 2012; 12:1902–1911.

44. Chen JJ, Wang SJ, Tsai CA, Lin CJ. Selection of differentially expressed genes in microarray data analysis. Pharmacogenomics J. 2007; 7:212–220.

45. Storey JD, Tibshirani R. Statistical significance for genomewide studies. Proc Natl Acad Sci U S A. 2003; 100:9440–9445.

46. Wu J, Liu W, Bemis A, Wang E, Qiu Y, Morris EA, Flannery CR, Yang Z. Comparative proteomic characterization of articular cartilage tissue from normal donors and patients with osteoarthritis. Arthritis Rheum. 2007; 56:3675–3684.

47. D'Eustachio P. Reactome knowledgebase of human biological pathways and processes. Methods Mol Biol. 2011; 694:49–61.

48. Ludyga N, Grunwald B, Azimzadeh O, Englert S, Hofler H, Tapio S, Aubele M. Nucleic acids from long-term preserved FFPE tissues are suitable for downstream analyses. Virchows Arch. 2012; 460:131–140.

49. Anastasov N, Hofig I, Vasconcellos IG, Rappl K, Braselmann H, Ludyga N, Auer G, Aubele M, Atkinson MJ. Radiation resistance due to high expression of miR-21 and G2/M checkpoint arrest in breast cancer cells. Radiat Oncol. 2012; 7:206.

2.3 The Presence or PPARα is Necessary for Radiation-induced Activation of Non-canonical TGFβ signaling

2.3.1 Publication

The scientific data included in the following original research paper published in the Journal of Proteome Research.

The Presence or PPARα is Necessary for Radiation-Induced Activation of Non-Canonical TGFβ signaling in the Heart

Vikram Subramanian, Sabine Borchard, Omid Azimzadeh, Wolfgang Sievert, Juliane Merl-Pham, Mariateresa Mancuso, Emanuela Pasquali, Gabriele Multhoff, Bastian Popper, Hans Zischka, Michael J. Atkinson, Soile Tapio

J Proteome Res. 2018 Apr 6;17(4):1677-1689

DOI: 10.1021/acs.jproteome.8b00001

2.3.2 Aim of this study

This study aimed to investigate how the observed radiation-induced changes in PPARα activity contributes to the radiation response of the murine heart, particularly the activation of the TGFβ1 mediated SMAD-dependent and SMAD-independent pathways and the energy metabolism of the heart.

2.3.3 Summary of results

Male wild-type (PPARα +/+), PPARα heterozygous (PPARα +/-) and PPARα homozygous null mutant (PPARα -/-) mice were bred, genotyped and locally irradiated to the heart at the age of 8 weeks with doses of 0, 8 and 16 Gy. Age-matched control mice of the appropriate genotypes were sham irradiated. Heart tissue was examined in all animals 20 weeks after treatment.

Quantitative proteomics data showed that PPAR mutation itself has a dramatic effect on the proteome of non-irradiated heart. Compared to wild-type group, 33 proteins were significantly deregulated in nonirradiated PPARα +/- heterozygous mutant group, whilst in

nonirradiated PPARα -/- homozygous mutant group 518 proteins were deregulated. In wild-type group, only 1 protein was deregulated at the dose of 8 Gy, whilst 84 proteins were deregulated at the higher dose of 16 Gy. In the PPARα +/- heterozygous group there were 32 proteins deregulated at 8 Gy, and 307 proteins deregulated at 16 Gy, compared to sham-irradiated PPARα +/- heterozygous mutant group. In the PPARα -/- homozygous mutant group 24 proteins were found to be deregulated at 8 Gy, and 14 proteins deregulated at 16 Gy compared to the sham-irradiated PPARα -/- homozygous mutant group.

Bioinformatic analysis was performed with deregulated protein list from all three groups using Ingenuity pathway analysis. Analysis predicted activation of TGFβ at the higher 16 Gy dose in wild-type (PPARα +/+) group, and this was also observed in the PPARα heterozygous (PPARα +/-) and PPARα homozygous mutant (PPARα -/-) groups. Analysis also showed predicted inhibition of PPARα at the higher dose in wild-type (PPARα +/+) and PPARα heterozygous mutant (PPARα +/-) groups. The transcriptional activity of PPARα in heart depends on phosphorylation of Ser12; higher phosphorylation signifies the deactivation of PPARα activity. Our data showed a significant increase in the phosphorylation of PPARα in wild-type and PPARα heterozygous mutant (PPARα +/-) group at 16 Gy compared to control group, indicating radiation-related less PPARα transcriptional activity in wild-type and PPARα heterozygous mutant (PPARα +/-) groups. Our result also showed a significant increase in the level of PPAR γ at both radiation doses in the wild-type group and PPARα +/- heterozygous mutant groups at 16 Gy dose. No significant changes in the level of phosphorylated form of PPARγ were observed in any genotype condition.

Interestingly this study showed activation of TGFβ mediated SMAD-dependent signaling pathway after irradiation was unaffected by PPARα status. Thus we conclude that SMAD-dependent signaling does not depend on status of PPARα in the heart. In contrast, we observed that radiation-induced activation of the SMAD-independent TGFβ signaling pathway did require the presence of PPARα in the heart.

To study the initiation of radiation-induced cardiac fibrosis in PPARα genotypes, the expression of marker proteins (α-SMA, vinculin, paxillin, and vimentin) involved in fibroblast to myofibroblast conversion were studied using western blotting in all three genotypes. Our result showed a significant increase in the expression of myofibroblast maturation marker

proteins (α-SMA, vinculin, paxillin, and vimentin) in wild-type group at 16 Gy dose. However, only the expression level of vimentin and paxillin reached to significant in PPARα mutated genotypes at 16 Gy dose. In general 8 Gy dose did not significantly induce the expression of any marker proteins irrespective of genotype. This study shows that the fibroblast to myofibroblast conversion process is inducted before the appearance of fibrotic tissue. This is indicative of a wound healing type response sustained for at least 20 weeks. This effect was completely dependent on PPARα status, being absent in both the PPARα heterozygous and homozygous animals.

Electron microscopy analysis revealed an influence of PPARα genotype on the size and morphology of cardiac mitochondria. Thus the number of mitochondria in both the nonirradiated PPARα +/- heterozygous and PPARα -/- homozygous mutant groups were significantly reduced compared to nonirradiated wild-type group. Interestingly, the mitochondria size of the nonirradiated PPARα -/- homozygous mutant group were significantly larger compared to mitochondria of nonirradiated wild-type group, signifying perturbed mitochondrial biogenesis and dynamics are associated with reduced levels of the PPARα protein. There was no apparent change in mitochondrial morphology in either of the mutant PPARα genotypes following irradiation, nor was there an obvious effect of radiation on the number of mitochondria in any of the PPARα genotypes.

Immunohistochemistry was used to analyze the impact of irradiation on the number of inflammatory macrophages in all three PPARα genotypic groups. The number of CD45 positive cells was decreased in wild-type mice after exposure to 16 Gy but were increased in the PPARα +/- heterozygous mutants. No significant changes in the number of CD45 positive cells were observed in PPARα -/- homozygous mutant group at 16 Gy dose compared to non-irradiated PPARα -/- homozygous mutant control group. To analyze the influence of ionizing radiation in cardiac inflammation, the level of matrix metalloprotease 9 (MMP 9), a biomarker for cardiac inflammation were studied using western blotting. The highest dose of 16 Gy triggered a significant increase in the expression of MMP 9 independent of the PPARα genotype. These data revealed, local high doses irradiation appears to function in a pro-inflammatory manner in the heart.

This is one of the first studies to show the effect of PPARα genotypic status on the cardiac proteome following irradiation in the heart. This study also showed that PPARα could have an influence on radiation-induced activation of TGFβ mediated SMAD-independent signaling pathway.

2.3.4 Contributions

I maintained the mouse breeding colonies and performed genotyping of all animals. I irradiated the animals together with Dr. Wolfgang Sievert. Prof. Dr. Gabriele Multhoff helped in the experimental design of the mouse irradiation as well as contributing scientific discussion of the experimental results. I sacrificed all the mice and together with Dr. Omid Azimzadeh prepared protein lysates of the heart samples for all experiments and submitted them to the proteomics core facility. The LC-MS/MS run was performed by Dr. Juliane Merl-Pham (PROT/HMGU). I performed all of the bioinformatic analysis of the proteomics data, as well as the western blotting for all pathways included in this study under the guidance of Dr. Soile Tapio and Dr. Omid Azimzadeh. I worked together with Dr. Omid Azimzadeh for some validation experiments. (Carbonylation, ELISA). I prepared heart samples for immunohistochemistry and electron microscopy study under the guidance of PD. Dr. Soile Tapio. Dr. Mariateresa Mancuso (ENEA, Rome, Italy) performed the immunohistochemistry experiment used in this study. Dr. Bastian Popper performed the electron microscopy, and I counted mitochondria and analyzed the area of mitochondria from all heart samples under the guidance of Sabine Borchard and Dr. Hans Zischka (HMGU). I helped in the preparation of the manuscript, created graphs with PD Dr. Soile Tapio. All co-authors in this manuscript also helped in scientific discussion and corrections of the manuscript.

2.3.5 Discussion

The primary purpose of this study was to examine how altered levels of PPARα impact the radiation response in the heart. We have focussed on two main functions of PPARα, specifically the TGFβ signaling pathway and energy metabolism in the heart exposure to radiation.

To succeed this purpose, wild-type mice that have a regular expression of PPARα and mice with a loss of one or both genes encoding PPARα were used in all experiments. Data from this

study showed that the irradiated wild-type group showed inactivation of PPARα due to increased phosphorylation at 16 Gy dose. In this group, proteomics data revealed most of the deregulated proteins belongs to the fatty acid oxidation pathway at 16 Gy dose. This is in good agreement with previously published data that showed similar changes following radiation-induced inhibition of PPARα activity in the heart [38] and with results presented in chapter 2.1 and chapter 2.2 of this thesis. In addition to this, the activation of TGFβ signaling mediated through SMAD-dependent and SMAD-independent pathways that were observed 40 weeks [37] after radiation exposure is now seen much earlier time point (20 weeks) after radiation exposure in wild-type group. In agreement with this, our study found a significant increase in the expression of marker proteins expressed during fibroblast to myofibroblast conversion process. This observed result suggests that cardiac reprogramming to induce cardiac fibrosis is initiated at much earlier time point, where no signs of fibrosis were detected.

In the PPARα +/- heterozygous mutant mice, data showed inactivation of PPARα due to increased phosphorylation at 16 Gy dose, suggesting a radiation-related alteration in the transcriptional activity of PPARα. PPARα +/- heterozygous mutant group displayed more changes in the heart proteome than wild-type group in a dose-dependent manner after radiation exposure. Of the more than 300 deregulated proteins at 16 Gy dose, most of these proteins found to be involved in the mitochondrial respiratory chain and fatty acid oxidation pathways, suggesting that metabolic function is significantly influenced by ionizing radiation than anti-inflammatory action of PPARα in the PPARα+/- heterozygous group. In the PPARα -/- homozygous mutant lacking PPARα, the analysis revealed more significant changes in the cardiac proteome (more deregulated proteins belong to lipid metabolism and mitochondrial proteins), enlarged mitochondria and reduced mitochondrial count compared to nonirradiated wild-type and PPARα +/- heterozygous mutant groups. The PPARα -/- homozygous mutant group does not provoke many alterations in the heart proteome after exposure to radiation.

Interestingly, our study found that radiation resulted in the loss of PPARα activity in the heart tissue of wild-type and PPARα +/- heterozygous mutant group with a simultaneous increase in the expression of PPARγ at 16 Gy dose. In line with our data, increased expression of PPARγ was observed in the heart of Sprague-Dawley rats 3 months after chest irradiation (15 Gy, 18 Gy) [237]. No radiation-induced increase in the expression of PPARγ was observed in

homozygous mutant mice lacking PPARα protein in the heart, this may be due to the presence of higher basal level of PPARγ in PPARα -/- homozygous mutant group. Studies have shown that these two members of the PPAR family have separate metabolic functions that are both pathway and tissue-dependent [232], and it is not probable to compensate one by another even though PPARγ and PPARα have common co-factors, but their target genes are not same [238].

Our data showed an increased expression of both TGFβ and downstream signaling proteins belongs to both the SMAD-dependent and SMAD-independent signaling pathways in wild-type group at 16 Gy dose, suggesting activation of TGFβ signaling in the heart is sustained for at least 20 weeks after irradiation. This observation is in line with the study that showed activation of TGFβ resulted in SMAD-dependent and SMAD-independent signaling pathways in the heart after 40 weeks of radiation exposure [239]. Also, we observed activation of Smad-dependent TGFβ signaling pathway at 16 Gy dose in wild-type and PPARα -/- homozygous mutant groups. In contrast, irradiation had no influence in the activation of TGFβ mediated SMAD-dependent pathway in PPARα deficient animals. Recently Bansal et al. showed that PPARα directly binds to TAK1 thereby inhibiting its phosphorylation and subsequent activation of downstream protein targets. This resulted in reduced collagen synthesis and reversion of cardiac fibrosis [240]. Activated TAK1 mediates the SMAD-independent TGFβ signaling pathway that involves activation of JNK2 and c-JUN N-terminal kinase[241-242]. In agreement with this, our data showed increased phosphorylation (activation) of TAK1, JNK2 and c-JUN in irradiated wild-type group (16 Gy) expressing active PPARα, but not in PPARα deficient groups. These data indicate that active PPARα inhibits SMAD-independent signaling pathway under normal physiological condition, likely through binding to TAK1. Irradiation resulted in the inactivation of PPARα that could then lead to activation of TGFβ mediated SMAD-independent pathway in wild-type group, due to reduced inhibitory effect by PPARα on TAK-1 protein. On the other hand, TGFβ mediated SMAD-dependent pathway was activated by irradiation independent of PPARα status. Activated TGFβ significantly transforms fibroblast function and phenotype [243] and stimulates myofibroblast differentiation [244]. In this study, we observed an augmented expression of several proteins that are involved in the conversion of fibroblast to myofibroblast in the wild-type animals at 16 Gy dose. This result implies that radiation-induced cardiac fibrosis may be initiated as early as week 20, even

though there are no histological signs of a fibrotic response reported at this time and dose [245].

Altogether, this study emphasized the role of PPARα in the radiation response in the heart. PPARα deficient mice show an altered response in the heart proteome, change in cardiac metabolism and TGFβ mediated signaling pathways in the heart after irradiation. This study suggests that active PPARα may be necessary to induce TGFβ mediated SMAD-independent signaling pathway in the heart after irradiation.

Journal of proteome research

Article

Cite This: J. Proteome Res. 2018, 17, 1677−1689

pubs.acs.org/jpr

PPARα Is Necessary for Radiation-Induced Activation of Noncanonical TGFβ Signaling in the Heart

Vikram Subramanian,[†] Sabine Borchard,[‡] Omid Azimzadeh,[†] Wolfgang Sievert,[§,¶] Juliane Merl-Pham,[⊥] Mariateresa Mancuso,[#] Emanuela Pasquali,[#] Gabriele Multhoff,[§,¶] Bastian Popper,[∥] Hans Zischka,[‡,△] Michael J. Atkinson,[†,●] and Soile Tapio*[,†]

[†]Institute of Radiation Biology, [‡]Institute of Molecular Toxicology and Pharmacology, [§]Institute of innovative Radiotherapy (iRT), and [⊥]Research Unit Protein Science, Helmholtz Zentrum München, German Research Center for Environmental Health GmbH, Munich 85764, Germany

[¶]Center for Translational Cancer Research (TranslaTUM), Radiation Immuno Oncology Group, Campus Klinikum rechts der Isar, Technical University of Munich, Munich 81675, Germany

[#]Laboratory of Radiation Biology and Biomedicine, Agenzia Nazionale per le Nuove Tecnologie, l'Energia e lo Sviluppo Economico Sostenibile (ENEA), Rome 00196, Italy

[∥]Department of Cell Biology and Core Facility Animal Models (CAM), Biomedical Center, Ludwig-Maximilians University Munich, Planegg 80539, Germany

[△]Institute of Toxicology and Environmental Hygiene and [●]Chair of Radiation Biology, Technical University of Munich, Munich 80333, Germany

Supporting Information

ABSTRACT: High-dose ionizing radiation is known to induce adverse effects such as inflammation and fibrosis in the heart. Transcriptional regulators PPARα and TGFβ are known to be involved in this radiation response. PPARα, an anti-inflammatory transcription factor controlling cardiac energy metabolism, is inactivated by irradiation. The pro-inflammatory and pro-fibrotic TGFβ is activated by irradiation via SMAD-dependent and SMAD-independent pathways. The goal of this study was to investigate how altering the level of PPARα influences the radiation response of these signaling pathways. For this purpose, we used genetically modified C57Bl/6 mice with wild type (+/+), heterozygous (+/−) or homozygous (−/−) PPARα genotype. Mice were locally irradiated to the heart using doses of 8 or 16 Gy; the controls were sham-irradiated. The heart tissue was investigated using label-free proteomics 20 weeks after the irradiation and the predicted pathways were validated using immunoblotting, ELISA, and immunohistochemistry. The heterozygous PPARα mice showed most radiation-induced changes in the cardiac proteome, whereas the homozygous PPARα mice showed the least changes. Irradiation induced SMAD-dependent TGFβ signaling independently of the PPARα status, but the presence of PPARα was necessary for the activation of the SMAD-independent pathway. These data indicate a central role of PPARα in cardiac response to ionizing radiation.

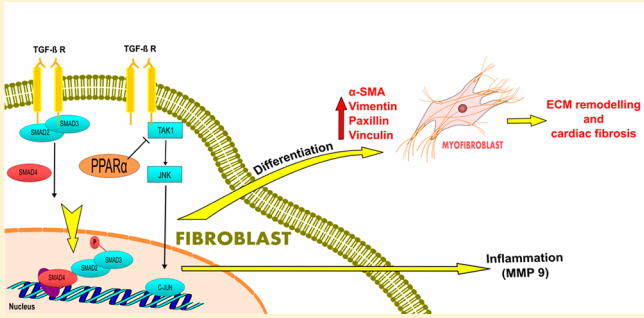

KEYWORDS: *ionizing radiation, proteomics, label-free quantification, PPARα, TGFβ, fibrosis, cardiovascular disease*

INTRODUCTION

Heart failure represents the major cause of cardiovascular disease mortality and morbidity worldwide and thereby contributes considerably to the health and economic burden in financial and health care systems.[1] Ionizing radiation is known to be a causal factor for heart disease in medical, occupational, or accidental exposure situations.[2−7] Typically, cardiac symptoms appear late, decades after the radiation exposure, and include increased inflammatory infiltrations and fibrosis of the myocardium, especially after high radiation doses.[8] Although the biological mechanisms behind the radiation-induced heart disease are not totally elucidated, adverse effects on cardiac blood vessels such as vascular inflammation, endothelial dysfunction, and premature senescence have been described in cellular and animal studies.[9−11] In addition to vascular abnormalities, recent studies have emphasized disturbances in myocardial energetics as a possible causal factor for radiation-induced heart disease.[12−17]

Received: January 2, 2018
Published: March 21, 2018

DOI: 10.1021/acs.jproteome.8b00001
J. Proteome Res. 2018, 17, 1677−1689

To fulfill its high energy demand, the heart produces large amounts of ATP, more than any other organ.[18] Normally, the main source of energy is free fatty acids[19] used in the oxidative phosphorylation to produce ATP by cardiac mitochondria.[20] The usage of free fatty acids for energy production inhibits the uptake and oxidation of glucose.[21] However, depending on substrate availability and energy demand, a rapid switch between energy sources is possible if necessary.[22]

Peroxisome proliferator-activated receptor alpha (PPARα) is a transcription factor that regulates energy metabolism in the heart. Together with PPARγ and PPARδ it belongs to the PPAR subfamily of nuclear receptors.[23] PPARs have both distinct and overlapping functions with some degree of tissue specificity, although all of them are expressed in the heart.[24] In its active form, PPARα builds a complex with the retinoid X receptor (RXR) and the coactivator 1 alpha (PCG1) to transcribe its target genes.[25,26] These genes largely code for enzymes used in fatty acid transport, fatty acid binding and activation, and peroxisomal and mitochondrial fatty acid β-oxidation[24] but also influence ketogenesis, triglyceride turnover, and gluconeogenesis.[24] The activity of PPARα is directly regulated by binding of ligand agonists that can be intracellular or dietary fatty acids or artificially administered fibrates.[27,28] It is also modulated by post-translational protein modifications such as phosphorylation.[29]

Mice overexpressing PPARα in the cardiac muscle show enhanced fatty acid oxidation rates, accumulation of triglycerides, reduction in glucose metabolism, and eventually cardiomyopathy.[30,31] In contrast, PPARα-null mice (PPARα −/−) show elevated free fatty acid levels as a consequence of inadequate fatty acid oxidation and dependency on glucose, decreased cardiac ATP production, abnormal mitochondrial cristae, and fibrosis.[32,33] Suppression of cellular fatty acid flux by chemical inhibition of mitochondrial fatty acid import caused massive hepatic and cardiac lipid accumulation, hypoglycemia, and death in 100% of male but only 25% of female PPARα −/− mice.[34] PPARα-null hearts exhibited 2−3-fold increase in oxidative damage, measured as oxidative protein adducts.[35]

In addition to its role in cardiac metabolism, PPARα has other important functions including regulation of cardiac inflammation, oxidative stress, and extracellular matrix remodeling.[36] Its anti-inflammatory effect is partly based on transcriptional inhibition of c-JUN and activator protein 1 (AP-1), downstream targets of noncanonical SMAD-independent TGFβ signaling, in a process called transrepression.[36−38]

TGFβ is the master regulator of heart fibrosis, influencing the alteration of normal quiescent cardiac fibroblasts to myofibroblasts.[39] It drives fibroblast-to-myofibroblast differentiation through activating both SMAD-dependent and SMAD-independent pathways,[40] which in turn stimulate the production of extracellular matrix proteins including α-smooth muscle actin (α-SMA), vimentin, paxillin, and vinculin.[41]

Recently, a direct interaction in was shown between PPARα and a member of the noncanonical SMAD-independent TGFβ signaling pathway, TGFβ activated kinase 1 (TAK1).[42] Activated by a specific ligand (arjulonic acid), PPARα was shown to inhibit the phosphorylation of TAK1 thereby leading to a blockage of the noncanonical pathway and inhibition of its downstream targets. This resulted in an amelioration of excess collagen synthesis and regression of cardiac fibrosis.[42]

We have previously shown PPARα to be a radiation target both in mouse and man.[12,16] In both cases, the total cardiac PPARα levels were not affected by irradiation, but increased inactivating phosphorylation (Ser12) of PPARα was observed. A study of late radiation-related effects using a mouse model (C57Bl/6J) showed increased cardiac inflammation, diffuse amyloidosis and severe fibrosis 40 weeks after local heart irradiation (16 Gy).[43] An integrated transcriptomics and proteomics study using the heart tissue of these mice indicated radiation-induced inhibition of PPARα and simultaneous activation of TGFβ by SMAD-dependent and SMAD-independent pathways.[44] This multiomics study indicated a crosstalk between PPARα and TGFβ signaling pathways.[44]

The aim of this study was to further investigate the possible role of PPARα on the radiation-induced activation of the TGFβ signaling using label-free proteomics and other methods. For this purpose, we used wild type, hetero- and homozygous mutant PPARα C57Bl/6 mice having normal, reduced, or absent PPARα gene expression, respectively.[45] The mice were irradiated locally to the heart (8 Gy, 16 Gy), the corresponding control mice were sham-irradiated, and the heart tissue was examined 20 weeks later. On the basis of the previous data, PPARα shows radiation-induced cardiac inactivation at this time point.[12] Furthermore, first signs of inflammation are being observed,[12] while no significant fibrosis is yet seen in the murine heart tissue.[43] This study now shows that irradiation induces SMAD-dependent TGFβ signaling independently of the PPARα status. However, the radiation-induced activation of the SMAD-independent pathway is not detected in the absence of PPARα. Furthermore, in mice expressing the wild type PPARα genotype, ionizing radiation induces the expression of PPARγ and marker proteins involved in fibroblast-to-myofibroblast conversion.

EXPERIMENTAL SECTION

Animals

Male PPARα −/− mice (B6;129S4-Pparatm1Gonz/J) were purchased from Jackson Laboratories (Sulzfeld, Germany) and mated with C57BL/6J wild type females to obtain hybrid PPARα +/− offspring that were the used to produce PPARα wild type, PPARα ± heterozygous, and PPARα −/− homozygous mutant mice.

The PPARα genotypes were confirmed by amplification of genomic DNA from ear punch blood samples. To isolate the DNA, the samples were treated with proteinase K (100 g/mL) in digestion buffer (1 M Tris, 0.5 M EDTA, 5 M NaCl, 20% SDS) overnight at 55 °C, followed by extraction and ethanol precipitation. The nucleotide sequences of PCR primers used for genotyping were: common primer 5′ GAGAAGTTGCAGGAGGGGATTGTG-3′ (oIMR8075), reverse wild type primer 5′-CCCATTTCGGTAGCAGGTAGTCTT-3′ (oIMR8076), and mutant reverse primer 5′-GCAATCCATCTTGTTCAATGGC-3′ (oIMR8077) (all primers from Eurofins genomics). The thermal cycles were followed according to the protocol of Jackson laboratory (https://www2.jax.org/protocolsdb/f?p=116:5:0::NO:5:P5_MASTER_PROTOCOL_ID,P5_JRS_CODE:23560,008154). The PCR products from all samples were electrophoresed on 1.5% agarose gel (Figure S-1).

At the age of 8 weeks, male mice with different genotypes for PPARα (wild type, heterozygous PPARα +/−, homozygous PPARα −/−) were randomly allocated to three different groups each containing at least 30 animals and housed in temperature controlled room with 12 h light−dark cycle. Standard mouse chow and water was provided *ad libitum*. Male

DOI: 10.1021/acs.jproteome.8b00001
J. Proteome Res. 2018, 17, 1677−1689

mice were used to provide the possibility to compare this study with our earlier ones where male mice were used.[12,44]

Irradiation and Sample Preparation

All animal experiments were approved and licensed under Bavarian federal law (Certificate No. AZ 55.2−1−54−2532−114−2014). Altogether, 90 mice were used in this study, with 10 mice in each group. Local heart irradiation was carried out at the age of 8 weeks as previously described.[12] Briefly, mice from the three genotypic groups were irradiated with a single X-ray dose of 8 or 16 Gy locally to the heart (200 kV, 10 mA) (Gulmay, UK). The age-matched control mice were sham irradiated. Mice were not anesthetized during irradiation but were held in a prone position in restraining jigs with thorax fixed using adjustable hinges. The position and field size (9 × 13 mm^2) of the heart was determined by pilot studies using soft X-rays; the rest of the body was shielded with a 2 mm thick lead plate. The radiation field by necessity included 30% of the lung volume. The animals were sacrificed 20 weeks after irradiation. The heart tissue was rapidly removed, rinsed with PBS and snap-frozen in liquid nitrogen and stored in −80 °C for further analysis. For histological analysis, heart samples were and fixed in 1% paraformaldehyde. For electron microscopy, heart tissue was fixed with 2.5% glutaraldehyde in 0.1 M sodium cacodylate buffer, pH 7.4 (Electron Microscopy Sciences, Pennsylvania).

Proteome Profiling

Frozen heart samples obtained from at least 5 mice per group were ground to a fine powder with a cold (−20 °C) mortar and pestle before being suspended in lysis buffer (SERVA).[46] Protein concentration was determined by the Bradford assay following the manufacturer's instructions (Thermo Fisher Scientific).

Protein lysates (10 μg) were digested using a modified filter-aided sample preparation (FASP) protocol[47] as described before with the use of cutoff filters from Sartorius.[44] Prior to LC−MS/MS analysis, the samples were centrifuged (16 000*g*) for 5 min at 4 °C.

Each sample (approximately 0.5 μg) was analyzed by LC−MS/MS on a Q-Exactive HF mass spectrometer (Thermo Fisher Scientific) online coupled to a nano-RSLC (Ultimate 3000 RSLC; Dionex) as described previously.[48] Tryptic peptides were accumulated on a nano trap column (300 μm inner diameter × 5 mm, packed with Acclaim PepMap100 C18, 5 μm, 100 Å; LC Packings) and then separated by reversed phase chromatography (customized ACQUITY UPLC M-Class HSS T3 Column, 1.8 μm, 75 μm × 250 mm; Waters) in a 80 min nonlinear gradient from 5 to 40% acetonitrile in 0.1% formic acid at a flow rate of 250 nL/min. Eluted peptides were analyzed by the Q-Exactive HF mass spectrometer equipped with a nanoflex ionization source. Full scan MS spectra (from m/z 300 to 1500) and MS/MS fragment spectra were acquired in the Orbitrap with a resolution of 60 000 or 15 000, respectively, with maximum injection times of 50 ms each. Up to ten most intense ions were selected for HCD fragmentation depending on signal intensity (TOP10 method). Target peptides already selected for MS/MS were dynamically excluded for 30 s.

The acquired spectra were loaded to the Progenesis QI software (version 3.0, Nonlinear) for label-free quantification and analyzed as previously described,[49,50] except that all features were exported as Mascot generic file (mgf) and used for peptide identification with Mascot (version 2.4) in the Ensembl Mouse protein database (release 80, 54 197 sequences, 24 204 564 residues). Search parameters used were: 10 ppm peptide mass tolerance and 0.02 Da fragment mass tolerance, one missed cleavage allowed, carbamidomethylation was set as fixed modification, methionine oxidation and asparagine or glutamine deamidation were allowed as variable modifications. A Mascot-integrated decoy database search calculated an average false discovery of <1%. The Mascot Percolator algorithm was used for the discrimination between correct and incorrect spectrum identifications.[51] Peptides with a minimum percolator score of 13 were reimported into the Progenesis QI software and the abundances of all unique peptides allocated to each individual protein were summed up and used for the calculation of abundance ratios and statistical analysis. Statistics was based on the ANOVA calculated by the Progenesis QI software, on arcsinh() transformed normalized protein abundances,[52] followed by FDR-correction, resulting in given q-values. Principal components analyses (PCAs) were performed within the Progenesis QI software.

For final quantifications, proteins identified with more than one unique peptide having ratios greater than 1.30-fold or less than 0.77-fold ($q \leq 0.05$) were defined as being significantly differentially expressed.

Interaction and Signaling Network Analysis

The signaling networks were analyzed using Ingenuity Pathway Analysis (IPA, QIAGEN Redwood City, www.qiagen.com/ingenuity).

Sandwich ELISA Assay

The alteration in the phosphorylation status of SMAD 2/3 was assessed using PathScan phospho-SMAD 2 (Ser465/467)/SMAD 3 (Ser423/425) Sandwich ELISA Kits (#120001). The data were compared to the level of total SMAD 2/3 sandwich ELISA kit (Cell Signaling) (#12000C). The measurement was performed using at least four biological replicates.

Immunoblot Analysis

Immunoblot analysis was performed as described previously[44] using anti-PPARα (bs-3614R) (Bioss Antibodies), antiphospho-PPARα (Ser12) (ab3484) (Abcam), anti-JNK1/JNK2 (ab179461) (Abcam), antiphospho-JNK1/JNK2 (Thr183/Tyr185) (ab4821) (Abcam), anti-TAK1 (ab109526) (Abcam), antiphospho-TAK1 (Thr187) (ab192443) (Abcam), anti-SMAD 4 (sc-7966) (Santa Cruz Biotechnologies), anti-c-JUN (60A8) (#9165) (Cell Signaling Technology), antiphospho-c-JUN (Ser63) (#2361) (Cell Signaling Technology), antivinculin (#4650) (Cell Signaling Technology), anti-α smooth muscle actin (ab32575) (Abcam), antivimentin (Sc-32322) (Santa Cruz Biotechnologies), anti-MMP9-(E-11) (Sc-393859) (Santa Cruz Biotechnologies), anti-DRP1 (ab54038) (Abcam), anti-PGC1 (Sc-13067) (Santa Cruz Biotechnologies), anti-PPARγ (#2443) (Cell Signaling Technology), antiphospho-PPARγ (Ser112) (PA5−35664) (Thermo Scientific), and antipaxillin (#12065) (Cell Signaling Technology). Reversible Ponceau S staining was used as loading control as the usual loading controls GAPDH, ATP5B, or tubulin showed changed levels of expression at least in one condition based on the proteomics data. Quantification of digitized images of immunoblot bands from four biological replicates were quantified using ImageJ 1.50f3 software (http://rsbweb.nih.gov/ij/).

DOI: 10.1021/acs.jproteome.8b00001
J. Proteome Res. 2018, 17, 1677−1689

Protein Carbonylation

Protein carbonylation assay was performed as a colorimetric measurement of protein oxidation level using the assay kit (#K830−100, Biovision) according to manufacturer's instructions.

Transmission Electron Microscopy

Sample fixation and embedding were done as described previously.[12] Briefly, the heart samples were postfixed with 2% osmium tetraoxide, dehydrated with gradual ethanol (30−100%), infiltrated with propylene oxide, embedded in Epon (Merck), and cured for 24 h at 60 °C. Semithin sections were cut and stained with toluidine blue. Ultrathin sections of 50 nm were collected onto 200 mesh copper girds, stained with uranyl acetate and lead citrate before the analysis by transmission electron microscopy (Jeol 1200 EXII; TEM) at 80 kV. Images were taken using a digital camera (KeenViewII, Olympus) and processed with the iTEM software package (anlySISFive, Olympus). The size and number of mitochondria were quantified in pictures of identical magnification from at least two biological replicates of each experimental group using ImageJ 1.50f3.

Serum Analysis

Blood samples were collected from all mice by cardiac puncture, and serum was isolated and kept at −80 °C. The levels of circulating free fatty acids were measured according to the manufacturer's prescriptions. The expression level of TGFβ was measured using mouse oxidative stress ELISA strip colorimetric kit (#EA-1401) (Signosis) according to the manufacturer's instructions.

Immunohistochemistry

Paraffin embedded heart tissue samples were cut in slices (4 μm) at the level of the mid horizontal plane. Heart sections from all groups with different treatment dose were stained with anti-CD45 (ab10558) to study the severity of inflammation after high-dose irradiation. Quantification of CD45 positive cells was carried out collecting four digital images per heart section (IAS image-processing software, Delta Sistemi, Rome, Italy) and carried out by investigators blinded to treatment groups.

Statistical Analysis

The student's t test (unpaired) and two-way ANOVA with Bonferroni posthoc test were used as statistical tests. Group difference was considered as statistically significant with values of $*p < 0.05$, $**p < 0.01$, and $***p < 0.001$. The error bars were calculated as standard deviation (SD). Proteomics analysis was done using five biological replicates. Immunoblotting, ELISA, and colorimetric experiments were done using four biological replicates.

Data Availability

The raw MS data can be accessed from the RBstore database (https://www.storedb.org/store_v3/study.jsp?studyId=1100).

RESULTS

Irradiation Induces Changes in the Cardiac Proteome Depending on the PPARα Status

The cardiac proteome of PPARα wild type, PPARα +/−, and PPARα −/− mice was analyzed 20 weeks after local heart X-ray irradiation (8 Gy, 16 Gy). Global label-free analysis of the cardiac tissue identified 2,736 proteins in total (Table S-1) of which 1750 could be quantified (Table S-1).

Among quantified proteins in the PPARα wild type, only one single protein, thyroid hormone receptor associated protein 3, was significantly differentially expressed at the dose of 8 Gy compared to the PPARα wild type sham-irradiated control group (Table S-3). At 16 Gy, 84 proteins were significantly differentially expressed, of which 46 were upregulated and 38 downregulated (Table S-4). Eight of the downregulated proteins belonged to the lipid metabolism pathway (Table S-3, orange color). Of these lipid metabolic enzymes, only annexin 1 (ANXA1), a negative regulator of the phospholipase family, was upregulated; all others were downregulated.

The total number of deregulated proteins at 8 and 16 Gy in the wild type mice are shown in the Venn diagram (Figure 1A).

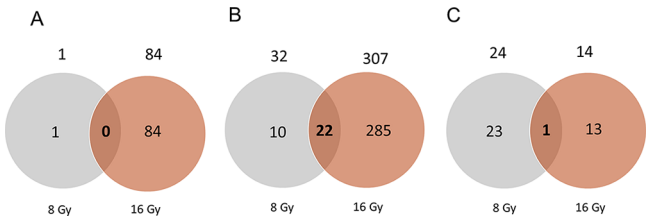

Figure 1. Radiation-induced alteration in the cardiac proteome. (A) Venn diagram shows the number of total and shared deregulated proteins at 8 and 16 Gy compared to control (0 Gy) of wild type mice (B) PPARα heterozygous (+/−) mutant mice and (C) PPARα homozygous (−/−) mutant mice.

In the PPARα heterozygous +/− mice, 32 proteins were significantly differentially expressed at 8 Gy (8 upregulated and 24 downregulated) if compared to the PPARα +/− control heart tissue (0 Gy) (Table S-5). At 16 Gy, 307 proteins were deregulated, of which 83 were upregulated and 224 downregulated (Table S-6). The largest group of these differentially regulated proteins belonged to the mitochondrial oxidative phosphorylation system (24 proteins); all of these were downregulated (Table S-6, gray color). The second largest group was proteins of lipid metabolism, all of which were downregulated with the exception of ANXA1 (Table S-6, orange color). The proteomics analysis showed that 22 proteins were shared between the two doses in the PPARα +/− mice (Figure 1B) (Table S-6, italics). All shared proteins with the exception of one (SPRY domain containing 4) showed same direction of deregulation (downregulation). One of the shared proteins was apolipoproteinA-II (APOA2) that was markedly downregulated at both doses (fold changes 0.26 and 0.23 at 8 and 16 Gy, respectively). *Apoa2* is a target gene of PPARα.[53] Altogether, 10 proteins known to be transcriptionally regulated by PPARα were found to be differentially regulated (16 Gy) with 7 downregulated and 3 upregulated proteins (Table S-6, bold).[54]

In the homozygous PPARα −/− mice, 24 proteins were significantly differentially expressed at 8 Gy, of which 18 proteins were upregulated and 6 downregulated compared to the PPARα −/− control group (Table S-7). At 16 Gy, 14 proteins were significantly differentially expressed, of which 8 proteins were upregulated and 6 downregulated (Table S-8), partly due to the high variability between the biological replicates. Of these, only one protein, podocalyxin-like protein, was shared between 8 and 16 Gy radiation doses (Figure 1C). It was downregulated at both doses (Tables S-7 and S-8).

Taken together, at the highest dose, the heterozygous mutant showed the largest number of significant radiation-induced

DOI: 10.1021/acs.jproteome.8b00001
J. Proteome Res. 2018, 17, 1677−1689

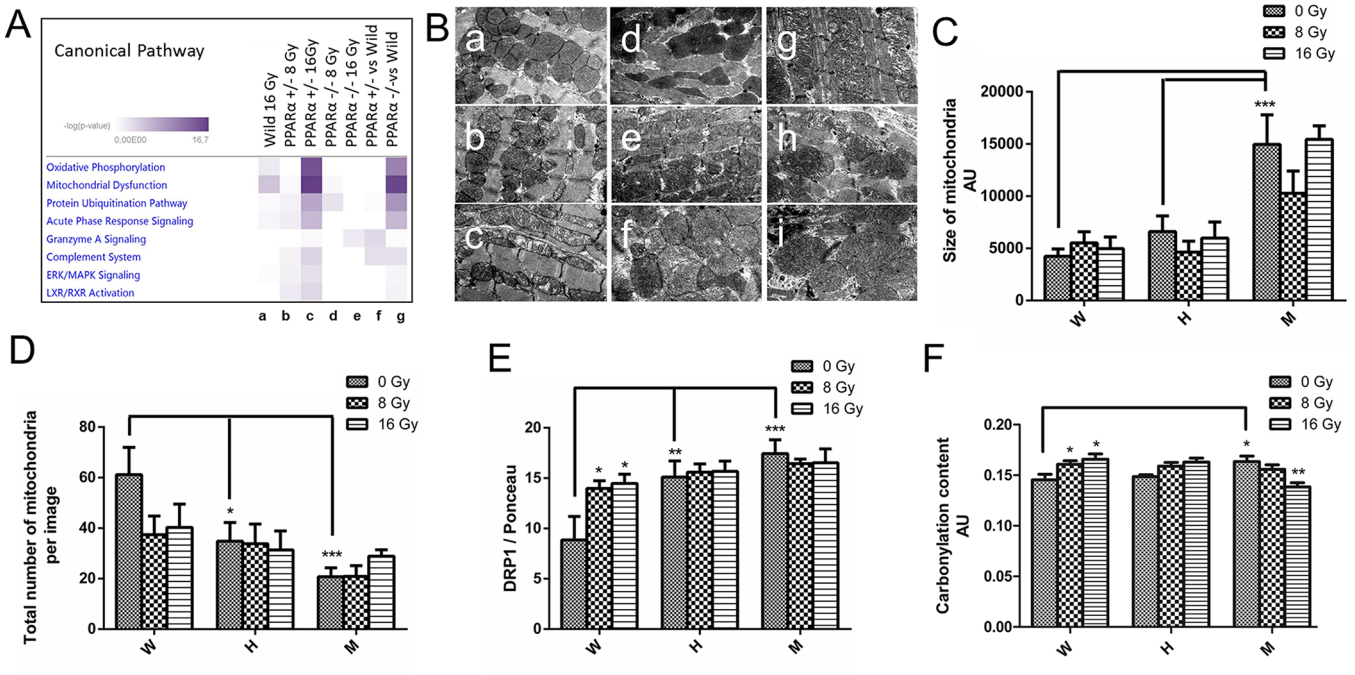

Figure 2. Radiation- and genotype-induced alterations in the mitochondria-associated features. (A) Most affected signaling pathways analysis according to IPA analysis are shown in (a) irradiated wild type (16 Gy vs 0 Gy); (b) irradiated heterozygous mutant (8 Gy vs 0 Gy); (c) irradiated heterozygous mutant (16 Gy vs 0 Gy); (d) irradiated homozygous mutant (8 Gy vs 0 Gy); (e) irradiated homozygous mutant (16 Gy vs 0 Gy); (f) nonirradiated heterozygous mutant vs nonirradiated wild type; (g) nonirradiated homozygous mutant vs nonirradiated wild type. High color intensity represents high significance (p-value). All colored boxes have a p-value of ≤ 0.05; white boxes have a p-value of ≥ 0.05 and are not significantly altered. (B) Typical electron microscopy images of heart sections of the (a) nonirradiated wild type mice, irradiated wild type mice at (b) 8 Gy, or (c) 16 Gy, (d) nonirradiated PPARα heterozygous mutant mice, heterozygous mutant mice irradiated at (e) 8 Gy or (f) 16 Gy, and (g) nonirradiated PPARα homozygous mutant mice, homozygous mutant mice irradiated at (h) 8 Gy or (i) 16 Gy. Magnification 2000×. (C) Size of mitochondria was analyzed using ImageJ, and the data are shown as mean ± SD. W, H, M correspond to wild type, heterozygous, and homozygous mutant, respectively. The radiation doses are indicated in the figure. For each condition, at least two biological replicates and >200 mitochondria were investigated at a magnification of 2000× (2-way ANOVA with Bonferroni posthoc test; $*p \leq 0.05$, $**p \leq 0.01$, $***p \leq 0.005$). (D) Total number of mitochondria per image was analyzed using ImageJ. W, H, M correspond to wild type, heterozygous, and homozygous mutant, respectively. The radiation doses are indicated in the figure. For each condition, at least two biological replicates and 10 electron micrographs were used for quantification. Data are shown as mean ± SD (2-way ANOVA with Bonferroni posthoc test; $*p \leq 0.05$, $**p \leq 0.01$, $***p \leq 0.005$). (E) Immunoblot analysis of the total protein level of DRP1 is shown in wild type (W), heterozygous (H), and homozygous (M) PPARα mice in control (0 Gy) and irradiated (8 and 16 Gy) animals. The columns represent the average ratios of relative protein expression in control and irradiated samples after background correction and normalization as described in the Experimental Section. The error bars are calculated as SD (2-way ANOVA with Bonferroni posthoc test; $*p \leq 0.05$, $**p \leq 0.01$, $***p \leq 0.005$; $n = 4$). (F) Protein carbonylation was calculated based on a colorimetric assay as described in Experimental Section in wild type (W), heterozygous (H), and homozygous (M) PPARα mice under control (0 Gy) and irradiated (8 and 16 Gy) conditions. The error bars are calculated as SD (2-way ANOVA with Bonferroni posthoc test; $*p \leq 0.05$, $**p \leq 0.01$; $n = 4$).

protein expression changes (307 proteins), while the homozygous mutant showed the least significant changes (14 proteins).

Absence of PPARα Influences the Cardiac Proteome

The low number of radiation-responsive deregulated proteins in the homozygous PPARα mutant compared to the large number in the heterozygous mutant prompted us to investigate possible differences between the nonirradiated heart proteomes.

In the nonirradiated heterozygous PPARα +/− mice heart tissue, 33 proteins were significantly differentially expressed in comparison to the nonirradiated wild type PPARα heart tissue (11 upregulated, 22 downregulated) (Table S-9). Of these 33 deregulated proteins, a great majority (29) were also found deregulated in the homozygous mutant, with 26 proteins showing the same direction of deregulation (Table S-10). Only three proteins showed different direction of deregulation (ARGHDIP, PLIN5, TCT38) (Table S-9, green text color).

The nonirradiated homozygous PPARα −/− mice heart tissue showed, in addition to the 29 proteins common with the heterozygous mutant, a large number of differentially expressed proteins (518) in comparison to the nonirradiated wild type PPARα heart proteome (Table S-10) with 364 proteins being upregulated and 154 downregulated. Of these, 31 deregulated proteins were known targets of PPARα.[54]

All in all, these results showed that the radiation-induced alterations in the heart proteome of the heterozygous +/− genotype were overlapping with those of the homozygous −/− genotype, but the homozygous proteome showed a great number of additional changes, mainly in proteins involved in lipid metabolism (27), most of these being downregulated (22) (S-10 Table, orange color). In addition, proteins of mitochondrial oxidative phosphorylation system or calcium transporters represented a large group of deregulated proteins (25 proteins) (Table S-10, gray color), 6 of which were mitochondrial encoded. Also 11 mitochondrial ribosomal proteins were found significantly deregulated (Table S-10,

DOI: 10.1021/acs.jproteome.8b00001
J. Proteome Res. 2018, 17, 1677−1689

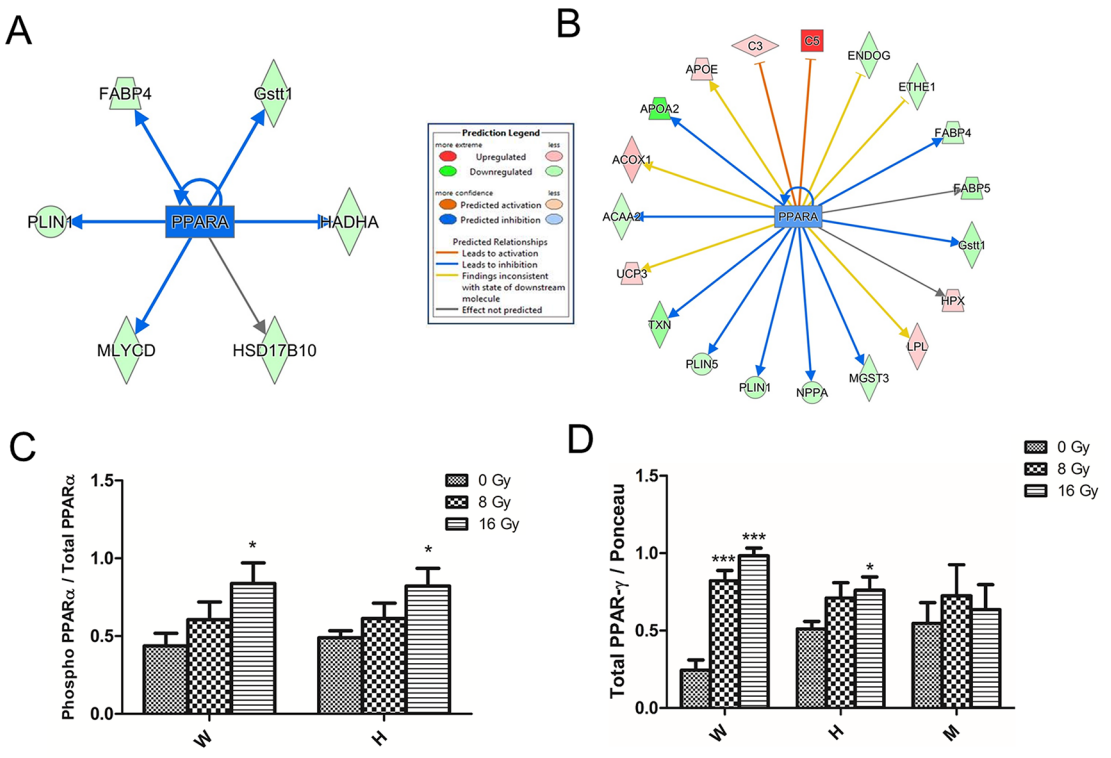

Figure 3. Radiation-induced inactivation of PPARα and increased expression of PPARγ in the heart tissue of wild type (W) and PPARα heterozygous (H) mutant mice. (A) Predicted inactivation (blue color) of PPARα is shown for wild type mice and (B) for heterozygous mutant mice based on the label-free proteomics at 16 Gy (http://www.INGENUITY.com). The upregulated proteins are marked in red and the downregulated in green. (C) Immunoblot analysis of phosphorylated and total levels PPARα is shown in wild type (W) and heterozygous (H) mice in control (0 Gy) and irradiated (8 and 16 Gy) animals. Columns represent the average ratios of relative protein expression in control and irradiated samples after background correction and normalization to Ponceau. The error bars are calculated as SD (t test; $*p \leq 0.05$; $n = 4$). (D) Immunoblot analysis of PPARγ is shown in wild type (W) and heterozygous (H) mice in control (0 Gy) and irradiated (8 and 16 Gy) mice. Columns represent the average ratios of relative protein expression in control and irradiated samples after background correction and normalization to Ponceau. The error bars are calculated as SD (t test; $*p \leq 0.05$; $n = 4$).

light green color). Proteins of oxidative stress response were also well represented (14 proteins) showing both up- and downregulation (Table S-10, red color).

Both Irradiation and the PPARα Genotype Influence the Mitochondrial Morphology

The results from the proteomics analyses were further investigated using the IPA software. The most affected canonical pathways in all proteome comparisons that were made in this study (Tables S-3 and S-10) were oxidative phosphorylation and mitochondrial dysfunction (Figure 2A). The dose of 16 Gy changed the mitochondrial proteome to a larger extent than that of 8 Gy in the wild type and heterozygous mutant while in the homozygous mutant no significant radiation effect was seen. However, the comparison between nonexposed wild type and homozygous mitochondrial proteomes indicated significant changes in the mitochondrial pathways (Figure 2A, high color intensity).

Electron microscopy (EM) imaging revealed differences in the mitochondrial size and morphology, depending on the genotypic status (Figure 2B, Figure S-1). In the homozygous mutant, several massively enlarged mitochondria were observed even in the nonirradiated control, indicating disturbed mitochondrial biogenesis and dynamics due to the lack of PPARα protein. The cristae patterns were more irregular with increased matrix parts than in the nonirradiated wild type.

On the basis of the EM images, the size of the mitochondria was quantified in each genotype and radiation condition (Figure 2C). Cardiac mitochondria of the homozygous nonirradiated mice were significantly larger compared to the mitochondria of nonirradiated wild type mice. No obvious radiation effect on the mitochondrial morphology was seen.

Additionally, the total number of the cardiac mitochondria per image was calculated for each genotype and radiation condition (Figure 2D). The number of cardiac mitochondria in the nonirradiated hetero- and homozygous mutants in comparison to that of nonirradiated wild type mice was significantly reduced. The reduction was larger in the case of the homozygous mutant than in the heterozygous one. Irradiation had no significant effect on the number of mitochondria.

The enlarged mitochondrial size suggested disturbance in the fusion and fission properties. For this reason, the expression of the dynamin 1-like protein (DRP1) that is responsible for the fission process and that of the fusion protein OPA1, mitochondrial dynamin like GTPase, were tested. The level of the total DRP1 was significantly increased in the non-irradiated hetero- and homozygous mutant compared to the wild type (Figure 2E, Figure S-3). Furthermore, irradiation increased the level of DRP1 in the wild type but had no effect in the hetero- or homozygous mutant (Figure 2E, Figure S-3). As increasing phosphorylation of DRP1 at Ser637 prevents mitochondrial fission in cardiomyocytes,[55] the level of phosphorylation at this site was measured. No significant changes were observed between the different genotypes or

DOI: 10.1021/acs.jproteome.8b00001
J. Proteome Res. 2018, 17, 1677−1689

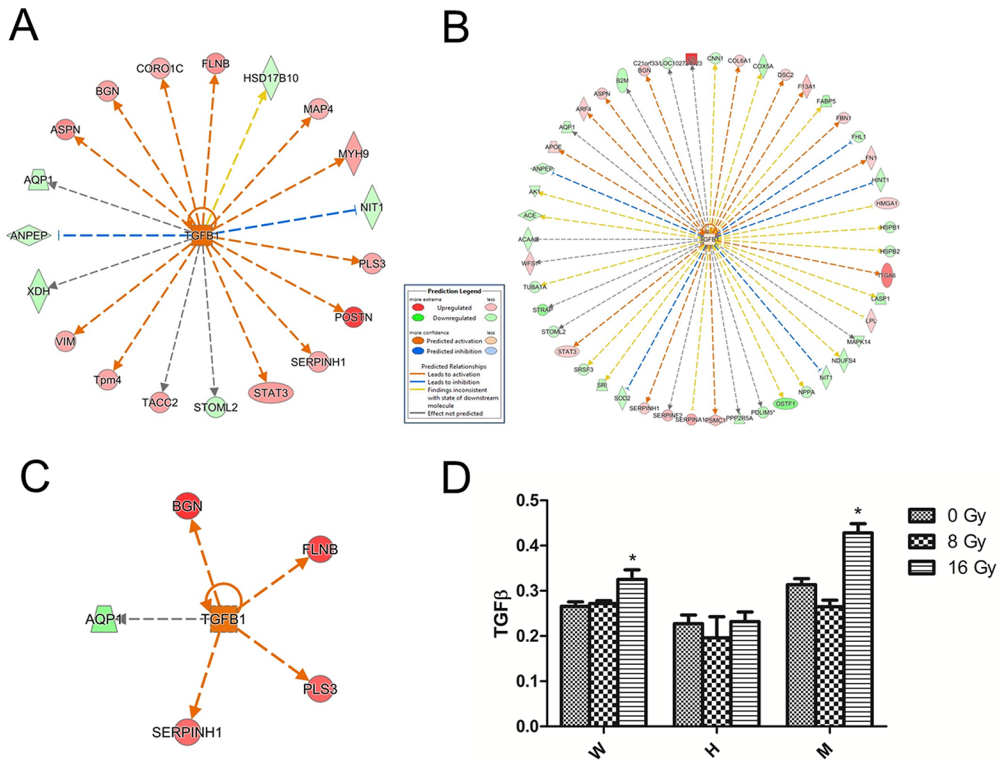

Figure 4. Analysis of the TGFβ status in the wild type (W), PPARα heterozygous (H), and PPARα homozygous (M) mice at 16 Gy. (A) Predicted activation (orange color) of TGFβ is shown for wild type, (B) heterozygous, and (C) homozygous mice (http://www.INGENUITY.com). The upregulated proteins are marked in red and the downregulated in green. (D) Level of TGFβ is shown in the serum of wild type (W) and heterozygous (H) PPARα mice in control (0 Gy) and irradiated (8 and 16 Gy) animals. Columns represent the average ratios of relative protein expression in control and irradiated samples after background correction and normalization as described in Experimental Section. The error bars are calculated as SD (t test; $*p \leq 0.05$; $n = 4$).

irradiation conditions (data not shown). No changes in the expression of OPA1 were found between the different genotypes in nonirradiated or irradiated samples (data not shown). In conclusion, the increased mitochondrial size seen in some conditions could not be explained based on the expression changes of OPA1 or DRP1.

As we have shown before that radiation-induced changes in the mitochondrial proteome are associated with increased mitochondrial reactive oxygen species (ROS),[56] the level of protein oxidation (carbonylation) in the heart tissue was measured (Figure 2F). The basal (nonirradiated) level of carbonylated proteins was higher in the homozygous mutant than in the wild type. Furthermore, irradiation significantly enhanced the protein carbonylation content in the wild type at 16 Gy but reduced it in the homozygous mutant (16 Gy).

In addition, the expression PGC1, a central regulator of the mitochondrial biogenesis[57] and a cofactor needed for the activation of PPARα,[58] was investigated in the different genotypic backgrounds at different radiation exposures. The level of PCG1 was significantly influenced by the genotype, its basal (nonirradiated) expression being increased in the homozygous mutant in comparison to the wild type (Figure S-4). No radiation effect on the level of PGC1 was seen.

Irradiation Induces Inactivation of PPARα and Increases PPARγ and TGFβ Expression

On the basis of IPA upstream regulator analysis, PPARα was predicted to be deactivated in both PPARα wild type and PPARα +/− mice at 16 Gy (Figure 3A,B). The activity of PPARα in the cardiac tissue depends on the phosphorylation of Ser12, increased phosphorylation meaning deactivation of this transcription factor.[12,59] The ratio of phosphorylated (inactive) to total protein was significantly increased in PPARα wild type and PPARα +/− mice at 16 Gy compared to the control group (Figure 3C, Figure S-5) suggesting radiation-related reduced PPAR alpha transcriptional activity in both genotypic groups.

It was also investigated whether the lack of PPARα is compensated by increasing levels of PPARγ as the functions of these two PPARs are partly overlapping.[36] The level of PPARγ was significantly increased by irradiation at both doses in the wild type mice and at the dose of 16 Gy in the heterozygous mutant (Figure 3D, Figure S-5). In the homozygous mutant, the basal level of PPARγ showed an increasing tendency compared to the wild type level that however did not reach significance ($p = 0.08$) (Figure 3D). It was also tested whether the level of phosphorylated (Ser112) PPARγ leading to its inactivation was altered due to irradiation or genotype.[60] No change in the phosphorylated status of PPARγ was observed in any condition (Figure S-5).

TGFβ1 was predicted to be significantly activated at 16 Gy in the heart tissue of wild type and homozygous −/− mice (Figure 4A,C; deep orange color of the central node) but less activated in the heterozygous +/− mice (Figure 4B, light orange color of the node). The level of TGFβ was measured in the serum of all mice. It was significantly increased at 16 Gy in the wild type and homozygous mutant but not in the heterozygous mutant (Figure 4D).

DOI: 10.1021/acs.jproteome.8b00001
J. Proteome Res. 2018, 17, 1677−1689

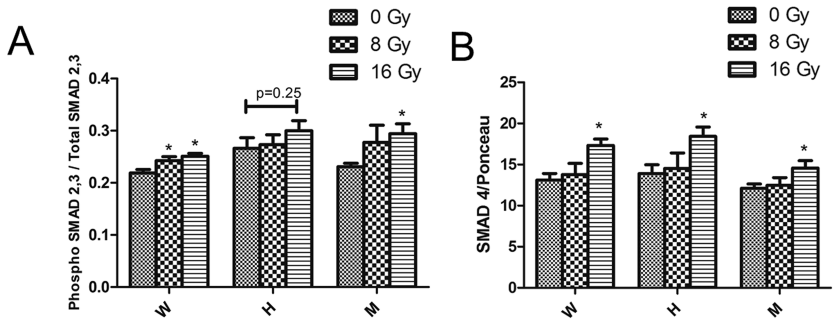

Figure 5. Influence of PPARα status on the SMAD-dependent TGFβ pathway. (A) ELISA analysis of phosphorylated and total levels of SMAD 2/3 is shown in wild type (W), heterozygous (H), and homozygous (M) PPARα mice in control (0 Gy) and irradiated (8 and 16 Gy) animals. (B) Immunoblot analysis of SMAD 4 expression is shown in W, H, and M PPARα mice in control (0 Gy) and irradiated (8 and 16 Gy) animals. The columns represent the average ratios of relative protein expression in control and irradiated samples after background correction and normalization as described in the Experimental Section. The error bars are calculated as SD (t test; $*p \leq 0.05$, $**p \leq 0.01$; $n = 4$).

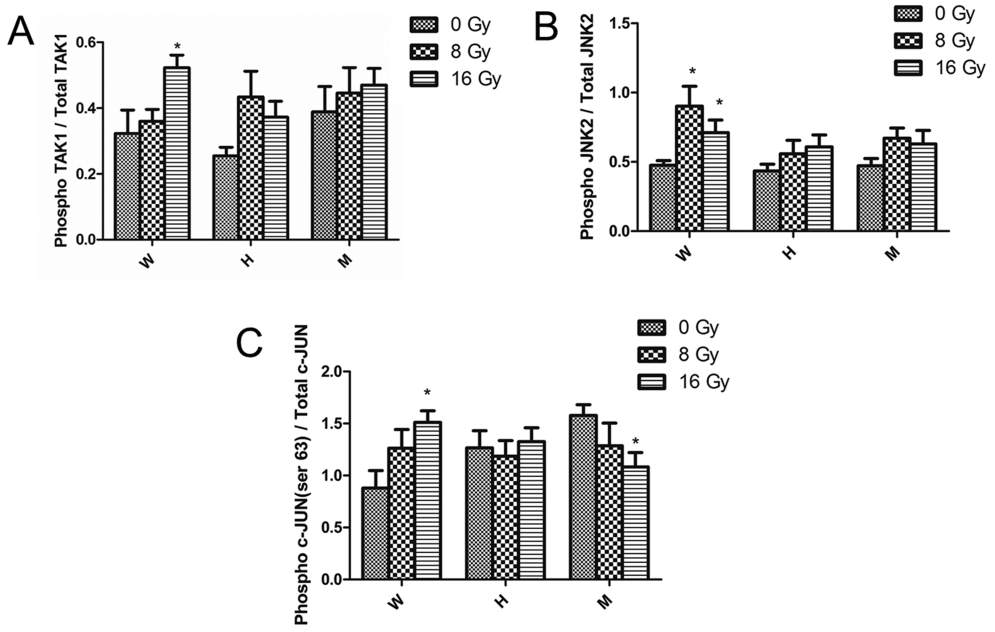

Figure 6. Influence of the PPARα status on the SMAD-independent TGFβ pathway. (A) Immunoblot analysis of phosphorylated and total levels of TAK1, (B) JNK2, and (C) c-JUN is shown in wild type (W), heterozygous (H), and homozygous (M) PPARα mice in control (0 Gy) and irradiated (8 and 16 Gy) animals. Columns represent the average ratios of relative protein expression in control and irradiated samples after background correction and normalization to Ponceau. The error bars are calculated as SD (t test; $*p \leq 0.05$; $n = 4$).

The level of free fatty acids in the serum was increased significantly only in the wild type mice at 16 Gy (data not shown) in agreement with our previous data.[12]

Irradiation Induces SMAD-Dependent TGFβ Signaling Independently of PPARα Status

We have shown previously that irradiation induces both SMAD-dependent and SMAD-independent TGFβ signaling in the heart.[44] Active SMAD2 and SMAD3 are known to interact with SMAD4 to assemble a complex that is required for efficient TGFβ–SMAD-dependent signal transduction.[61] To see whether the expression of PPARα has an effect on SMAD-dependent pathway the levels of total and phosphorylated forms of SMAD2, SMAD3, and SMAD4 were measured in wild type, hetero-, and homozygous mutant. The analysis showed a small but significant increase in the ratio of phosphorylated/total level of SMAD2, 3, and 4 in PPARα wild type and homozygous mutant at 16 Gy (Figure 5, Figure S-6). The heterozygous mutant showed significant increase of SMAD4 at 16 Gy, while the increase in the level of SMAD2, 3 did not reach statistical significance ($p = 0.25$). These data suggest that the status of PPARα does not influence the radiation-induced activation of the SMAD-dependent pathway.

Irradiation Does Not Influence the SMAD-Independent TGFβ Signaling in the Absence of PPARα

To estimate the effect of irradiation on the SMAD-independent TGFβ signaling, the total and phosphorylated forms of protein components of this pathway, TGFβ associated kinase 1 (TAK1), c-JUN N-terminal kinase (JNK2), and c-JUN were analyzed. A significant increase in the ratio of phosphorylated to total level of TAK1 was observed at 16 Gy in PPARα wild type but not in heterozygous PPARα +/− or homozygous PPARα −/− mice at 8 or 16 Gy (Figure 6A, Figure S-7). Activated TAK1 has been shown to induce activation (phosphorylation) of the JNK2 protein that in its turn activates

DOI: 10.1021/acs.jproteome.8b00001
J. Proteome Res. 2018, 17, 1677−1689

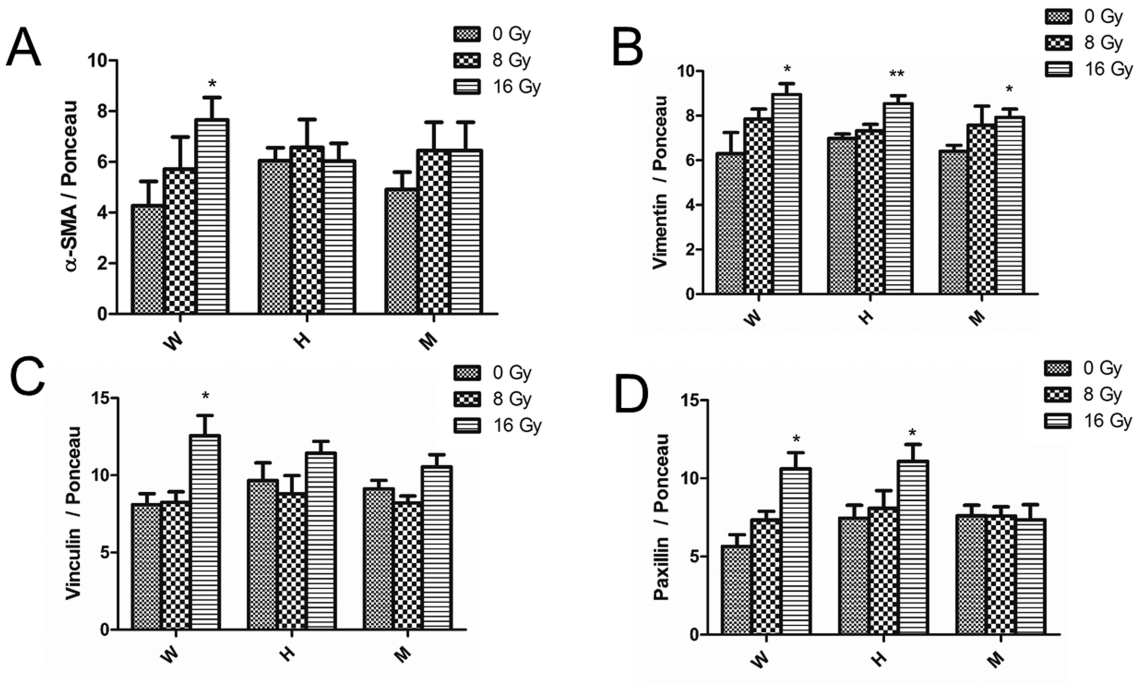

Figure 7. Expression of marker proteins involved in the fibroblast to myofibroblast differentiation. (A) Immunoblot analysis of the levels of α-SMA, (B) vimentin, (C) vinculin, and (D) paxillin is shown in wild type (W), heterozygous (H), and homozygous (M) PPARα mice in control (0 Gy) and irradiated (8 and 16 Gy) animals. The columns represent the average ratios of relative protein expression in control and irradiated samples after background correction and normalization to Ponceau. The error bars are calculated as SD (t test; $*p \leq 0.05$, $**p \leq 0.01$; $n = 4$).

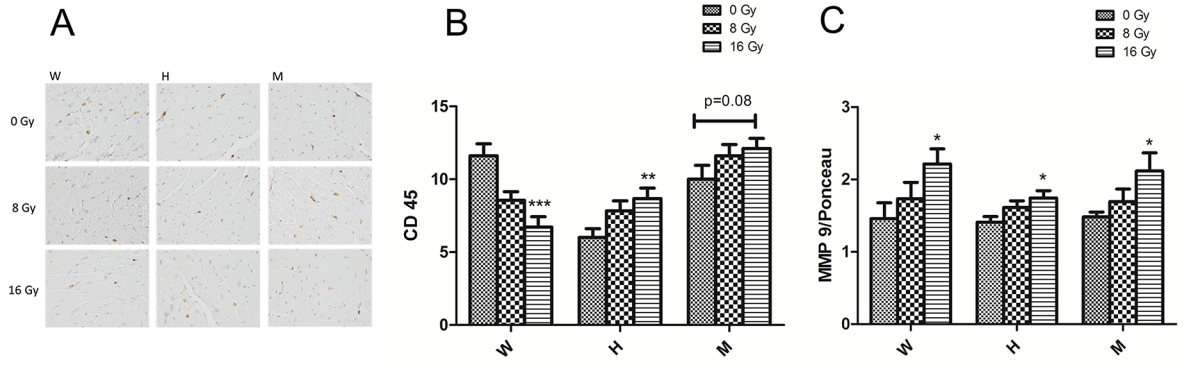

Figure 8. Validation of inflammation marker proteins CD45 and MMP9. (A) Typical CD45 immunohistochemistry images detecting inflammatory infiltrations in the heart tissue are shown. (B) Number of CD45 positive cells normalized to the heart area (number of positive cells per mm^2) in control and irradiated wild type (W), heterozygous (H), and homozygous (M) PPARα mice is shown (t test; $*p \leq 0.05$, $**p \leq 0.01$, $***p \leq 0.005$; $n = 3$). (C) Immunoblot analysis of the level of MMP 9 is shown. The columns represent the average ratios of relative protein expression in control and irradiated wild type (W), heterozygous (H), and homozygous (M) PPARα mice after background correction and normalization to Ponceau. The error bars are calculated as SD (t test; $*p \leq 0.05$; $n = 4$).

c-JUN protein and thereby triggers the transcription of target genes that are involved in inflammatory and fibrotic responses.[62] Significant increase in the ratio of phosphorylated/total level of JNK2 was found in the PPARα wild type mice at 8 and 16 Gy but no significant alteration was observed in PPARα ± and PPARα −/− mice at either radiation dose (Figure 6B, Figure S-7). Furthermore, radiation-induced activation of c-JUN was seen in PPARα wild type mice (16 Gy), while no radiation effect was seen in the heterozygous +/− mice. Interestingly, a significant decrease in the ratio of phosphorylated to total level of c-JUN was observed in PPARα −/− group at 16 Gy (Figure 6C, Figure S-7). These data indicate that the presence of PPARα is necessary for the radiation-induced activation of the noncanonical TGFβ signaling.

Irradiation Enhances the Expression of Marker Proteins Involved in the Fibroblast to Myofibroblast Conversion

The expression of protein markers involved in the fibroblast to myofibroblast differentiation (α-SMA, vinculin, paxillin, and vimentin) was measured to investigate the initiation of radiation-induced cardiac fibrosis in PPARα wild type, PPARα +/−, and PPARα −/− mice. Our analysis showed a significant increase in the level of α-SMA in PPARα wild type at 16 Gy but no significant alteration in PPARα +/− or PPARα −/− mice at either dose (Figure 7A, Figure S-8). The level of vimentin, however, was significantly increased in all mice at 16

DOI: 10.1021/acs.jproteome.8b00001
J. Proteome Res. 2018, 17, 1677−1689

Gy (Figure 7B, Figure S-8). Similar to α-SMA, the protein expression of vinculin was only increased in the wild type mouse (Figure 7C, Figure S-8), while the level of paxillin was significantly enhanced at 16 Gy in wild type and heterozygous PPARα mice (Figure 7D, Figure S-8). Taken together, the dose of 16 Gy was able to increase the expression of myofibroblast maturation markers in the wild type mouse, while only the levels of vimentin and paxillin were affected in the PPARα mutated genotypes at this dose. The dose of 8 Gy did not significantly affect the expression of any of the investigated proteins irrespective of the genotype. These data show that the fibroblast to myofibroblast conversion is initiated early, weeks before the appearance of fibrotic tissue.[43]

Irradiation Induces Inflammation of the Heart Tissue

The effect of irradiation on the number of inflammatory macrophages in the cardiac tissue was tested in all three genotypes using immunohistochemistry (Figure 8A). In the wild type, the number of CD45 positive cells was significantly decreased at the 16 Gy dose, which is in contrast with our previous results 16 weeks postirradiation.[12] However, in the heterozygous mutant, the level of inflammatory infiltrates was significantly increased at the dose of 16 Gy, and an increasing tendency was also seen in the homozygous mutant ($p = 0.08$) (Figure 8B).

The influence of ionizing radiation on the level of matrix metalloprotease 9 (MMP9), a biomarker for cardiac inflammation,[63] was also tested in the heart tissue of the genotypic different mice. The highest dose (16 Gy) caused significantly increased expression of MMP9 independent of the genotype (Figure 8C, Figure S-6). In conclusion, local heart irradiation at high doses appears to function in a pro-inflammatory manner, in agreement with previous studies.[12,44]

DISCUSSION

The goal of this study was to investigate how altering the basal level of PPARα in the heart influences the radiation response, focusing on the two distinct functions of PPARα, namely the regulation of energy metabolism and the anti-inflammatory effect via the TGFβ signaling. For this purpose, in addition to the wild type mice with normal expression of PPARα, also mice that show a loss of one or both genes encoding PPARα were used in all irradiation experiments.

In the wild type mice, the data of this study confirm our previous results showing radiation-induced inactivation of PPARα in the heart.[12] The inhibiting effect of irradiation (16 Gy) on fatty acid oxidation, based on the large number of downregulated proteins of this pathway, is obvious in this study. Furthermore, the activation of TGFβ signaling via SMAD-dependent and SMAD-independent pathways that was previously observed 40 weeks postirradiation[44] is now seen at a much earlier time point (20 weeks). In line with this, we observe radiation-induced increase in the level of proteins important in the conversion of fibroblasts to myofibroblasts. This suggests that a reprogramming for cardiac fibrosis starts relatively early, at a time point where no histological signs of fibrosis are present (ref 43 and data not shown).

In the heterozygous mutant mice, a systemic reduction of the PPARα level leads to reduced mitochondrial number in the heart. Furthermore, the heterozygous mutant shows more radiation-induced changes in the heart proteome than the wild type. However, similar to the wild type mice, the number of differentially regulated proteins increases in a dose-dependent manner. Of the more than 300 differentially regulated proteins (16 Gy), the majority are downregulated and belong to metabolic pathways (mitochondrial respiratory chain and fatty acid oxidation) suggesting that ionizing radiation greatly influences the metabolic function but less the anti-inflammatory function of PPARα in the heterozygous genotype.

In the homozygous mutant lacking PPARα, the cardiac mitochondria are found to be significantly enlarged and their number greatly reduced compared to the wild type or the heterozygous mutant mitochondria. The heart proteome of this mutant, published for the first time in this study, shows severely abnormal features with most protein changes affecting the lipid metabolism and mitochondrial proteins. These proteins are encoded either in the nucleus or in the mitochondria. Radiation exposure does not induce much alteration in this cardiac proteome.

This study shows that in the mice having genotypically reduced or absent expression of PPARα, SMAD-dependent activation of TGFβ pathway is enhanced in a dose-dependent manner as seen in the wild type. In contrast, irradiation shows no effect on the activation of the noncanonical SMAD-independent TGFβ pathway. It was recently shown by Bansal et al. that active PPARα is able to directly bind to TAK1, an upstream member of the noncanonical pathway, thereby inhibiting its phosphorylation and activating the downstream targets.[42] This was ultimately resulting in reduced collagen synthesis and regression of cardiac fibrosis.[42] TAK1-mediated downstream effects involve activation of JNK2, and c-JUN N-terminal kinase.[39,64] We show here that the level of active (phosphorylated) forms of TAK1, JNK2, and c-JUN is only increased by irradiation in wild type mice expressing normal levels of PPARα. These data suggest that under normal physiological conditions (with no radiation exposure) active PPARα inhibits the noncanonical TGFβ signaling, presumably by binding to TAK1. High-dose irradiation inactivates PPARα that subsequently leads to activation of the SMAD-independent TGFβ signaling. In contrast, the SMAD-dependent TGFβ signaling appears to be activated by irradiation independent of the PPARα status.

Interestingly, we observe in the heart tissue of the wild type and heterozygous mice that show radiation-induced loss of active PPARα a simultaneous radiation-induced increase in the expression of PPARγ. In line with our study, the level of PPARγ was increased 3 months after high-dose chest irradiation (15 Gy, 18 Gy) in Sprague−Dawley rats.[65] No radiation-induced enhancement in the PPARγ level is seen in the homozygous mutant lacking the PPARα protein. This may be due to the higher basal level of PPARγ in the homozygous mutant that is indicated by our data in this tudy but did not reach statistical significance. As these two PPAR family members have distinct metabolic functions that are both tissue- and pathway-dependent,[66] a full compensation of one by another is not probable. Although both PPARs have common cofactors, the target genes are not similar.[33] It is assumed that PPARγ is not involved in the activation of fatty acid oxidation in the heart.[67] However, some studies showed anti-inflammatory properties of PPARγ agonists in cardiomyocytes *in vitro* and in cardiac tissue *in vivo*.[68]

All in all, these data emphasize the important role of PPARα in the metabolic and inflammatory response to ionizing radiation in the heart. They suggest that activating PPARα by appropriate ligands could be used to alleviate metabolic abnormalities and inflammation after cardiac radiation ex-

DOI: 10.1021/acs.jproteome.8b00001
J. Proteome Res. 2018, 17, 1677−1689

posure. However, ligand-based activation of PPARα in "normal" myocardial ischemia cases is still a subject of controversy as recently reviewed.[17] Clinical studies suggest that inducing the anti-inflammatory effects of PPARα is clearly protective while the systemic stimulatory effect on fatty acid oxidation in the whole body may be detrimental as it reduces the lipid and thereby energy supply to the heart.[69] The separation of the metabolic and nonmetabolic functions of PPARα may not be conceivable with classical ligands. A targeted inhibition of proteins cooperating with PPARα may be necessary to accomplish a tailor-made prevention of radiation-induced heart disease.[70]

■ ASSOCIATED CONTENT

Supporting Information

The Supporting Information is available free of charge on the ACS Publications website at DOI: 10.1021/acs.jproteome.8b00001.

Genotyping of wild type, PPARα heterozygous, and PPARα homozygous mutant mice; typical electron microscopy images of heart sections; immunoblot analysis of phosphorylated and total levels of DRP1; immunoblot analysis of total levels of PGC1; immunoblot analysis of phosphorylated and total levels PPARα and PPARγ; immunoblot analysis of MMP9 and SMAD 4 expression; immunoblot analysis of phosphorylated and total levels TAK1, JNK2, c-JUN; immunoblot analysis of expression of α-SMA, vimentin, vinculin, and paxillin (PDF)

All proteins identified by label-free proteomics; all proteins quantified by label-free proteomics; significantly deregulated proteins in irradiated heart after 8 Gy in PPARα wild type, 16 Gy in PPARα wild type, 8 Gy in PPARα +/−, 16 Gy in PPARα +/−, 8 Gy in PPARα −/−, 16 Gy in PPARα −/−; significantly deregulated proteins in sham-irradiated PPARα +/− compared to sham-irradiated PPARα +/+; significantly deregulated proteins in sham-irradiated PPARα −/− compared to the sham-irradiated PPARα +/+ (XLS)

■ AUTHOR INFORMATION

Corresponding Author

*E-mail: soile.tapio@helmholtz-muenchen.de. Phone: +49-89-3187-3445. Fax: +49-89-3187-3378.

ORCID

Omid Azimzadeh: 0000-0001-8984-0388
Soile Tapio: 0000-0001-9860-3683

Notes

The authors declare no competing financial interest.

■ ACKNOWLEDGMENTS

V.S. is a recipient of a scholarship from the German Academic Exchange Service (DAAD) Grant No. 91524248. We thank Dr. Michael Rosemann for the help and advice with mouse breeding and Carola Eberhagen and Stefanie Winkler for excellent technical assistance.

■ ABBREVIATIONS

PPARα, peroxisome proliferator activated receptor alpha; TGFβ, transforming growth factor beta; IPA, ingenuity pathway analysis; Gy, gray

■ REFERENCES

(1) Yancy, C. W.; Jessup, M.; Bozkurt, B.; Butler, J.; Casey, D. E., Jr.; Drazner, M. H.; Fonarow, G. C.; Geraci, S. A.; Horwich, T.; Januzzi, J. L.; Johnson, M. R.; Kasper, E. K.; Levy, W. C.; Masoudi, F. A.; McBride, P. E.; McMurray, J. J.; Mitchell, J. E.; Peterson, P. N.; Riegel, B.; Sam, F.; Stevenson, L. W.; Tang, W. H.; Tsai, E. J.; Wilkoff, B. L. 2013 ACCF/AHA guideline for the management of heart failure: a report of the American College of Cardiology Foundation/American Heart Association Task Force on Practice Guidelines. *J. Am. Coll. Cardiol.* **2013**, *62*, e147−239.

(2) Swerdlow, A. J.; Higgins, C. D.; Smith, P.; Cunningham, D.; Hancock, B. W.; Horwich, A.; Hoskin, P. J.; Lister, A.; Radford, J. A.; Rohatiner, A. Z.; Linch, D. C. Myocardial infarction mortality risk after treatment for Hodgkin disease: a collaborative British cohort study. *J. Natl. Cancer Inst* **2007**, *99*, 206−14.

(3) Darby, S. C.; Ewertz, M.; McGale, P.; Bennet, A. M.; Blom-Goldman, U.; Bronnum, D.; Correa, C.; Cutter, D.; Gagliardi, G.; Gigante, B.; Jensen, M. B.; Nisbet, A.; Peto, R.; Rahimi, K.; Taylor, C.; Hall, P. Risk of ischemic heart disease in women after radiotherapy for breast cancer. *N. Engl. J. Med.* **2013**, *368*, 987−98.

(4) Carr, Z. A.; Land, C. E.; Kleinerman, R. A.; Weinstock, R. W.; Stovall, M.; Griem, M. L.; Mabuchi, K. Coronary heart disease after radiotherapy for peptic ulcer disease. *Int. J. Radiat. Oncol., Biol., Phys.* **2005**, *61*, 842−50.

(5) Tukenova, M.; Guibout, C.; Oberlin, O.; Doyon, F.; Mousannif, A.; Haddy, N.; Guerin, S.; Pacquement, H.; Aouba, A.; Hawkins, M.; Winter, D.; Bourhis, J.; Lefkopoulos, D.; Diallo, I.; de Vathaire, F. Role of cancer treatment in long-term overall and cardiovascular mortality after childhood cancer. *J. Clin. Oncol.* **2010**, *28*, 1308−15.

(6) Azizova, T. V.; Muirhead, C. R.; Druzhinina, M. B.; Grigoryeva, E. S.; Vlasenko, E. V.; Sumina, M. V.; O'Hagan, J. A.; Zhang, W.; Haylock, R. G.; Hunter, N. Cardiovascular diseases in the cohort of workers first employed at Mayak PA in 1948−1958. *Radiat. Res.* **2010**, *174*, 155−68.

(7) Shimizu, Y.; Kodama, K.; Nishi, N.; Kasagi, F.; Suyama, A.; Soda, M.; Grant, E. J.; Sugiyama, H.; Sakata, R.; Moriwaki, H.; Hayashi, M.; Konda, M.; Shore, R. E. Radiation exposure and circulatory disease risk: Hiroshima and Nagasaki atomic bomb survivor data, 1950−2003. *Bmj* **2010**, *340*, b5349.

(8) Tapio, S. Pathology and biology of radiation-induced cardiac disease. *J. Radiat. Res.* **2016**, *57*, 439−448.

(9) Di Maggio, F. M.; Minafra, L.; Forte, G. I.; Cammarata, F. P.; Lio, D.; Messa, C.; Gilardi, M. C.; Bravata, V. Portrait of inflammatory response to ionizing radiation treatment. *J. Inflammation (London, U. K.)* **2015**, *12*, 14.

(10) Wang, Y.; Boerma, M.; Zhou, D. Ionizing Radiation-Induced Endothelial Cell Senescence and Cardiovascular Diseases. *Radiat. Res.* **2016**, *186*, 153−61.

(11) Azimzadeh, O.; Sievert, W.; Sarioglu, H.; Merl-Pham, J.; Yentrapalli, R.; Bakshi, M. V.; Janik, D.; Ueffing, M.; Atkinson, M. J.; Multhoff, G.; Tapio, S. Integrative proteomics and targeted transcriptomics analyses in cardiac endothelial cells unravel mechanisms of long-term radiation-induced vascular dysfunction. *J. Proteome Res.* **2015**, *14*, 1203−19.

(12) Azimzadeh, O.; Sievert, W.; Sarioglu, H.; Yentrapalli, R.; Barjaktarovic, Z.; Sriharshan, A.; Ueffing, M.; Janik, D.; Aichler, M.; Atkinson, M. J.; Multhoff, G.; Tapio, S. PPAR Alpha: A Novel Radiation Target in Locally Exposed Mus musculus Heart Revealed by Quantitative Proteomics. *J. Proteome Res.* **2013**, *12*, 2700−14.

(13) Franco, A.; Ciccarelli, M.; Sorriento, D.; Napolitano, L.; Fiordelisi, A.; Trimarco, B.; Durante, M.; Iaccarino, G. Rays Sting: The Acute Cellular Effects of Ionizing Radiation Exposure. *Transl Med. UniSa* **2016**, *14*, 42−53.

DOI: 10.1021/acs.jproteome.8b00001
J. Proteome Res. 2018, 17, 1677−1689

(14) Sridharan, V.; Seawright, J. W.; Antonawich, F. J.; Garnett, M.; Cao, M.; Singh, P.; Boerma, M. Late Administration of a Palladium Lipoic Acid Complex (POLY-MVA) Modifies Cardiac Mitochondria but Not Functional or Structural Manifestations of Radiation-Induced Heart Disease in a Rat Model. *Radiat. Res.* **2017**, *187*, 361−366.
(15) Sridharan, V.; Thomas, C. J.; Cao, M.; Melnyk, S. B.; Pavliv, O.; Joseph, J.; Singh, S. P.; Sharma, S.; Moros, E. G.; Boerma, M. Effects of local irradiation combined with sunitinib on early remodeling, mitochondria, and oxidative stress in the rat heart. *Radiother. Oncol.* **2016**, *119*, 259−64.
(16) Azimzadeh, O.; Azizova, T.; Merl-Pham, J.; Subramanian, V.; Bakshi, M. V.; Moseeva, M.; Zubkova, O.; Hauck, S. M.; Anastasov, N.; Atkinson, M. J.; Tapio, S. A dose-dependent perturbation in cardiac energy metabolism is linked to radiation-induced ischemic heart disease in Mayak nuclear workers. *Oncotarget* **2017**, *8*, 9067−9078.
(17) Azimzadeh, O.; Tapio, S. Proteomics landscape of radiation-induced cardiovascular disease: somewhere over the paradigm. *Expert Rev. Proteomics* **2017**, *14*, 987−996.
(18) Azevedo, P. S.; Minicucci, M. F.; Santos, P. P.; Paiva, S. A.; Zornoff, L. A. Energy metabolism in cardiac remodeling and heart failure. *Cardiol Rev.* **2013**, *21*, 135−40.
(19) Taegtmeyer, H. Energy metabolism of the heart: from basic concepts to clinical applications. *Curr. Probl Cardiol* **1994**, *19*, 59−113.
(20) Lopaschuk, G. D. Metabolic Modulators in Heart Disease: Past, Present, and Future. *Can. J. Cardiol.* **2017**, *33*, 838−849.
(21) Lopaschuk, G. D.; Belke, D. D.; Gamble, J.; Toshiyuki, I.; Schonekess, B. O. Regulation of fatty acid oxidation in the mammalian heart in health and disease. *Biochim. Biophys. Acta, Lipids Lipid Metab.* **1994**, *1213*, 263−76.
(22) Sarma, S.; Ardehali, H.; Gheorghiade, M. Enhancing the metabolic substrate: PPAR-alpha agonists in heart failure. *Heart Failure Rev.* **2012**, *17*, 35−43.
(23) Dreyer, C.; Krey, G.; Keller, H.; Givel, F.; Helftenbein, G.; Wahli, W. Control of the peroxisomal beta-oxidation pathway by a novel family of nuclear hormone receptors. *Cell* **1992**, *68*, 879−87.
(24) Kersten, S. Integrated physiology and systems biology of PPARalpha. *Mol. Metab.* **2014**, *3*, 354−71.
(25) Tugwood, J. D.; Issemann, I.; Anderson, R. G.; Bundell, K. R.; McPheat, W. L.; Green, S. The mouse peroxisome proliferator activated receptor recognizes a response element in the 5′ flanking sequence of the rat acyl CoA oxidase gene. *EMBO J.* **1992**, *11*, 433−9.
(26) Sanderson, L. M.; Degenhardt, T.; Koppen, A.; Kalkhoven, E.; Desvergne, B.; Muller, M.; Kersten, S. Peroxisome proliferator-activated receptor beta/delta (PPARbeta/delta) but not PPARalpha serves as a plasma free fatty acid sensor in liver. *Mol. Cell. Biol.* **2009**, *29*, 6257−67.
(27) Haemmerle, G.; Moustafa, T.; Woelkart, G.; Buttner, S.; Schmidt, A.; van de Weijer, T.; Hesselink, M.; Jaeger, D.; Kienesberger, P. C.; Zierler, K.; Schreiber, R.; Eichmann, T.; Kolb, D.; Kotzbeck, P.; Schweiger, M.; Kumari, M.; Eder, S.; Schoiswohl, G.; Wongsiriroj, N.; Pollak, N. M.; Radner, F. P.; Preiss-Landl, K.; Kolbe, T.; Rulicke, T.; Pieske, B.; Trauner, M.; Lass, A.; Zimmermann, R.; Hoefler, G.; Cinti, S.; Kershaw, E. E.; Schrauwen, P.; Madeo, F.; Mayer, B.; Zechner, R. ATGL-mediated fat catabolism regulates cardiac mitochondrial function via PPAR-alpha and PGC-1. *Nat. Med.* **2011**, *17*, 1076−85.
(28) Cornu-Chagnon, M. C.; Dupont, H.; Edgar, A. Fenofibrate: metabolism and species differences for peroxisome proliferation in cultured hepatocytes. *Toxicol. Sci.* **1995**, *26*, 63−74.
(29) Barger, P. M.; Brandt, J. M.; Leone, T. C.; Weinheimer, C. J.; Kelly, D. P. Deactivation of peroxisome proliferator-activated receptor-alpha during cardiac hypertrophic growth. *J. Clin. Invest.* **2000**, *105*, 1723−30.
(30) Finck, B. N.; Han, X.; Courtois, M.; Aimond, F.; Nerbonne, J. M.; Kovacs, A.; Gross, R. W.; Kelly, D. P. A critical role for PPARalpha-mediated lipotoxicity in the pathogenesis of diabetic cardiomyopathy: modulation by dietary fat content. *Proc. Natl. Acad. Sci. U. S. A.* **2003**, *100*, 1226−31.
(31) Finck, B. N.; Lehman, J. J.; Leone, T. C.; Welch, M. J.; Bennett, M. J.; Kovacs, A.; Han, X.; Gross, R. W.; Kozak, R.; Lopaschuk, G. D.; Kelly, D. P. The cardiac phenotype induced by PPARalpha overexpression mimics that caused by diabetes mellitus. *J. Clin. Invest.* **2002**, *109*, 121−30.
(32) Watanabe, K.; Fujii, H.; Takahashi, T.; Kodama, M.; Aizawa, Y.; Ohta, Y.; Ono, T.; Hasegawa, G.; Naito, M.; Nakajima, T.; Kamijo, Y.; Gonzalez, F. J.; Aoyama, T. Constitutive regulation of cardiac fatty acid metabolism through peroxisome proliferator-activated receptor alpha associated with age-dependent cardiac toxicity. *J. Biol. Chem.* **2000**, *275*, 22293−9.
(33) el Azzouzi, H.; Leptidis, S.; Bourajjaj, M.; Armand, A. S.; van der Nagel, R.; van Bilsen, M.; Da Costa Martins, P. A.; De Windt, L. J. Peroxisome proliferator-activated receptor (PPAR) gene profiling uncovers insulin-like growth factor-1 as a PPARalpha target gene in cardioprotection. *J. Biol. Chem.* **2011**, *286*, 14598−607.
(34) Djouadi, F.; Weinheimer, C. J.; Saffitz, J. E.; Pitchford, C.; Bastin, J.; Gonzalez, F. J.; Kelly, D. P. A gender-related defect in lipid metabolism and glucose homeostasis in peroxisome proliferator-activated receptor alpha- deficient mice. *J. Clin. Invest.* **1998**, *102*, 1083−91.
(35) Guellich, A.; Damy, T.; Lecarpentier, Y.; Conti, M.; Claes, V.; Samuel, J. L.; Quillard, J.; Hebert, J. L.; Pineau, T.; Coirault, C. Role of oxidative stress in cardiac dysfunction of PPARalpha−/− mice. *Am. J. Physiol Heart Circ Physiol* **2007**, *293*, H93−H102.
(36) Lockyer, P.; Schisler, J. C.; Patterson, C.; Willis, M. S. Minireview: Won't get fooled again: the nonmetabolic roles of peroxisome proliferator-activated receptors (PPARs) in the heart. *Mol. Endocrinol.* **2010**, *24*, 1111−9.
(37) Venteclef, N.; Jakobsson, T.; Steffensen, K. R.; Treuter, E. Metabolic nuclear receptor signaling and the inflammatory acute phase response. *Trends Endocrinol. Metab.* **2011**, *22*, 333−43.
(38) Ajith, T. A.; Jayakumar, T. G. Peroxisome proliferator-activated receptors in cardiac energy metabolism and cardiovascular disease. *Clin. Exp. Pharmacol. Physiol.* **2016**, *43*, 649−58.
(39) Liu, G.; Ma, C.; Yang, H.; Zhang, P. Y. Transforming growth factor beta and its role in heart disease. *Exp. Ther. Med.* **2017**, *13*, 2123−2128.
(40) Hong, K. M.; Belperio, J. A.; Keane, M. P.; Burdick, M. D.; Strieter, R. M. Differentiation of human circulating fibrocytes as mediated by transforming growth factor-beta and peroxisome proliferator-activated receptor gamma. *J. Biol. Chem.* **2007**, *282*, 22910−20.
(41) Santiago, J. J.; Dangerfield, A. L.; Rattan, S. G.; Bathe, K. L.; Cunnington, R. H.; Raizman, J. E.; Bedosky, K. M.; Freed, D. H.; Kardami, E.; Dixon, I. M. Cardiac fibroblast to myofibroblast differentiation in vivo and in vitro: expression of focal adhesion components in neonatal and adult rat ventricular myofibroblasts. *Dev. Dyn.* **2010**, *239*, 1573−84.
(42) Bansal, T.; Chatterjee, E.; Singh, J.; Ray, A.; Kundu, B.; Thankamani, V.; Sengupta, S.; Sarkar, S. Arjunolic acid, a peroxisome proliferator-activated receptor alpha agonist, regresses cardiac fibrosis by inhibiting non-canonical TGF-beta signaling. *J. Biol. Chem.* **2017**, *292*, 16440−16462.
(43) Seemann, I.; Gabriels, K.; Visser, N. L.; Hoving, S.; te Poele, J. A.; Pol, J. F.; Gijbels, M. J.; Janssen, B. J.; van Leeuwen, F. W.; Daemen, M. J.; Heeneman, S.; Stewart, F. A. Irradiation induced modest changes in murine cardiac function despite progressive structural damage to the myocardium and microvasculature. *Radiother. Oncol.* **2012**, *103*, 143−50.
(44) Subramanian, V.; Seemann, I.; Merl-Pham, J.; Hauck, S. M.; Stewart, F. A.; Atkinson, M. J.; Tapio, S.; Azimzadeh, O. Role of TGF Beta and PPAR Alpha Signaling Pathways in Radiation Response of Locally Exposed Heart: Integrated Global Transcriptomics and Proteomics Analysis. *J. Proteome Res.* **2017**, *16*, 307−318.
(45) Lee, S. S.; Pineau, T.; Drago, J.; Lee, E. J.; Owens, J. W.; Kroetz, D. L.; Fernandez-Salguero, P. M.; Westphal, H.; Gonzalez, F. J. Targeted disruption of the alpha isoform of the peroxisome proliferator-activated receptor gene in mice results in abolishment of

DOI: 10.1021/acs.jproteome.8b00001
J. Proteome Res. 2018, 17, 1677−1689

the pleiotropic effects of peroxisome proliferators. *Mol. Cell. Biol.* **1995**, *15*, 3012−22.
(46) Azimzadeh, O.; Sievert, W.; Sarioglu, H.; Yentrapalli, R.; Barjaktarovic, Z.; Sriharshan, A.; Ueffing, M.; Janik, D.; Aichler, M.; Atkinson, M. J.; Multhoff, G.; Tapio, S. PPAR Alpha: A Novel Radiation Target in Locally Exposed Mus musculus Heart Revealed by Quantitative Proteomics. *J. Proteome Res.* **2013**, *12*, 2700−2714.
(47) Wisniewski, J. R.; Zougman, A.; Nagaraj, N.; Mann, M. Universal sample preparation method for proteome analysis. *Nat. Methods* **2009**, *6*, 359−62.
(48) Philipp, J.; Azimzadeh, O.; Subramanian, V.; Merl-Pham, J.; Lowe, D.; Hladik, D.; Erbeldinger, N.; Ktitareva, S.; Fournier, C.; Atkinson, M. J.; Raj, K.; Tapio, S. Radiation-Induced Endothelial Inflammation Is Transferred via the Secretome to Recipient Cells in a STAT-Mediated Process. *J. Proteome Res.* **2017**, *16*, 3903−3916.
(49) Hauck, S. M.; Dietter, J.; Kramer, R. L.; Hofmaier, F.; Zipplies, J. K.; Amann, B.; Feuchtinger, A.; Deeg, C. A.; Ueffing, M. Deciphering membrane-associated molecular processes in target tissue of autoimmune uveitis by label-free quantitative mass spectrometry. *Mol. Cell. Proteomics* **2010**, *9*, 2292−305.
(50) Merl, J.; Ueffing, M.; Hauck, S. M.; von Toerne, C. Direct comparison of MS-based label-free and SILAC quantitative proteome profiling strategies in primary retinal Muller cells. *Proteomics* **2012**, *12*, 1902−11.
(51) Brosch, M.; Yu, L.; Hubbard, T.; Choudhary, J. Accurate and sensitive peptide identification with Mascot Percolator. *J. Proteome Res.* **2009**, *8*, 3176−81.
(52) Grosche, A.; Hauser, A.; Lepper, M. F.; Mayo, R.; von Toerne, C.; Merl-Pham, J.; Hauck, S. M. The Proteome of Native Adult Muller Glial Cells From Murine Retina. *Mol. Cell. Proteomics* **2016**, *15*, 462−80.
(53) Blanquart, C.; Barbier, O.; Fruchart, J. C.; Staels, B.; Glineur, C. Peroxisome proliferator-activated receptor alpha (PPARalpha) turnover by the ubiquitin-proteasome system controls the ligand-induced expression level of its target genes. *J. Biol. Chem.* **2002**, *277*, 37254−9.
(54) Rakhshandehroo, M.; Knoch, B.; Muller, M.; Kersten, S. Peroxisome proliferator-activated receptor alpha target genes. *PPAR Res.* **2010**, *2010*, 1.
(55) Yang, Y.; Tian, Y.; Hu, S.; Bi, S.; Li, S.; Hu, Y.; Kou, J.; Qi, J.; Yu, B. Extract of Sheng-Mai-San Ameliorates Myocardial Ischemia-Induced Heart Failure by Modulating Ca2+-Calcineurin-Mediated Drp1 Signaling Pathways. *Int. J. Mol. Sci.* **2017**, *18*, 1825.
(56) Barjaktarovic, Z.; Schmaltz, D.; Shyla, A.; Azimzadeh, O.; Schulz, S.; Haagen, J.; Dorr, W.; Sarioglu, H.; Schafer, A.; Atkinson, M. J.; Zischka, H.; Tapio, S. Radiation-induced signaling results in mitochondrial impairment in mouse heart at 4 weeks after exposure to X-rays. *PLoS One* **2011**, *6*, e27811.
(57) Dorn, G. W., 2nd; Vega, R. B.; Kelly, D. P. Mitochondrial biogenesis and dynamics in the developing and diseased heart. *Genes Dev.* **2015**, *29*, 1981−91.
(58) Fan, W.; Evans, R. PPARs and ERRs: molecular mediators of mitochondrial metabolism. *Curr. Opin. Cell Biol.* **2015**, *33*, 49−54.
(59) Azimzadeh, O.; Azizova, T.; Merl-Pham, J.; Subramanian, V.; Bakshi, M. V.; Moseeva, M.; Zubkova, O.; Hauck, S. M.; Anastasov, N.; Atkinson, M. J.; et al. A dose-dependent perturbation in cardiac energy metabolism is linked to radiation-induced ischemic heart disease in Mayak nuclear workers. *Oncotarget* **2017**, *8*, 9067.
(60) Burns, K. A.; Vanden Heuvel, J. P. Modulation of PPAR activity via phosphorylation. *Biochim. Biophys. Acta, Mol. Cell Biol. Lipids* **2007**, *1771*, 952−60.
(61) Shi, Y.; Massague, J. Mechanisms of TGF-beta signaling from cell membrane to the nucleus. *Cell* **2003**, *113*, 685−700.
(62) Hocevar, B. A.; Prunier, C.; Howe, P. H. Disabled-2 (Dab2) mediates transforming growth factor beta (TGFbeta)-stimulated fibronectin synthesis through TGFbeta-activated kinase 1 and activation of the JNK pathway. *J. Biol. Chem.* **2005**, *280*, 25920−25927.
(63) Halade, G. V.; Jin, Y. F.; Lindsey, M. L. Matrix metalloproteinase (MMP)-9: a proximal biomarker for cardiac remodeling and a distal biomarker for inflammation. *Pharmacol. Ther.* **2013**, *139*, 32−40.
(64) Li, L.; Chen, Y.; Doan, J.; Murray, J.; Molkentin, J. D.; Liu, Q. Transforming growth factor beta-activated kinase 1 signaling pathway critically regulates myocardial survival and remodeling. *Circulation* **2014**, *130*, 2162−72.
(65) Gao, S.; Wu, R.; Zeng, Y. Up-regulation of peroxisome proliferator-activated receptor gamma in radiation-induced heart injury in rats. *Radiat. Environ. Biophys.* **2012**, *51*, 53−9.
(66) Lee, W. S.; Kim, J. Peroxisome Proliferator-Activated Receptors and the Heart: Lessons from the Past and Future Directions. *PPAR Res.* **2015**, *2015*, 271983.
(67) Finck, B. N. The PPAR regulatory system in cardiac physiology and disease. *Cardiovasc. Res.* **2007**, *73*, 269−77.
(68) Ehara, N.; Ono, K.; Morimoto, T.; Kawamura, T.; Abe, M.; Hasegawa, K. The possible role of peroxisome proliferator-activated receptor gamma in heart failure. *Exp Clin Cardiol* **2004**, *9*, 169−73.
(69) van Bilsen, M.; van Nieuwenhoven, F. A. PPARs as therapeutic targets in cardiovascular disease. *Expert Opin. Ther. Targets* **2010**, *14*, 1029−45.
(70) Tapio, S. Using proteomics to explore the effects of radiation on the heart - impacts for medicine. *Expert Rev. Proteomics* **2017**, *14*, 277−279.

DOI: 10.1021/acs.jproteome.8b00001
J. Proteome Res. 2018, 17, 1677−1689

Chapter 3: Conclusion and outlook

In chapter 2.1, our study document the involvement of PPARα and TGFβ in the development of long-term radiation-induced myocardial damage. Significantly, PPARα activity remains repressed whilst TGFβ signaling is upregulated in a persistent manner, remaining even after 40 weeks of post-irradiation. This imbalance was associated with changes in the proteome and transcriptome that indicate an impaired cardiac lipid metabolism, an ongoing inflammatory response, and activation of wound healing (fibrosis) in the heart. Our Study also found that MAPK signaling pathway as a possible source of crosstalk between the PPARα and TGFβ signaling pathways to regulate the outcome of these two signaling pathways. This confirms the hypothesis that PPARα and TGFβ plays a role in the progression of radiation-induced pathological consequences after radiation exposure in the heart.

Moreover, the study from Chapter 2.2, revealed workplace exposure to an external radiation dose increases the risk of developing ischemic heart disease due to impaired activity of PPARα protein with increased phosphorylation that is accompanied by changes in the expression of structural and antioxidant proteins and microRNAs in the heart. This data support the role of PPARα in the development of ischemic heart disease due to chronic radiation exposure.

In Chapter 2.3, this study challenged the hypothesis that manipulation of the basal level of PPARα in the heart alters the radiation response and that this may prevent radiation-induced cardiovascular disease phenotype. This study demonstrates that haploinsufficiency of the PPARα gene may increase radiation-induced proteomic changes in the heart. Interestingly, high dose irradiation induced less deregulated proteins in the absence of PPARα. This observed result suggests that radiation may not add more effects in the heart already maximally damaged by the absence of PPARα. This study also revealed that a basal level of PPARα is necessary to induce activation of Smad-independent signaling via TGFβ. These observations confirm the hypothesis that genetic manipulation of the level of PPARα in the heart can able to alter the radiation response in the heart.

All in all, the three published studies included in this thesis demonstrate that PPARα is a central player in generating the observed effects of ionizing radiation on the heart.

Additionally, the data also provide evidence for a role of TGFβ through activation of both SMAD-dependent and SMAD-independent signaling in the heart following exposure to high dose irradiation. These observations suggest that activating PPARα using appropriate ligands or targeted inhibition of TGFβ mediated signaling pathways may help to accomplish tailor-made prevention of radiation-induced heart disease and if true it will be valuable countermeasure in populations occupationally or clinically exposed to ionizing radiation.

Acknowledgments

I write my acknowledgments to express my sincere and humble thanks to the people who supported and helped me in this journey.

First and foremost, my humble and sincere thanks to my God Almighty, my creator, my strong pillar, my source of inspiration, and understanding. He has been the source of my strength throughout this Ph.D. work. Thank you for protecting me, mentally, physically and spiritually in all my way in this land.

Next, I would like to say my thanks to Prof. Michael J. Atkinson, my first supervisor for giving an excellent opportunity to pursue my doctoral thesis at the Institute of Radiation Biology (ISB). His guidance and continuous support from beginning to the end of my Ph.D. research was excellent and helped me to improve myself in the relevant scientific area. His expertise in the field of radiation biology enabled me to have a sound scientific discussion with him, which permitted me to develop relevant knowledge during my doctoral study.

I am so grateful to my supervisor and mentor PD. Dr. Soile Tapio for giving me a chance to work on my Ph.D. thesis in her research group at the Institute of Radiation Biology (ISB). I thank you very much for your research instruction and committed guidance in my doctoral research work.

My next sincere thanks to my second supervisor Prof. Dr. Gabriele Multhoff of TUM. I thank you for your excellent scientific advice and constructive feedbacks during my scientific meetings.

My special thanks go to Dr. Omid Azimzadeh for his great support in my DAAD application process, scientific teachings in the field of proteomics, providing an opportunity to work in multiple projects to learn more about scientific techniques in much more detail through research experiments and scientific discussions.

I am thankful to Dr. Julianne Merl-Pham, Dr. Stefanie M. Hauck from the core-facility proteomics at HMGU, Dr. Wolfgang Sievert from Klinikum rechts der Isar and Dr. Ingar Seemann, Fiona A. Stewart from the Netherlands Cancer Institute and to the many other

research groups and collaboration partners for their tremendous research support in my research work.

I would like to share my thanks to all my friends in ISB and special thanks to Sabine for being with me during good and tough times in my journey as a good friend.

I sincerely appreciate Silvia and Solvejg for their help in supporting office works and making me practice the German language. My sincere thanks to Bahar for arranging all lab meetings, seminars, thesis committee meetings and providing free concert by listening to her songs to forget my academic stress. Few times it was additional stress (Its Joke), most of the time it is not (Its true). I express my sincere thanks to Steffi for all of her technical help related to my research work.

My additional thanks to all other group leaders and their group members of ISB for their support and good scientific discussions during institute scientific meetings. My special thanks to Dr. Michael Rosemann for teaching me skills related to mice experiments and scientific discussion in my Ph.D. project. My profound thanks to all past and present members of the Institute of Radiation Biology (ISB) for their co-operation and help.

I feel proud to say my sincere thanks to my parents, brothers, friends, and extended relatives, who provided all type of support in during my studies and stay in Germany. My great thanks to Dr. Ravikumar, Dr. Sheela Priyadarshini, Dr. Gabriel Milchias, Dr. Antony Prabu, Dr. Edward, Dr. A.P Sasi Kumar, who provided encouragement and excellent support in my education. My special thanks to Dr. Ananthram Devaraj, my beloved brother for his constant guidance in DAAD application process and all type of scientific help, encouragement, support etc. Finally, my words are not enough to thank you all, without you all I would not have reached this level in my life.

Last but not least, extraordinary gratitude goes to The German Academic Exchange Service (DAAD) providing funding for my Ph.D. study and introducing me to Germany to learn new culture, language, people, etc.

Abbreviations

AF1	activating function 1
AF2	activating function 2
CVD	cardiovascular disease
DBD	DNA binding domain
DDA	data dependent aquistation
DTT	dithiothreitol
ELISA	enzyme linked immunosorbent assay
EC	endothelial cells
ERK	extracellular regulated kinase
FASP	filter aided separation of proteins
FDR	false discovery rate
FFA	free fatty acid
GO	gene ontology
Gy	gray
IHC	immunohistochemistry
IPA	ingenuity pathway analysis
IR	irradiation
LBD	ligand binding domain
LC-MS	liquid chromatography-mass spectrometry
M/Z	mass to charge
MAPK	mitogen activated kinase
MMP9	matrix metalloprotein 9
NR	nuclear receptor
PCR	polymerase chain reaction
PKC	protein kinase C
PPARα	peroxisome proliferator activated receptor alpha
PPARβ	peroxisome proliferator activated receptor beta
PPARγ	peroxisome proliferator activated receptor gamma

PPRE	PPAR response element
RBE	relative biological effectiveness
ROS	reactive oxygen species
RT	radiation therapy
SD	standard deviation
SDS	sodium dodecyl sulfate
STRING	search tool for the retrieval of interacting genes and proteins
TAK1	transforming growth factor beta activated kinase 1
TG	triglyceride
TGFβ	transforming growth factor beta
WB	western blotting
IHC	immunohistochemistry
TEM	transmission electron microscopy

Bibliography

1. Swerdlow, A. J.; Higgins, C. D.; Smith, P.; Cunningham, D.; Hancock, B. W.; Horwich, A.; Hoskin, P. J.; Lister, A.; Radford, J. A.; Rohatiner, A. Z. S.; Linch, D. C., Myocardial infarction mortality risk after treatment for Hodgkin disease: a collaborative British cohort study. *Journal of the National Cancer Institute* **2007,** *99* (3), 206–214.
2. Darby, S. C.; Ewertz, M.; McGale, P.; Bennet, A. M.; Blom-Goldman, U.; Brønnum, D.; Correa, C.; Cutter, D.; Gagliardi, G.; Gigante, B.; Jensen, M.-B.; Nisbet, A.; Peto, R.; Rahimi, K.; Taylor, C.; Hall, P., Risk of ischemic heart disease in women after radiotherapy for breast cancer. *The New England journal of medicine* **2013,** *368* (11), 987–998.
3. Azizova, T. V.; Muirhead, C. R.; Druzhinina, M. B.; Grigoryeva, E. S.; Vlasenko, E. V.; Sumina, M. V.; O'Hagan, J. A.; Zhang, W.; Haylock, R. G. E.; Hunter, N., Cardiovascular diseases in the cohort of workers first employed at Mayak PA in 1948-1958. *Radiation research* **2010,** *174* (2), 155–168.
4. Shimizu, Y.; Kodama, K.; Nishi, N.; Kasagi, F.; Suyama, A.; Soda, M.; Grant, E. J.; Sugiyama, H.; Sakata, R.; Moriwaki, H., Radiation exposure and circulatory disease risk: Hiroshima and Nagasaki atomic bomb survivor data, 1950-2003. *Bmj* **2010,** *340*, b5349.
5. Tapio, S., Pathology and biology of radiation-induced cardiac disease. *Journal of radiation research* **2016,** *57* (5), 439-448.
6. Baker, J. E.; Moulder, J. E.; Hopewell, J. W., Radiation as a risk factor for cardiovascular disease. *Antioxidants & redox signaling* **2011,** *15* (7), 1945–1956.
7. Hall, E. J.; Giaccia, A. J., *Radiobiology for the Radiologist*. Lippincott Williams & Wilkins: 2006.
8. Fleet, A., Radiobiology for the Radiologist: Eric J. Hall, Amato J. Giaccia, Lippincott Williams and Wilkins Publishing; ISBN 0-7817-4151-3; 656 pages; 2006; Hardback;£ 53. *Journal of Radiotherapy in Practice* **2006,** *5* (4), 237-237.
9. Little, J. B., Genomic instability and bystander effects: a historical perspective. *Oncogene* **2003,** *22* (45), 6978-6987.
10. Little, M. P., A review of non-cancer effects, especially circulatory and ocular diseases. *Radiation and environmental biophysics* **2013,** *52* (4), 435–449.
11. McGale, P.; Darby, S. C.; Hall, P.; Adolfsson, J.; Bengtsson, N.-O.; Bennet, A. M.; Fornander, T.; Gigante, B.; Jensen, M.-B.; Peto, R., Incidence of heart disease in 35,000 women treated with radiotherapy for breast cancer in Denmark and Sweden. *Radiotherapy and Oncology* **2011,** *100* (2), 167-175.
12. Yeoh, K.-W.; Mikhaeel, N. G., Role of radiotherapy in modern treatment of Hodgkin's lymphoma. *Advances in hematology* **2011,** *2011*.
13. Rutqvist, L. E.; Rose, C.; Cavallin-Ståhl, E., A systematic overview of radiation therapy effects in breast cancer. *Acta oncologica* **2003,** *42* (5-6), 532-545.
14. Hurkmans, C. W.; Borger, J. H.; Bos, L. J.; van der Horst, A.; Pieters, B. R.; Lebesque, J. V.; Mijnheer, B. J., Cardiac and lung complication probabilities after breast cancer irradiation. *Radiotherapy and oncology* **2000,** *55* (2), 145-151.
15. Johansen, S.; Tjessem, K. H.; Fosså, K.; Bosse, G.; Danielsen, T.; Malinen, E.; Fosså, S. D., Dose distribution in the heart and cardiac chambers following 4-field radiation therapy of breast cancer: a retrospective study. *Breast cancer: basic and clinical research* **2013,** *7*, BCBCR. S11118.

16. Darby, S.; McGale, P.; Peto, R.; Granath, F.; Hall, P.; Ekbom, A., Mortality from cardiovascular disease more than 10 years after radiotherapy for breast cancer: nationwide cohort study of 90 000 Swedish women. *Bmj* **2003,** *326* (7383), 256-257.
17. Darby, S. C.; McGale, P.; Taylor, C. W.; Peto, R., Long-term mortality from heart disease and lung cancer after radiotherapy for early breast cancer: Prospective cohort study of about 300 000 women in US SEER cancer registries. *The Lancet Oncology* **2005,** *6* (8), 557–565.
18. Carr, Z. A.; Land, C. E.; Kleinerman, R. A.; Weinstock, R. W.; Stovall, M.; Griem, M. L.; Mabuchi, K., Coronary heart disease after radiotherapy for peptic ulcer disease. *International Journal of Radiation Oncology• Biology• Physics* **2005,** *61* (3), 842-850.
19. Tukenova, M.; Guibout, C.; Oberlin, O.; Doyon, F.; Mousannif, A.; Haddy, N.; Guérin, S.; Pacquement, H.; Aouba, A.; Hawkins, M., Role of cancer treatment in long-term overall and cardiovascular mortality after childhood cancer. *Journal of clinical oncology* **2010,** *28* (8), 1308-1315.
20. Group, E. B. C. T. C., Effects of radiotherapy and of differences in the extent of surgery for early breast cancer on local recurrence and 15-year survival: an overview of the randomised trials. *The Lancet* **2005,** *366* (9503), 2087-2106.
21. Darby, S. C.; Cutter, D. J.; Boerma, M.; Constine, L. S.; Fajardo, L. F.; Kodama, K.; Mabuchi, K.; Marks, L. B.; Mettler, F. A.; Pierce, L. J., Radiation-related heart disease: current knowledge and future prospects. *International journal of radiation oncology, biology, physics* **2010,** *76* (3), 656.
22. Carlson, R. G.; Mayfield, W. R.; Normann, S.; Alexander, J. A., Radiation-associated valvular disease. *Chest* **1991,** *99* (3), 538-545.
23. Hooning, M. J.; Botma, A.; Aleman, B. M.; Baaijens, M. H.; Bartelink, H.; Klijn, J. G.; Taylor, C. W.; Van Leeuwen, F. E., Long-term risk of cardiovascular disease in 10-year survivors of breast cancer. *Journal of the National Cancer Institute* **2007,** *99* (5), 365-375.
24. Darby, S. C.; Ewertz, M.; Hall, P., Ischemic heart disease after breast cancer radiotherapy. *The New England journal of medicine* **2013,** *368* (26), 2527.
25. Taylor, C.; Darby, S. C., Ischemic heart disease and breast cancer radiotherapy: the way forward. *JAMA internal medicine* **2014,** *174* (1), 160-161.
26. Hauptmann, M.; Mohan, A. K.; Doody, M. M.; Linet, M. S.; Mabuchi, K., Mortality from diseases of the circulatory system in radiologic technologists in the United States. *American journal of epidemiology* **2003,** *157* (3), 239-248.
27. Hayashi, T.; Kusunoki, Y.; Hakoda, M.; Morishita, Y.; Kubo, Y.; Maki, M.; Kasagi, F.; Kodama, K.; Macphee, D.; Kyoizumi, S., Radiation dose-dependent increases in inflammatory response markers in A-bomb survivors. *International journal of radiation biology* **2003,** *79* (2), 129-136.
28. Tomasek, L.; Swerdlow, A.; Darby, S.; Placek, V.; Kunz, E., Mortality in uranium miners in west Bohemia: a long-term cohort study. *Occupational and environmental medicine* **1994,** *51* (5), 308-315.
29. Nusinovici, S.; Vacquier, B.; Leuraud, K.; Metz-Flamant, C.; Caër-Lorho, S.; Acker, A.; Laurier, D., Mortality from circulatory system diseases and low-level radon exposure in the French cohort study of uranium miners, 1946-1999. *Scandinavian journal of work, environment & health* **2010**, 373-383.
30. Azizova, T.; Haylock, R.; Moseeva, M.; Bannikova, M.; Grigoryeva, E., Cerebrovascular diseases incidence and mortality in an extended Mayak Worker Cohort 1948–1982. *Radiation research* **2014,** *182* (5), 529-544.

31. Azizova, T. V.; Muirhead, C. R.; Moseeva, M. B.; Grigoryeva, E. S.; Vlasenko, E. V.; Hunter, N.; Haylock, R. G. E.; O'Hagan, J. A., Ischemic heart disease in nuclear workers first employed at the Mayak PA in 1948-1972. *Health physics* **2012,** *103* (1), 3–14.
32. Preston, D. L.; Shimizu, Y.; Pierce, D. A.; Suyama, A.; Mabuchi, K., Studies of mortality of atomic bomb survivors. Report 13: Solid cancer and noncancer disease mortality: 1950–1997. *Radiation research* **2003,** *160* (4), 381-407.
33. Fajardo, L.; Stewart, J., Experimental radiation-induced heart disease. I. Light microscopic studies. *The American journal of pathology* **1970,** *59* (2), 299.
34. Lauk, S.; Kiszel, Z.; Buschmann, J.; Trott, K.-R., Radiation-induced heart disease in rats. *International Journal of Radiation Oncology* Biology* Physics* **1985,** *11* (4), 801-808.
35. Boerma, M.; Kruse, J. J.; van Loenen, M.; Klein, H. R.; Bart, C. I.; Zurcher, C.; Wondergem, J., Increased deposition of von Willebrand factor in the rat heart after local ionizing irradiation. *Strahlentherapie und Onkologie* **2004,** *180* (2), 109-116.
36. Boerma, M.; Wang, J.; Wondergem, J.; Joseph, J.; Qiu, X.; Kennedy, R. H.; Hauer-Jensen, M., Influence of mast cells on structural and functional manifestations of radiation-induced heart disease. *Cancer research* **2005,** *65* (8), 3100-3107.
37. Seemann, I.; Gabriels, K.; Visser, N. L.; Hoving, S.; te Poele, J. A.; Pol, J. F.; Gijbels, M. J.; Janssen, B. J.; van Leeuwen, F. W.; Daemen, M. J.; Heeneman, S.; Stewart, F. A., Irradiation induced modest changes in murine cardiac function despite progressive structural damage to the myocardium and microvasculature. *Radiotherapy and oncology : journal of the European Society for Therapeutic Radiology and Oncology* **2012,** *103* (2), 143–150.
38. Azimzadeh, O.; Sievert, W.; Sarioglu, H.; Yentrapalli, R.; Barjaktarovic, Z.; Sriharshan, A.; Ueffing, M.; Janik, D.; Aichler, M.; Atkinson, M. J.; Multhoff, G.; Tapio, S., PPAR alpha: a novel radiation target in locally exposed Mus musculus heart revealed by quantitative proteomics. *J Proteome Res* **2013,** *12* (6), 2700-14.
39. Azimzadeh, O.; Scherthan, H.; Sarioglu, H.; Barjaktarovic, Z.; Conrad, M.; Vogt, A.; Calzada-Wack, J.; Neff, F.; Aubele, M.; Buske, C., Rapid proteomic remodeling of cardiac tissue caused by total body ionizing radiation. *Proteomics* **2011,** *11* (16), 3299-3311.
40. Azimzadeh, O.; Subramanian, V.; Ständer, S.; Merl-Pham, J.; Lowe, D.; Barjaktarovic, Z.; Moertl, S.; Raj, K.; Atkinson, M. J.; Tapio, S., Proteome analysis of irradiated endothelial cells reveals persistent alteration in protein degradation and the RhoGDI and NO signalling pathways. *International journal of radiation biology* **2017,** *93* (9), 920-928.
41. Panganiban, R. A. M.; Mungunsukh, O.; Day, R. M., X-irradiation induces ER stress, apoptosis, and senescence in pulmonary artery endothelial cells. *International journal of radiation biology* **2013,** *89* (8), 656-667.
42. Waters, C. M.; Taylor, J. M.; Molteni, A.; Ward, W. F., Dose-response effects of radiation on the permeability of endothelial cells in culture. *Radiation research* **1996,** *146* (3), 321-328.
43. Kim, E. M.; Yang, H. S.; Kang, S. W.; Ho, J.-N.; Lee, S. B.; Um, H.-D., Amplification of the γ-irradiation-induced cell death pathway by reactive oxygen species in human U937 cells. *Cellular signalling* **2008,** *20* (5), 916-924.
44. Azimzadeh, O.; Sievert, W.; Sarioglu, H.; Merl-Pham, J.; Yentrapalli, R.; Bakshi, M. V.; Janik, D.; Ueffing, M.; Atkinson, M. J.; Multhoff, G., Integrative proteomics and targeted transcriptomics analyses in cardiac endothelial cells unravel mechanisms of long-term radiation-induced vascular dysfunction. *Journal of proteome research* **2015,** *14* (2), 1203-1219.

45. Yentrapalli, R.; Azimzadeh, O.; Sriharshan, A.; Malinowsky, K.; Merl, J.; Wojcik, A.; Harms-Ringdahl, M.; Atkinson, M. J.; Becker, K.-F.; Haghdoost, S., The PI3K/Akt/mTOR pathway is implicated in the premature senescence of primary human endothelial cells exposed to chronic radiation. *PloS one* **2013,** *8* (8), e70024.
46. Yentrapalli, R.; Azimzadeh, O.; Barjaktarovic, Z.; Sarioglu, H.; Wojcik, A.; Harms-Ringdahl, M.; Atkinson, M. J.; Haghdoost, S.; Tapio, S., Quantitative proteomic analysis reveals induction of premature senescence in human umbilical vein endothelial cells exposed to chronic low-dose rate gamma radiation. *Proteomics* **2013,** *13* (7), 1096-1107.
47. Sander, V.; Suñe, G.; Jopling, C.; Morera, C.; Belmonte, J. C. I., Isolation and in vitro culture of primary cardiomyocytes from adult zebrafish hearts. *Nature protocols* **2013,** *8* (4), 800.
48. Louch, W. E.; Sheehan, K. A.; Wolska, B. M., Methods in cardiomyocyte isolation, culture, and gene transfer. *Journal of molecular and cellular cardiology* **2011,** *51* (3), 288-298.
49. Frieß, J. L.; Heselich, A.; Ritter, S.; Haber, A.; Kaiser, N.; Layer, P. G.; Thielemann, C., Electrophysiologic and cellular characteristics of cardiomyocytes after X-ray irradiation. *Mutation research* **2015,** *777*, 1–10.
50. Committee, N. R. N., A unified nomenclature system for the nuclear receptor superfamily. *Cell* **1999,** *97* (2), 161-163.
51. Carson-Jurica, M. A.; Schrader, W. T.; O'MALLEY, B. W., Steroid receptor family: structure and functions. *Endocrine Reviews* **1990,** *11* (2), 201-220.
52. Moras, D.; Gronemeyer, H., The nuclear receptor ligand-binding domain: structure and function. *Current opinion in cell biology* **1998,** *10* (3), 384-391.
53. Gervois, P.; Torra, I. P.; Chinetti, G.; Grötzinger, T.; Dubois, G.; Fruchart, J. C.; Fruchart-Najib, J.; Leitersdorf, E.; Staels, B., A truncated human peroxisome proliferator-activated receptor alpha splice variant with dominant negative activity. *Molecular endocrinology (Baltimore, Md.)* **1999,** *13* (9), 1535–1549.
54. Michalik, L.; Auwerx, J.; Berger, J. P.; Chatterjee, V. K.; Glass, C. K.; Gonzalez, F. J.; Grimaldi, P. A.; Kadowaki, T.; Lazar, M. A.; O'Rahilly, S., International Union of Pharmacology. LXI. Peroxisome proliferator-activated receptors. *Pharmacological reviews* **2006,** *58* (4), 726-741.
55. Kliewer, S.; Forman, B.; Blumberg, B.; Ong, E.; Borgmeyer, U.; Mangelsdorf, D.; Umesono, K.; Evans, R., Differential expression and activation of a family of murine peroxisome proliferator-activated receptors. *Proceedings of the National Academy of Sciences* **1994,** *91* (15), 7355-7359.
56. Braissant, O.; Foufelle, F.; Scotto, C.; Dauça, M.; Wahli, W., Differential expression of peroxisome proliferator-activated receptors (PPARs): tissue distribution of PPAR-alpha,-beta, and-gamma in the adult rat. *Endocrinology* **1996,** *137* (1), 354-366.
57. Auboeuf, D.; Rieusset, J.; Fajas, L.; Vallier, P.; Frering, V.; Riou, J. P.; Staels, B.; Auwerx, J.; Laville, M.; Vidal, H., Tissue distribution and quantification of the expression of mRNAs of peroxisome proliferator–activated receptors and liver X receptor-α in humans: no alteration in adipose tissue of obese and NIDDM patients. *Diabetes* **1997,** *46* (8), 1319-1327.
58. Lefebvre, P.; Chinetti, G.; Fruchart, J.-C.; Staels, B., Sorting out the roles of PPARα in energy metabolism and vascular homeostasis. *Journal of Clinical Investigation* **2006,** *116* (3), 571.
59. Feige, J. N.; Gelman, L.; Michalik, L.; Desvergne, B.; Wahli, W., From molecular action to physiological outputs: peroxisome proliferator-activated receptors are nuclear receptors at the crossroads of key cellular functions. *Progress in lipid research* **2006,** *45* (2), 120-159.

60. Pyper, S. R.; Viswakarma, N.; Yu, S.; Reddy, J. K., PPARα: energy combustion, hypolipidemia, inflammation and cancer. *Nuclear receptor signaling* **2010,** *8*.
61. Kim, T.; Yang, Q., Peroxisome-proliferator-activated receptors regulate redox signaling in the cardiovascular system. *World journal of cardiology* **2013,** *5* (6), 164.
62. Chen, K. C.; Chang, S. S.; Huang, H. J.; Lin, T. L.; Wu, Y. J.; Chen, C. Y., Three-in-one agonists for PPAR-alpha, PPAR-gamma, and PPAR-delta from traditional Chinese medicine. *J Biomol Struct Dyn* **2012,** *30* (6), 662-83.
63. Barish, G. D.; Narkar, V. A.; Evans, R. M., PPARδ: a dagger in the heart of the metabolic syndrome. *The Journal of clinical investigation* **2006,** *116* (3), 590.
64. Kilgore, K. S.; Billin, A. N., PPARbeta/delta ligands as modulators of the inflammatory response. *Current opinion in investigational drugs (London, England: 2000)* **2008,** *9* (5), 463-469.
65. Wang, Y.-X.; Lee, C.-H.; Tiep, S.; Ruth, T. Y.; Ham, J.; Kang, H.; Evans, R. M., Peroxisome-proliferator-activated receptor δ activates fat metabolism to prevent obesity. *Cell* **2003,** *113* (2), 159-170.
66. Cheng, L.; Ding, G.; Qin, Q.; Xiao, Y.; Woods, D.; Chen, Y. E.; Yang, Q., Peroxisome proliferator-activated receptor δ activates fatty acid oxidation in cultured neonatal and adult cardiomyocytes. *Biochemical and biophysical research communications* **2004,** *313* (2), 277-286.
67. Tanaka, T.; Yamamoto, J.; Iwasaki, S.; Asaba, H.; Hamura, H.; Ikeda, Y.; Watanabe, M.; Magoori, K.; Ioka, R. X.; Tachibana, K., Activation of peroxisome proliferator-activated receptor δ induces fatty acid β-oxidation in skeletal muscle and attenuates metabolic syndrome. *Proceedings of the National Academy of Sciences* **2003,** *100* (26), 15924-15929.
68. Attianese, G. M. G.; Desvergne, B., Integrative and systemic approaches for evaluating PPARβ/δ (PPARD) function. *Nuclear receptor signaling* **2015,** *13*.
69. Lee, C.-H.; Olson, P.; Evans, R. M., Minireview: lipid metabolism, metabolic diseases, and peroxisome proliferator-activated receptors. *Endocrinology* **2003,** *144* (6), 2201-2207.
70. Barak, Y.; Nelson, M. C.; Ong, E. S.; Jones, Y. Z.; Ruiz-Lozano, P.; Chien, K. R.; Koder, A.; Evans, R. M., PPARγ is required for placental, cardiac, and adipose tissue development. *Molecular cell* **1999,** *4* (4), 585-595.
71. Picard, F.; Auwerx, J., PPARγ and glucose homeostasis. *Annual review of nutrition* **2002,** *22* (1), 167-197.
72. Rosen, E. D.; Spiegelman, B. M., PPARγ: a nuclear regulator of metabolism, differentiation, and cell growth. *Journal of Biological Chemistry* **2001**.
73. Kang, Y. R.; Kwak, C. H.; Hwang, J. Y., Safety and Efficacy of Peroxisome Proliferator-Activated Receptor-alpha Agonist for Treating Cardiovascular Disease. *Korean Circulation Journal* **2007,** *37* (12), 599-608.
74. Bugge, A.; Mandrup, S., Molecular mechanisms and genome-wide aspects of PPAR subtype specific transactivation. *PPAR research* **2010,** *2010*.
75. JUGE-AUBRY, C. E.; KUENZLI, S.; SANCHEZ, J.-C.; HOCHSTRASSER, D.; MEIER, C. A., Peroxisomal bifunctional enzyme binds and activates the activationfunction-1 region of the peroxisome proliferator-activated receptor α. *Biochemical Journal* **2001,** *353* (2), 253-258.
76. Barger, P. M.; Browning, A. C.; Garner, A. N.; Kelly, D. P., p38 Mitogen-activated protein kinase activates peroxisome proliferator-activated receptor α a potential role in the cardiac metabolic stress response. *Journal of Biological Chemistry* **2001,** *276* (48), 44495-44501.

77. Feige, J. N.; Gelman, L.; Tudor, C.; Engelborghs, Y.; Wahli, W.; Desvergne, B., Fluorescence imaging reveals the nuclear behavior of peroxisome proliferator-activated receptor/retinoid X receptor heterodimers in the absence and presence of ligand. *Journal of Biological Chemistry* **2005,** *280* (18), 17880-17890.
78. Tomaru, T.; Satoh, T.; Yoshino, S.; Ishizuka, T.; Hashimoto, K.; Monden, T.; Yamada, M.; Mori, M., Isolation and characterization of a transcriptional cofactor and its novel isoform that bind the deoxyribonucleic acid-binding domain of peroxisome proliferator-activated receptor-γ. *Endocrinology* **2006,** *147* (1), 377-388.
79. Gray, J. P.; Burns, K. A.; Leas, T. L.; Perdew, G. H.; Vanden Heuvel, J. P., Regulation of peroxisome proliferator-activated receptor α by protein kinase C. *Biochemistry* **2005,** *44* (30), 10313-10321.
80. Sung, C. K.; She, H.; Xiong, S.; Tsukamoto, H., Tumor necrosis factor-α inhibits peroxisome proliferator-activated receptor γ activity at a posttranslational level in hepatic stellate cells. *American Journal of Physiology-Gastrointestinal and Liver Physiology* **2004,** *286* (5), G722-G729.
81. Puigserver, P.; Wu, Z.; Park, C. W.; Graves, R.; Wright, M.; Spiegelman, B. M., A cold-inducible coactivator of nuclear receptors linked to adaptive thermogenesis. *Cell* **1998,** *92* (6), 829-839.
82. Li, D.; Kang, Q.; Wang, D.-M., Constitutive coactivator of peroxisome proliferator-activated receptor (PPARγ), a novel coactivator of PPARγ that promotes adipogenesis. *Molecular Endocrinology* **2007,** *21* (10), 2320-2333.
83. Gervois, P.; Torra, I. s. P.; Chinetti, G.; Grötzinger, T.; Dubois, G.; Fruchart, J.-C.; Fruchart-Najib, J.; Leitersdorf, E.; Staels, B., A truncated human peroxisome proliferator-activated receptor α splice variant with dominant negative activity. *Molecular Endocrinology* **1999,** *13* (9), 1535-1549.
84. Xu, H. E.; Lambert, M. H.; Montana, V. G.; Plunket, K. D.; Moore, L. B.; Collins, J. L.; Oplinger, J. A.; Kliewer, S. A.; Gampe, R. T.; McKee, D. D., Structural determinants of ligand binding selectivity between the peroxisome proliferator-activated receptors. *Proceedings of the National Academy of Sciences* **2001,** *98* (24), 13919-13924.
85. Xu, H. E.; Lambert, M. H.; Montana, V. G.; Parks, D. J.; Blanchard, S. G.; Brown, P. J.; Sternbach, D. D.; Lehmann, J. M.; Wisely, G. B.; Willson, T. M., Molecular recognition of fatty acids by peroxisome proliferator–activated receptors. *Molecular cell* **1999,** *3* (3), 397-403.
86. Nolte, R. T.; Wisely, G. B.; Westin, S.; Cobb, J. E.; Lambert, M. H.; Kurokawa, R.; Rosenfeld, M. G.; Willson, T. M.; Glass, C. K.; Milburn, M. V., Ligand binding and co-activator assembly of the peroxisome proliferator-activated receptor-γ. *Nature* **1998,** *395* (6698), 137-143.
87. Leuenberger, N.; Pradervand, S.; Wahli, W., Sumoylated PPARα mediates sex-specific gene repression and protects the liver from estrogen-induced toxicity in mice. *The Journal of clinical investigation* **2009,** *119* (10), 3138.
88. McKenna, N. J.; Lanz, R. B.; O'malley, B. W., Nuclear receptor coregulators: cellular and molecular biology. *Endocrine reviews* **1999,** *20* (3), 321-344.
89. Moraes, L. A.; Piqueras, L.; Bishop-Bailey, D., Peroxisome proliferator-activated receptors and inflammation. *Pharmacology & therapeutics* **2006,** *110* (3), 371-385.
90. Schupp, M.; Lazar, M. A., Endogenous ligands for nuclear receptors: digging deeper. *Journal of Biological Chemistry* **2010,** *285* (52), 40409-40415.
91. Azhar, S., Peroxisome proliferator-activated receptors, metabolic syndrome and cardiovascular disease. *Future cardiology* **2010,** *6* (5), 657-691.

92. Taegtmeyer, H., Energy metabolism of the heart: from basic concepts to clinical applications. *Current problems in cardiology* **1994,** *19* (2), 59-113.
93. Neely, J.; Rovetto, M. a.; Oram, J., Myocardial utilization of carbohydrate and lipids. *Progress in cardiovascular diseases* **1972,** *15* (3), 289-329.
94. Madrazo, J. A.; Kelly, D. P., The PPAR trio: regulators of myocardial energy metabolism in health and disease. *Journal of molecular and cellular cardiology* **2008,** *44* (6), 968-975.
95. Vosper, H.; Khoudoli, G. A.; Graham, T. L.; Palmer, C. N., Peroxisome proliferator-activated receptor agonists, hyperlipidaemia, and atherosclerosis. *Pharmacology & therapeutics* **2002,** *95* (1), 47-62.
96. van der Lee, K. A.; Vork, M. M.; De Vries, J. E.; Willemsen, P. H.; Glatz, J. F.; Reneman, R. S.; Van der Vusse, G. J.; Van Bilsen, M., Long-chain fatty acid-induced changes in gene expression in neonatal cardiac myocytes. *Journal of lipid research* **2000,** *41* (1), 41-47.
97. Brandt, J. M.; Djouadi, F.; Kelly, D. P., Fatty acids activate transcription of the muscle carnitine palmitoyltransferase I gene in cardiac myocytes via the peroxisome proliferator-activated receptor α. *Journal of Biological Chemistry* **1998,** *273* (37), 23786-23792.
98. Gilde, A. J.; van der Lee, K. A.; Willemsen, P. H.; Chinetti, G.; van der Leij, F. R.; van der Vusse, G. J.; Staels, B.; van Bilsen, M., Peroxisome proliferator-activated receptor (PPAR) alpha and PPARbeta/delta, but not PPARgamma, modulate the expression of genes involved in cardiac lipid metabolism. *Circ Res* **2003,** *92* (5), 518-24.
99. Barger, P. M.; Brandt, J. M.; Leone, T. C.; Weinheimer, C. J.; Kelly, D. P., Deactivation of peroxisome proliferator-activated receptor-alpha during cardiac hypertrophic growth. *The Journal of clinical investigation* **2000,** *105* (12), 1723–1730.
100. Huss, J. M.; Levy, F. H.; Kelly, D. P., Hypoxia Inhibits the Peroxisome Proliferator-activated Receptor α/Retinoid X Receptor Gene Regulatory Pathway in Cardiac Myocytes A MECHANISM FOR O2-DEPENDENT MODULATION OF MITOCHONDRIAL FATTY ACID OXIDATION. *Journal of Biological Chemistry* **2001,** *276* (29), 27605-27612.
101. Staels, B.; Dallongeville, J.; Auwerx, J.; Schoonjans, K.; Leitersdorf, E.; Fruchart, J.-C., Mechanism of action of fibrates on lipid and lipoprotein metabolism. *Circulation* **1998,** *98* (19), 2088-2093.
102. Krauss, R. M., Lipids and lipoproteins in patients with type 2 diabetes. *Diabetes care* **2004,** *27* (6), 1496-1504.
103. Tenenbaum, A.; Fisman, E. Z., Fibrates are an essential part of modern anti-dyslipidemic arsenal: spotlight on atherogenic dyslipidemia and residual risk reduction. *Cardiovascular diabetology* **2012,** *11* (1), 125.
104. YOUNG, M. E.; PATIL, S.; Ying, J.; DEPRE, C.; AHUJA, H. S.; SHIPLEY, G. L.; STEPKOWSKI, S. M.; DAVIES, P. J.; TAEGTMEYER, H., Uncoupling protein 3 transcription is regulated by peroxisome proliferator-activated receptor α in the adult rodent heart. *The FASEB Journal* **2001,** *15* (3), 833-845.
105. Duan, S. Z.; Usher, M. G.; Mortensen, R. M., PPARs: the vasculature, inflammation and hypertension. *Current opinion in nephrology and hypertension* **2009,** *18* (2), 128-133.
106. Chinetti-Gbaguidi, G.; Staels, B., PPARβ in macrophages and atherosclerosis. *Biochimie* **2016**.
107. Lockyer, P.; Schisler, J. C.; Patterson, C.; Willis, M. S., Minireview: Won't get fooled again: the nonmetabolic roles of peroxisome proliferator-activated receptors (PPARs) in the heart. *Molecular endocrinology (Baltimore, Md.)* **2010,** *24* (6), 1111–1119.

108. Diep, Q. N.; Benkirane, K.; Amiri, F.; Cohn, J. S.; Endemann, D.; Schiffrin, E. L., PPAR alpha activator fenofibrate inhibits myocardial inflammation and fibrosis in angiotensin II-infused rats. *J Mol Cell Cardiol* **2004,** *36* (2), 295-304.
109. Ajith, T. A.; Jayakumar, T. G., Peroxisome proliferator-activated receptors in cardiac energy metabolism and cardiovascular disease. *Clinical and Experimental Pharmacology and Physiology* **2016,** *43* (7), 649-658.
110. Venteclef, N.; Jakobsson, T.; Steffensen, K. R.; Treuter, E., Metabolic nuclear receptor signaling and the inflammatory acute phase response. *Trends in Endocrinology & Metabolism* **2011,** *22* (8), 333-343.
111. Marx, N.; Sukhova, G. K.; Collins, T.; Libby, P.; Plutzky, J., PPARα activators inhibit cytokine-induced vascular cell adhesion molecule-1 expression in human endothelial cells. *Circulation* **1999,** *99* (24), 3125-3131.
112. Delerive, P.; Martin-Nizard, F.; Chinetti, G.; Trottein, F.; Fruchart, J.; Duriez, P.; Staels, B., PPAR activators inhibit thrombin-induced endothelin-1 production in human vascular endothelial cells by inhibiting the AP-1 signaling pathway. *Circ Res* **1999,** *85* (5), 394-402.
113. Staels, B.; Koenig, W.; Habib, A.; Merval, R.; Lebret, M.; Torra, I. P.; Delerive, P.; Fadel, A.; Chinetti, G.; Fruchart, J.-C., Activation of human aortic smooth-muscle cells is inhibited by PPARα but not by PPARγ activators. *Nature* **1998,** *393* (6687), 790-793.
114. Delerive, P.; De Bosscher, K.; Besnard, S.; Berghe, W. V.; Peters, J. M.; Gonzalez, F. J.; Fruchart, J.-C.; Tedgui, A.; Haegeman, G.; Staels, B., Peroxisome proliferator-activated receptor α negatively regulates the vascular inflammatory gene response by negative cross-talk with transcription factors NF-κB and AP-1. *Journal of Biological Chemistry* **1999,** *274* (45), 32048-32054.
115. Delerive, P.; Gervois, P.; Fruchart, J.-C.; Staels, B., Induction of IkBa expression as a mechanism contributing to the anti-inflammatory activities of PPARa activators. *Journal of Biological Chemistry* **2000**.
116. Shalev, A.; Siegrist-Kaiser, C.; Yen, P.; Wahli, W.; Burger, A.; Chin, W.; Meier, C., The peroxisome proliferator-activated receptor alpha is a phosphoprotein: regulation by insulin. *Endocrinology* **1996,** *137* (10), 4499-4502.
117. Barger, P. M.; Brandt, J. M.; Leone, T. C.; Weinheimer, C. J.; Kelly, D. P., Deactivation of peroxisome proliferator–activated receptor-α during cardiac hypertrophic growth. *Journal of Clinical Investigation* **2000,** *105* (12), 1723.
118. Djouadi, F.; Weinheimer, C. J.; Saffitz, J. E.; Pitchford, C.; Bastin, J.; Gonzalez, F. J.; Kelly, D. P., A gender-related defect in lipid metabolism and glucose homeostasis in peroxisome proliferator-activated receptor alpha-deficient mice. *The Journal of clinical investigation* **1998,** *102* (6), 1083-1091.
119. Watanabe, K.; Fujii, H.; Takahashi, T.; Kodama, M.; Aizawa, Y.; Ohta, Y.; Ono, T.; Hasegawa, G.; Naito, M.; Nakajima, T., Constitutive regulation of cardiac fatty acid metabolism through peroxisome proliferator-activated receptor α associated with age-dependent cardiac toxicity. *Journal of Biological Chemistry* **2000,** *275* (29), 22293-22299.
120. Campbell, F. M.; Kozak, R.; Wagner, A.; Altarejos, J. Y.; Dyck, J. R.; Belke, D. D.; Severson, D. L.; Kelly, D. P.; Lopaschuk, G. D., A Role for Peroxisome Proliferator-activated Receptor α (PPARα) in the Control of Cardiac Malonyl-CoA Levels, reduced fatty acid oxidation rates and increased glucose oxidation rates in the hearts of mice lacking PPARα are associated with higher concentrations of maloyl-CoA and reduced expression of malonyl-CoA decarboxylase. *Journal of Biological Chemistry* **2002,** *277* (6), 4098-4103.

121. Gonzalez, F. J., Recent update on the PPAR alpha-null mouse. *Biochimie* **1997,** *79* (2-3), 139-44.
122. Kersten, S.; Seydoux, J.; Peters, J. M.; Gonzalez, F. J.; Desvergne, B.; Wahli, W., Peroxisome proliferator–activated receptor α mediates the adaptive response to fasting. *Journal of clinical investigation* **1999,** *103* (11), 1489.
123. Smeets, P. J.; Teunissen, B. E.; Willemsen, P. H.; van Nieuwenhoven, F. A.; Brouns, A. E.; Janssen, B. J.; Cleutjens, J. P.; Staels, B.; van der Vusse, G. J.; van Bilsen, M., Cardiac hypertrophy is enhanced in PPAR alpha-/- mice in response to chronic pressure overload. *Cardiovasc Res* **2008,** *78* (1), 79-89.
124. Guellich, A.; Damy, T.; Lecarpentier, Y.; Conti, M.; Claes, V.; Samuel, J.-L.; Quillard, J.; Hébert, J.-L.; Pineau, T.; Coirault, C., Role of oxidative stress in cardiac dysfunction of PPARα−/− mice. *American Journal of Physiology-Heart and Circulatory Physiology* **2007,** *293* (1), H93-H102.
125. Poynter, M. E.; Daynes, R. A., Peroxisome proliferator-activated receptor α activation modulates cellular redox status, represses nuclear factor-κB signaling, and reduces inflammatory cytokine production in aging. *Journal of biological chemistry* **1998,** *273* (49), 32833-32841.
126. Finck, B. N.; Lehman, J. J.; Leone, T. C.; Welch, M. J.; Bennett, M. J.; Kovacs, A.; Han, X.; Gross, R. W.; Kozak, R.; Lopaschuk, G. D., The cardiac phenotype induced by PPARα overexpression mimics that caused by diabetes mellitus. *The Journal of clinical investigation* **2002,** *109* (1), 121-130.
127. Finck, B. N.; Han, X.; Courtois, M.; Aimond, F.; Nerbonne, J. M.; Kovacs, A.; Gross, R. W.; Kelly, D. P., A critical role for PPARα-mediated lipotoxicity in the pathogenesis of diabetic cardiomyopathy: modulation by dietary fat content. *Proceedings of the National Academy of Sciences* **2003,** *100* (3), 1226-1231.
128. Finck, B. N., The PPAR regulatory system in cardiac physiology and disease. *Cardiovascular research* **2007,** *73* (2), 269–277.
129. Border, W. A.; Noble, N. A., Interactions of transforming growth factor-β and angiotensin II in renal fibrosis. *Hypertension* **1998,** *31* (1), 181-188.
130. Schiller, M.; Javelaud, D.; Mauviel, A., TGF-β-induced SMAD signaling and gene regulation: consequences for extracellular matrix remodeling and wound healing. *Journal of dermatological science* **2004,** *35* (2), 83-92.
131. Letterio, J. J.; Roberts, A. B., Regulation of immune responses by TGF-β. *Annual review of immunology* **1998,** *16* (1), 137-161.
132. Suthanthiran, M.; Li, B.; Song, J. O.; Ding, R.; Sharma, V. K.; Schwartz, J. E.; August, P., Transforming growth factor-β1 hyperexpression in African-American hypertensives: a novel mediator of hypertension and/or target organ damage. *Proceedings of the National Academy of Sciences* **2000,** *97* (7), 3479-3484.
133. Khan, R.; Agrotis, A.; Bobik, A., Understanding the role of transforming growth factor-β1 in intimal thickening after vascular injury. *Cardiovascular research* **2007,** *74* (2), 223-234.
134. Schulick, A. H.; Taylor, A. J.; Zuo, W.; Qiu, C.-b.; Dong, G.; Woodward, R. N.; Agah, R.; Roberts, A. B.; Virmani, R.; Dichek, D. A., Overexpression of transforming growth factor β1 in arterial endothelium causes hyperplasia, apoptosis, and cartilaginous metaplasia. *Proceedings of the National Academy of Sciences* **1998,** *95* (12), 6983-6988.
135. Majesky, M. W.; Lindner, V.; Twardzik, D. R.; Schwartz, S. M.; Reidy, M. A., Production of transforming growth factor beta 1 during repair of arterial injury. *Journal of Clinical Investigation* **1991,** *88* (3), 904.

136. Thompson, N. L.; Flanders, K. C.; Smith, J. M.; Ellingsworth, L. R.; Roberts, A. B.; Sporn, M. B., Expression of transforming growth factor-beta 1 in specific cells and tissues of adult and neonatal mice. *The Journal of Cell Biology* **1989,** *108* (2), 661-669.
137. Dubois, C. M.; Laprise, M.-H.; Blanchette, F.; Gentry, L. E.; Leduc, R., Processing of transforming growth factor 1 precursor by human furin convertase. *Journal of Biological Chemistry* **1995,** *270* (18), 10618-10624.
138. Munger, J. S.; Harpel, J. G.; Gleizes, P.-E.; Mazzieri, R.; Nunes, I.; Rifkin, D. B., Latent transforming growth factor-β: structural features and mechanisms of activation. *Kidney international* **1997,** *51* (5), 1376-1382.
139. Hynes, R. O., The extracellular matrix: not just pretty fibrils. *Science* **2009,** *326* (5957), 1216-1219.
140. Lyons, R. M.; Keski-Oja, J.; Moses, H. L., Proteolytic activation of latent transforming growth factor-beta from fibroblast-conditioned medium. *The Journal of cell biology* **1988,** *106* (5), 1659-1665.
141. Miyazawa, K.; Shinozaki, M.; Hara, T.; Furuya, T.; Miyazono, K., Two major Smad pathways in TGF-β superfamily signalling. *Genes to Cells* **2002,** *7* (12), 1191-1204.
142. Massagué, J.; Chen, Y.-G., Controlling TGF-β signaling. *Genes & development* **2000,** *14* (6), 627-644.
143. Gilboa, L.; Wells, R. G.; Lodish, H. F.; Henis, Y. I., Oligomeric structure of type I and type II transforming growth factor β receptors: homodimers form in the ER and persist at the plasma membrane. *The Journal of cell biology* **1998,** *140* (4), 767-777.
144. Shi, Y.; Massagué, J., Mechanisms of TGF-β Signaling from Cell Membrane to the Nucleus. *Cell* **2003,** *113* (6), 685–700.
145. Weiss, A.; Attisano, L., The TGFbeta superfamily signaling pathway. *Wiley interdisciplinary reviews. Developmental biology* **2013,** *2* (1), 47–63.
146. Feng, X.-H.; Derynck, R., Specificity and versatility in TGF-β signaling through Smads. *Annu. Rev. Cell Dev. Biol.* **2005,** *21*, 659-693.
147. Cunnington, R. H.; Nazari, M.; Dixon, I. M., c-Ski, Smurf2, and Arkadia as regulators of TGF-β signaling: new targets for managing myofibroblast function and cardiac fibrosis. *Canadian journal of physiology and pharmacology* **2009,** *87* (10), 764-772.
148. Whitman, M., Signal transduction: Feedback from inhibitory SMADs. *Nature* **1997,** *389* (6651), 549.
149. Jonk, L. J.; Itoh, S.; Heldin, C.-H.; ten Dijke, P.; Kruijer, W., Identification and functional characterization of a Smad binding element (SBE) in the JunB promoter that acts as a transforming growth factor-β, activin, and bone morphogenetic protein-inducible enhancer. *Journal of Biological Chemistry* **1998,** *273* (33), 21145-21152.
150. Chen, S.-J.; Yuan, W.; Mori, Y.; Levenson, A.; Varga, J.; Trojanowska, M., Stimulation of type I collagen transcription in human skin fibroblasts by TGF-β: involvement of Smad 3. *Journal of Investigative Dermatology* **1999,** *112* (1), 49-57.
151. Nagarajan, R. P.; Zhang, J.; Li, W.; Chen, Y., Regulation of Smad7 promoter by direct association with Smad3 and Smad4. *Journal of Biological Chemistry* **1999,** *274* (47), 33412-33418.
152. Dennler, S.; Itoh, S.; Vivien, D.; ten Dijke, P.; Huet, S.; Gauthier, J. M., Direct binding of Smad3 and Smad4 to critical TGFβ-inducible elements in the promoter of human plasminogen activator inhibitor-type 1 gene. *The EMBO journal* **1998,** *17* (11), 3091-3100.

153. Taylor, L. M.; Khachigian, L. M., Induction of platelet-derived growth factor B-chain expression by transforming growth factor-β involves transactivation by Smads. *Journal of Biological Chemistry* **2000,** *275* (22), 16709-16716.
154. Lai, C.-F.; Feng, X.; Nishimura, R.; Teitelbaum, S. L.; Avioli, L. V.; Ross, F. P.; Cheng, S.-L., Transforming Growth Factor-β up-regulates the β5Integrin subunit expression via Sp1 and Smad signaling. *Journal of Biological Chemistry* **2000,** *275* (46), 36400-36406.
155. Holmes, A.; Abraham, D. J.; Sa, S.; Shiwen, X.; Black, C. M.; Leask, A., CTGF and SMADs, maintenance of scleroderma phenotype is independent of SMAD signaling. *Journal of Biological Chemistry* **2001,** *276* (14), 10594-10601.
156. Verrecchia, F.; Chu, M.-L.; Mauviel, A., Identification of novel TGF-beta/Smad gene targets in dermal fibroblasts using a combined cDNA microarray/promoter transactivation approach. *Journal of Biological Chemistry* **2001**.
157. Burks, T. N.; Cohn, R. D., Role of TGF-β signaling in inherited and acquired myopathies. *Skeletal Muscle* **2011,** *1* (1).
158. Massagué, J., How cells read TGF-beta signals. *Nature reviews. Molecular cell biology* **2000,** *1* (3), 169–178.
159. Derynck, R.; Zhang, Y. E., Smad-dependent and Smad-independent pathways in TGF-beta family signalling. *Nature* **2003,** *425* (6958), 577–584.
160. Wakefield, L. M.; Roberts, A. B., TGF-β signaling: positive and negative effects on tumorigenesis. *Current opinion in genetics & development* **2002,** *12* (1), 22-29.
161. Li, J.; Zhao, Z.; Liu, J.; Huang, N.; Long, D.; Wang, J.; Li, X.; Liu, Y., MEK/ERK and p38 MAPK regulate chondrogenesis of rat bone marrow mesenchymal stem cells through delicate interaction with TGF-β1/Smads pathway. *Cell proliferation* **2010,** *43* (4), 333-343.
162. Burch, M. L.; Yang, S. N.; Ballinger, M. L.; Getachew, R.; Osman, N.; Little, P. J., TGF-β stimulates biglycan synthesis via p38 and ERK phosphorylation of the linker region of Smad2. *Cellular and Molecular Life Sciences* **2010,** *67* (12), 2077-2090.
163. Mao, R.; Fan, Y.; Mou, Y.; Zhang, H.; Fu, S.; Yang, J., TAK1 lysine 158 is required for TGF-β-induced TRAF6-mediated Smad-independent IKK/NF-κB and JNK/AP-1 activation. *Cellular signalling* **2011,** *23* (1), 222-227.
164. Hartsough, M. T.; Mulder, K. M., Transforming growth factor β activation of p44mapk in proliferating cultures of epithelial cells. *Journal of Biological Chemistry* **1995,** *270* (13), 7117-7124.
165. Mucsi, I.; Skorecki, K. L.; Goldberg, H. J., Extracellular signal-regulated kinase and the small GTP-binding protein, Rac, contribute to the effects of transforming growth factor-β1 on gene expression. *Journal of Biological Chemistry* **1996,** *271* (28), 16567-16572.
166. Lee, M. K.; Pardoux, C.; Hall, M. C.; Lee, P. S.; Warburton, D.; Qing, J.; Smith, S. M.; Derynck, R., TGF-β activates Erk MAP kinase signalling through direct phosphorylation of ShcA. *The EMBO journal* **2007,** *26* (17), 3957-3967.
167. Yamashita, M.; Fatyol, K.; Jin, C.; Wang, X.; Liu, Z.; Zhang, Y. E., TRAF6 mediates Smad-independent activation of JNK and p38 by TGF-β. *Molecular cell* **2008,** *31* (6), 918-924.
168. Sorrentino, A.; Thakur, N.; Grimsby, S.; Marcusson, A.; Von Bulow, V.; Schuster, N.; Zhang, S.; Heldin, C.-H.; Landström, M., The type I TGF-β receptor engages TRAF6 to activate TAK1 in a receptor kinase-independent manner. *Nature cell biology* **2008,** *10* (10), 1199-1207.
169. Zhang, Y. E., Non-Smad pathways in TGF-β signaling. *Cell research* **2009,** *19* (1), 128-139.
170. Yu, L.; Hébert, M. C.; Zhang, Y. E., TGF-β receptor-activated p38 MAP kinase mediates Smad-independent TGF-β responses. *The EMBO journal* **2002,** *21* (14), 3749-3759.

171. Hanafusa, H.; Ninomiya-Tsuji, J.; Masuyama, N.; Nishita, M.; Fujisawa, J.-i.; Shibuya, H.; Matsumoto, K.; Nishida, E., Involvement of the p38 mitogen-activated protein kinase pathway in transforming growth factor-β-induced gene expression. *Journal of Biological Chemistry* **1999,** *274* (38), 27161-27167.
172. Zhang, D.; Gaussin, V.; Taffet, G. E.; Belaguli, N. S.; Yamada, M.; Schwartz, R. J.; Michael, L. H.; Overbeek, P. A.; Schneider, M. D., TAK1 is activated in the myocardium after pressure overload and is sufficient to provoke heart failure in transgenic mice. *Nature medicine* **2000,** *6* (5), 556–563.
173. Lijnen, P.; Petrov, V., Transforming Growth Factor-b1-Induced Collagen Production in Cultures of Cardiac Fibroblasts is the Result of the Appearance of Myofibroblasts. *Methods and findings in experimental and clinical pharmacology* **2002,** *24* (6), 333-344.
174. Kimura, N.; Matsuo, R.; Shibuya, H.; Nakashima, K.; Taga, T., BMP2-induced apoptosis is mediated by activation of TAK1-p38 kinase pathway that is negatively regulated by Smad6. *Journal of Biological Chemistry* **2000**.
175. Edlund, S.; Bu, S.; Schuster, N.; Aspenstrom, P.; Heuchel, R.; Heldin, N.-E.; ten Dijke, P.; Heldin, C.-H.; Landstrom, M., Transforming growth factor-β1 (TGF-β)–induced apoptosis of prostate cancer cells involves Smad7-dependent activation of p38 by TGF-β-activated kinase 1 and mitogen-activated protein kinase kinase 3. *Molecular biology of the cell* **2003,** *14* (2), 529-544.
176. Hao, J.; Wang, B.; Jones, S. C.; Jassal, D. S.; Dixon, I. M., Interaction between angiotensin II and Smad proteins in fibroblasts in failing heart and in vitro. *American journal of physiology. Heart and circulatory physiology* **2000,** *279* (6), H3020-30.
177. Yang, Y. Z.; Fan, T. T.; Gao, F.; Fu, J.; Liu, Q., Exogenous cytochrome c inhibits the expression of transforming growth factor-β1 in a mouse model of sepsis-induced myocardial dysfunction via the SMAD1/5/8 signaling pathway. *Molecular medicine reports* **2015,** *12* (2), 2189-2196.
178. Gabriel, V. A., Transforming growth factor-β and angiotensin in fibrosis and burn injuries. *Journal of burn care & research* **2009,** *30* (3), 471-481.
179. Rosenkranz, S., TGF-beta1 and angiotensin networking in cardiac remodeling. *Cardiovascular research* **2004,** *63* (3), 423–432.
180. Rosenkranz, S.; Flesch, M.; Amann, K.; Haeuseler, C.; Kilter, H.; Seeland, U.; Schlüter, K.-D.; Böhm, M., Alterations of beta-adrenergic signaling and cardiac hypertrophy in transgenic mice overexpressing TGF-beta(1). *American journal of physiology. Heart and circulatory physiology* **2002,** *283* (3), H1253-62.
181. Wei, H.; Bedja, D.; Koitabashi, N.; Xing, D.; Chen, J.; Fox-Talbot, K.; Rouf, R.; Chen, S.; Steenbergen, C.; Harmon, J. W., Endothelial expression of hypoxia-inducible factor 1 protects the murine heart and aorta from pressure overload by suppression of TGF-β signaling. *Proceedings of the National Academy of Sciences* **2012,** *109* (14), E841-E850.
182. Sun, F.; Duan, W.; Zhang, Y.; Zhang, L.; Qile, M.; Liu, Z.; Qiu, F.; Zhao, D.; Lu, Y.; Chu, W., Simvastatin alleviates cardiac fibrosis induced by infarction via up-regulation of TGF-β receptor III expression. *British journal of pharmacology* **2015,** *172* (15), 3779-3792.
183. Yeh, C. C.; Li, H.; Malhotra, D.; Turcato, S.; Nicholas, S.; Tu, R.; Zhu, B. Q.; Cha, J.; Swigart, P. M.; Myagmar, B. E., Distinctive ERK and p38 signaling in remote and infarcted myocardium during post-MI remodeling in the mouse. *Journal of cellular biochemistry* **2010,** *109* (6), 1185-1191.
184. Zhang, D.; Gaussin, V.; Taffet, G. E.; Belaguli, N. S.; Yamada, M.; Schwartz, R. J.; Michael, L. H.; Overbeek, P. A.; Schneider, M. D., TAK1 is activated in the myocardium after

pressure overload and is sufficient to provoke heart failure in transgenic mice. *Nature medicine* **2000,** *6* (5), 556.
185. Hong, K. M.; Belperio, J. A.; Keane, M. P.; Burdick, M. D.; Strieter, R. M., Differentiation of human circulating fibrocytes as mediated by transforming growth factor-β and peroxisome proliferator-activated receptor γ. *Journal of Biological Chemistry* **2007,** *282* (31), 22910-22920.
186. Hein, S.; Arnon, E.; Kostin, S.; Schönburg, M.; Elsässer, A.; Polyakova, V.; Bauer, E. P.; Klövekorn, W.-P.; Schaper, J., Progression from compensated hypertrophy to failure in the pressure-overloaded human heart: structural deterioration and compensatory mechanisms. *Circulation* **2003,** *107* (7), 984–991.
187. Matsumoto-Ida, M.; Takimoto, Y.; Aoyama, T.; Akao, M.; Takeda, T.; Kita, T., Activation of TGF-β1-TAK1-p38 MAPK pathway in spared cardiomyocytes is involved in left ventricular remodeling after myocardial infarction in rats. *American Journal of Physiology-Heart and Circulatory Physiology* **2006,** *290* (2), H709-H715.
188. Rosenkranz, S.; Flesch, M.; Amann, K.; Haeuseler, C.; Kilter, H.; Seeland, U.; Schlüter, K.-D.; Böhm, M., Alterations of β-adrenergic signaling and cardiac hypertrophy in transgenic mice overexpressing TGF-β1. *American Journal of Physiology-Heart and Circulatory Physiology* **2002,** *283* (3), H1253-H1262.
189. Pauschinger, M.; Knopf, D.; Petschauer, S.; Doerner, A.; Poller, W.; Schwimmbeck, P. L.; Kühl, U.; Schultheiss, H.-P., Dilated cardiomyopathy is associated with significant changes in collagen type I/III ratio. *Circulation* **1999,** *99* (21), 2750-2756.
190. Li, R.-K.; Li, G.; Mickle, D. A.; Weisel, R. D.; Merante, F.; Luss, H.; Rao, V.; Christakis, G. T.; Williams, W. G., Overexpression of transforming growth factor-β1 and insulin-like growth factor-I in patients with idiopathic hypertrophic cardiomyopathy. *Circulation* **1997,** *96* (3), 874-881.
191. Fielitz, J.; Hein, S.; Mitrovic, V.; Pregla, R.; Zurbrügg, H. R.; Warnecke, C.; Schaper, J.; Fleck, E.; Regitz-Zagrosek, V., Activation of the cardiac renin-angiotensin system and increased myocardial collagen expression in human aortic valve disease. *Journal of the American College of Cardiology* **2001,** *37* (5), 1443–1449.
192. Anscher, M. S., Targeting the TGF-β1 pathway to prevent normal tissue injury after cancer therapy. *The oncologist* **2010,** *15* (4), 350-359.
193. Barcellos-Hoff, M.; Derynck, R.; Tsang, M.; Weatherbee, J., Transforming growth factor-beta activation in irradiated murine mammary gland. *The Journal of clinical investigation* **1994,** *93* (2), 892-899.
194. Fruchart, J.-C., Peroxisome proliferator-activated receptor-alpha (PPARalpha): at the crossroads of obesity, diabetes and cardiovascular disease. *Atherosclerosis* **2009,** *205* (1), 1–8.
195. Merl, J.; Ueffing, M.; Hauck, S. M.; von Toerne, C., Direct comparison of MS-based label-free and SILAC quantitative proteome profiling strategies in primary retinal Müller cells. *Proteomics* **2012,** *12* (12), 1902-1911.
196. Hauck, S. M.; Dietter, J.; Kramer, R. L.; Hofmaier, F.; Zipplies, J. K.; Amann, B.; Feuchtinger, A.; Deeg, C. A.; Ueffing, M., Deciphering membrane-associated molecular processes in target tissue of autoimmune uveitis by label-free quantitative mass spectrometry. *Molecular & cellular proteomics : MCP* **2010,** *9* (10), 2292–2305.
197. Wiśniewski, J. R.; Zougman, A.; Nagaraj, N.; Mann, M., Universal sample preparation method for proteome analysis. *Nature methods* **2009,** *6* (5), 359.

198. Azimzadeh, O.; Sievert, W.; Sarioglu, H.; Merl-Pham, J.; Yentrapalli, R.; Bakshi, M. V.; Janik, D.; Ueffing, M.; Atkinson, M. J.; Multhoff, G.; Tapio, S., Integrative proteomics and targeted transcriptomics analyses in cardiac endothelial cells unravel mechanisms of long-term radiation-induced vascular dysfunction. *Journal of proteome research* **2015,** *14* (2), 1203–1219.
199. Philipp, J.; Azimzadeh, O.; Subramanian, V.; Merl-Pham, J.; Lowe, D.; Hladik, D.; Erbeldinger, N.; Ktitareva, S.; Fournier, C.; Atkinson, M. J., Radiation-induced endothelial inflammation is transferred via the secretome to recipient cells in a STAT-Mediated Process. *Journal of proteome research* **2017,** *16* (10), 3903-3916.
200. Hauck, S. M.; Dietter, J.; Kramer, R. L.; Hofmaier, F.; Zipplies, J. K.; Amann, B.; Feuchtinger, A.; Deeg, C. A.; Ueffing, M., Deciphering membrane-associated molecular processes in target tissue of autoimmune uveitis by label-free quantitative mass spectrometry. *Molecular & cellular proteomics : MCP* **2010,** *9* (10), 2292-305.
201. Merl, J.; Ueffing, M.; Hauck, S. M.; von Toerne, C., Direct comparison of MS-based label-free and SILAC quantitative proteome profiling strategies in primary retinal Muller cells. *Proteomics* **2012,** *12* (12), 1902-11.
202. Chen, J.; Wang, S.; Tsai, C.; Lin, C., Selection of differentially expressed genes in microarray data analysis. *The pharmacogenomics journal* **2007,** *7* (3), 212.
203. Storey, J. D.; Tibshirani, R., Statistical significance for genomewide studies. *Proceedings of the National Academy of Sciences* **2003,** *100* (16), 9440-9445.
204. Chen, J. J.; Wang, S. J.; Tsai, C. A.; Lin, C. J., Selection of differentially expressed genes in microarray data analysis. *The pharmacogenomics journal* **2007,** *7* (3), 212-20.
205. Storey, J. D.; Tibshirani, R., Statistical significance for genomewide studies. *Proc Natl Acad Sci U S A* **2003,** *100* (16), 9440-5.
206. Seemann, I.; te Poele, J. A.; Luikinga, S. J.; Hoving, S.; Stewart, F. A., Endoglin haplo-insufficiency modifies the inflammatory response in irradiated mouse hearts without affecting structural and mircovascular changes. *PloS one* **2013,** *8* (7), e68922.
207. Szklarczyk, D.; Franceschini, A.; Wyder, S.; Forslund, K.; Heller, D.; Huerta-Cepas, J.; Simonovic, M.; Roth, A.; Santos, A.; Tsafou, K. P., STRING v10: protein–protein interaction networks, integrated over the tree of life. *Nucleic acids research* **2014,** *43* (D1), D447-D452.
208. Sekiguchi, K.; Tian, Q.; Ishiyama, M.; Burchfield, J.; Gao, F.; Mann, D. L.; Barger, P. M., Inhibition of PPAR-α activity in mice with cardiac-restricted expression of tumor necrosis factor: potential role of TGF-β/Smad3. *American Journal of Physiology-Heart and Circulatory Physiology* **2007,** *292* (3), H1443-H1451.
209. Derynck, R.; Zhang, Y. E., Smad-dependent and Smad-independent pathways in TGF-β family signalling. *Nature* **2003,** *425* (6958), 577.
210. Sun, W.; Ni, X.; Sun, S.; Cai, L.; Yu, J.; Wang, J.; Nie, B.; Sun, Z.; Ni, X.; Cao, X., Adipose-derived stem cells alleviate radiation-induced muscular fibrosis by suppressing the expression of TGF-β1. *Stem cells international* **2016,** *2016*.
211. Westermann, D.; Mersmann, J.; Petrik, C.; Melchior, A.; Rauch, R. L.; Young, M. F.; Levkau, B.; Baba, H.; Zacharowski, K.; Unger, T., Biglycan is Required for Adaptive Remodelling After Myocardial Infarction. Am Heart Assoc: 2006.
212. Díez, J., Altered degradation of extracellular matrix in myocardial remodelling: the growing role of cathepsins and cystatins. Oxford University Press: 2010.
213. Taunk, N. K.; Haffty, B. G.; Kostis, J. B.; Goyal, S., Radiation-induced heart disease: pathologic abnormalities and putative mechanisms. *Frontiers in oncology* **2015,** *5*, 39.

214. Fruchart, J.-C., Peroxisome proliferator-activated receptor-alpha (PPARα): at the crossroads of obesity, diabetes and cardiovascular disease. *Atherosclerosis* **2009,** *205* (1), 1-8.
215. Marx, N.; Kehrle, B.; Kohlhammer, K.; Grüb, M.; Koenig, W.; Hombach, V.; Libby, P.; Plutzky, J., PPAR activators as antiinflammatory mediators in human T lymphocytes: implications for atherosclerosis and transplantation-associated arteriosclerosis. *Circulation research* **2002,** *90* (6), 703-710.
216. Sievert, W.; Trott, K.-R.; Azimzadeh, O.; Tapio, S.; Zitzelsberger, H.; Multhoff, G., Late proliferating and inflammatory effects on murine microvascular heart and lung endothelial cells after irradiation. *Radiotherapy and Oncology* **2015,** *117* (2), 376-381.
217. Wang, T.; Zhang, L.; Shi, C.; Sun, H.; Wang, J.; Li, R.; Zou, Z.; Ran, X.; Su, Y., TGF-β-induced miR-21 negatively regulates the antiproliferative activity but has no effect on EMT of TGF-β in HaCaT cells. *The international journal of biochemistry & cell biology* **2012,** *44* (2), 366-376.
218. Zhou, J.; Wang, K.-C.; Wu, W.; Subramaniam, S.; Shyy, J. Y.-J.; Chiu, J.-J.; Li, J. Y.-S.; Chien, S., MicroRNA-21 targets peroxisome proliferators-activated receptor-alpha in an autoregulatory loop to modulate flow-induced endothelial inflammation. *Proceedings of the National Academy of Sciences of the United States of America* **2011,** *108* (25), 10355–10360.
219. Cheng, Y.; Zhang, C., MicroRNA-21 in cardiovascular disease. *Journal of cardiovascular translational research* **2010,** *3* (3), 251–255.
220. Lowes, B. D.; Minobe, W.; Abraham, W. T.; Rizeq, M. N.; Bohlmeyer, T. J.; Quaife, R. A.; Roden, R. L.; Dutcher, D. L.; Robertson, A. D.; Voelkel, N. F.; Badesch, D. B.; Groves, B. M.; Gilbert, E. M.; Bristow, M. R., Changes in gene expression in the intact human heart. Downregulation of alpha-myosin heavy chain in hypertrophied, failing ventricular myocardium. *The Journal of clinical investigation* **1997,** *100* (9), 2315–2324.
221. Litten, R. Z.; Fein, H. G.; Gainey, G. T.; Walden, T. L.; Smallridge, R. C., Alterations in rat cardiac myosin isozymes induced by whole-body irradiation are prevented by 3, 5, 3'-L-triiodothyronine. *Metabolism* **1990,** *39* (1), 64-68.
222. Azizova, T. V.; Grigoryeva, E. S.; Haylock, R. G.; Pikulina, M. V.; Moseeva, M. B., Ischaemic heart disease incidence and mortality in an extended cohort of Mayak workers first employed in 1948–1982. *The British journal of radiology* **2015,** *88* (1054), 20150169.
223. Simonetto, C.; Azizova, T. V.; Grigoryeva, E. S.; Kaiser, J. C.; Schöllnberger, H.; Eidemüller, M., Ischemic heart disease in workers at Mayak PA: latency of incidence risk after radiation exposure. *PloS one* **2014,** *9* (5), e96309.
224. Barjaktarovic, Z.; Shyla, A.; Azimzadeh, O.; Schulz, S.; Haagen, J.; Dörr, W.; Sarioglu, H.; Atkinson, M. J.; Zischka, H.; Tapio, S., Ionising radiation induces persistent alterations in the cardiac mitochondrial function of C57BL/6 mice 40 weeks after local heart exposure. *Radiotherapy and oncology : journal of the European Society for Therapeutic Radiology and Oncology* **2013,** *106* (3), 404–410.
225. Azimzadeh, O.; Scherthan, H.; Yentrapalli, R.; Barjaktarovic, Z.; Ueffing, M.; Conrad, M.; Neff, F.; Calzada-Wack, J.; Aubele, M.; Buske, C.; Atkinson, M. J.; Hauck, S. M.; Tapio, S., Label-free protein profiling of formalin-fixed paraffin-embedded (FFPE) heart tissue reveals immediate mitochondrial impairment after ionising radiation. *Journal of proteomics* **2012,** *75* (8), 2384–2395.
226. Fillmore, N.; Mori, J.; Lopaschuk, G., Mitochondrial fatty acid oxidation alterations in heart failure, ischaemic heart disease and diabetic cardiomyopathy. *British journal of pharmacology* **2014,** *171* (8), 2080-2090.

227. Heather, L. C.; Carr, C. A.; Stuckey, D. J.; Pope, S.; Morten, K. J.; Carter, E. E.; Edwards, L. M.; Clarke, K., Critical role of complex III in the early metabolic changes following myocardial infarction. *Cardiovascular research* **2010,** *85* (1), 127–136.
228. Barjaktarovic, Z.; Schmaltz, D.; Shyla, A.; Azimzadeh, O.; Schulz, S.; Haagen, J.; Dörr, W.; Sarioglu, H.; Schäfer, A.; Atkinson, M. J., Radiation–induced signaling results in mitochondrial impairment in mouse heart at 4 weeks after exposure to X-rays. *PloS one* **2011,** *6* (12), e27811.
229. Ji, G.; Lv, K.; Chen, H.; Wang, T.; Wang, Y.; Zhao, D.; Qu, L.; Li, Y., MiR-146a regulates SOD2 expression in H2O2 stimulated PC12 cells. *PloS one* **2013,** *8* (7), e69351.
230. Bayeva, M.; Ardehali, H., Mitochondrial dysfunction and oxidative damage to sarcomeric proteins. *Current hypertension reports* **2010,** *12* (6), 426-432.
231. Dalle-Donne, I.; Rossi, R.; Giustarini, D.; Gagliano, N.; Lusini, L.; Milzani, A.; Di Simplicio, P.; Colombo, R., Actin carbonylation: from a simple marker of protein oxidation to relevant signs of severe functional impairment. *Free Radical Biology and Medicine* **2001,** *31* (9), 1075-1083.
232. Lee, W.-S.; Kim, J., Peroxisome Proliferator-Activated Receptors and the Heart: Lessons from the Past and Future Directions. *PPAR research* **2015,** *2015* (5), 1–18.
233. Kida, K.; Nakajima, M.; Mohri, T.; Oda, Y.; Takagi, S.; Fukami, T.; Yokoi, T., PPARα is regulated by miR-21 and miR-27b in human liver. *Pharmaceutical research* **2011,** *28* (10), 2467-2476.
234. Gomez, I. G.; MacKenna, D. A.; Johnson, B. G.; Kaimal, V.; Roach, A. M.; Ren, S.; Nakagawa, N.; Xin, C.; Newitt, R.; Pandya, S., Anti–microRNA-21 oligonucleotides prevent Alport nephropathy progression by stimulating metabolic pathways. *The Journal of clinical investigation* **2015,** *125* (1), 141-156.
235. Schroen, B.; Heymans, S., Small but smart—microRNAs in the centre of inflammatory processes during cardiovascular diseases, the metabolic syndrome, and ageing. *Cardiovascular research* **2011,** *93* (4), 605-613.
236. Thum, T.; Gross, C.; Fiedler, J.; Fischer, T.; Kissler, S.; Bussen, M.; Galuppo, P.; Just, S.; Rottbauer, W.; Frantz, S., MicroRNA-21 contributes to myocardial disease by stimulating MAP kinase signalling in fibroblasts. *Nature* **2008,** *456* (7224), 980.
237. Gao, S.; Wu, R.; Zeng, Y., Up-regulation of peroxisome proliferator-activated receptor gamma in radiation-induced heart injury in rats. *Radiation and environmental biophysics* **2012,** *51* (1), 53-59.
238. el Azzouzi, H.; Leptidis, S.; Bourajjaj, M.; Armand, A.-S.; van der Nagel, R.; van Bilsen, M.; Martins, P. A. D. C.; De Windt, L. J., Peroxisome proliferator-activated receptor (PPAR) gene profiling uncovers insulin-like growth factor-1 as a PPARα target gene in cardioprotection. *Journal of Biological Chemistry* **2011,** *286* (16), 14598-14607.
239. Subramanian, V.; Seemann, I.; Merl-Pham, J.; Hauck, S. M.; Stewart, F. A.; Atkinson, M. J.; Tapio, S.; Azimzadeh, O., Role of TGF Beta and PPAR Alpha Signaling Pathways in Radiation Response of Locally Exposed Heart: Integrated Global Transcriptomics and Proteomics Analysis. *Journal of proteome research* **2016,** *16* (1), 307-318.
240. Bansal, T.; Chatterjee, E.; Singh, J.; Ray, A.; Kundu, B.; Thankamani, V.; Sengupta, S.; Sarkar, S., Arjunolic Acid, a Peroxisome Proliferator-Activated Receptor Alpha Agonist Regresses Cardiac Fibrosis by Inhibiting Non-canonical TGF-β Signaling. *Journal of Biological Chemistry* **2017**, jbc. M117. 788299.

241. Li, L.; Chen, Y.; Doan, J.; Murray, J.; Molkentin, J. D.; Liu, Q., Transforming growth factor β-activated kinase 1 signaling pathway critically regulates myocardial survival and remodeling. *Circulation* **2014,** *130* (24), 2162–2172.
242. Biernacka, A.; Dobaczewski, M.; Frangogiannis, N. G., TGF-β signaling in fibrosis. *Growth factors* **2011,** *29* (5), 196-202.
243. Akhurst, R. J.; Hata, A., Targeting the TGFβ signalling pathway in disease. *Nature reviews. Drug discovery* **2012,** *11* (10), 790–811.
244. Desmoulière, A.; Geinoz, A.; Gabbiani, F.; Gabbiani, G., Transforming growth factor-beta 1 induces alpha-smooth muscle actin expression in granulation tissue myofibroblasts and in quiescent and growing cultured fibroblasts. *The Journal of cell biology* **1993,** *122* (1), 103-111.
245. Seemann, I.; Gabriels, K.; Visser, N. L.; Hoving, S.; te Poele, J. A.; Pol, J. F.; Gijbels, M. J.; Janssen, B. J.; van Leeuwen, F. W.; Daemen, M. J.; Heeneman, S.; Stewart, F. A., Irradiation induced modest changes in murine cardiac function despite progressive structural damage to the myocardium and microvasculature. *Radiother Oncol* **2012,** *103* (2), 143-50.